12-2018

ADENYLYL CYCLASE TYPE 9: REGULATION AND CARDIAC FUNCTION

Tanya A. Baldwin

Tanya A. Baldwin

ADENYLYL CYCLASE TYPE 9: REGULATION AND CARDIAC FUNCTION

by

Tanya A. Baldwin, B.S.

APPROVED:

_____
Carmen W. Dessauer, Ph.D.
Advisory Professor

_____
Darren F. Boehning, Ph.D.

_____
Xiaodong C. Cheng, Ph.D.

_____
Vasanthi Jayaraman, Ph.D.

_____
Heinrich Taegtmeyer, M.D., D.Phil.

APPROVED:

_____
Dean, The University of Texas
MD Anderson Cancer Center UTHealth Graduate School of Biomedical Sciences

ADENYLYL CYCLASE TYPE 9: REGULATION AND CARDIAC FUNCTION

A

DISSERTATION

Presented to the Faculty of

The University of Texas

MD Anderson Cancer Center UTHealth

Graduate School of Biomedical Sciences

in Partial Fulfillment

of the Requirements

for the Degree of

DOCTOR OF PHILOSOPHY

by

Tanya Ann Baldwin, B.S.

Houston, Texas

December 2018

Dedication

I dedicate this work to Thomas and everyone who has cheered, mentored, pushed, and pulled me along the way.

Acknowledgements

At the beginning, never would I have imagined my PhD journey would be so complex. Despite the ups and the downs, I am thankful for the process and to those who helped me along the way.

To my parents, who loved and encouraged me from the very start. You fostered my love of science from an early age whether it was helping me collect bugs, showing me how to make cheese, or teaching me the names of bones. Brad, thank you for the random phone calls and for always being excited about what I am doing. You never ceased to encourage me. And to the countless family members and friends who have cheered me on along the way, your love and support was appreciated.

To Thomas, thank you from the bottom of my heart for helping me through every part of this process and for never letting me quite or give less than my best. You provided a never-ending source of love, encouragement, and updates about what was going on in the world. This journey would not have been as amusing or informative without you.

A scientist in isolation misses out on a wealth of knowledge and insight. None of this would have been possible without the core and extended members of the Dessauer Lab, present and past. Cameron, Yong, and Yan thank you for showing me the ways of the lab from teaching me techniques to assisting with experiment. I am better having learned from you. Cameron, the late evening spent in lab or the ice palace would have drudged on without you. Max, Sam, Anibal, Alexis, and Simi your help, feedback, and shenanigans made the long days seem shorter.

I am also thankful for wonderful collaborators, in particular Dr. Val Watts. Thank you for including me in your work, the AC1 inhibitor paper was my very first publication! The reagents you provided were invaluable to helping me finish.

To my committee: Drs. Heinrich Taegtmeyer, Vasanthi Jayaraman, Xiaodong Cheng, and Darren Boehning, thank you for your valuable feedback and guidance from the very start. Also, thank you for having fantastic lab members whose insights, protocols, and willingness to lend resources helped my project along the way.

Dr. T, I cannot thank you enough for your guidance and insights into my science and career development (especially all of the letters of recommendation). I am thankful you agreed to let me shadow you in the clinic and take the time to give me invaluable advice. I am indebted to a number of your lab members for helping me as well. Especially, Dr. Giovanni Davogustto, I appreciate you taking the time to teach and help me with my mouse cardiac Doppler and echocardiograms.

Dr. Shane Cunha, thank you for stepping in last minute as a stand in committee member for my defense. I am thankful to have had you as a mentor during my PhD. Your relentless questioning and constructive feedback have made me a better scientist. Plus, you let me take/borrow anything I needed for experiments and provided me with countless adult/neonatal cardiac myocytes, thank you!

There are too many people in the Integrative Biology and Pharmacology department and McGovern Medical School to thank, I appreciate everyone who has given me constructive feedback on my project, lent me reagents, cells, and whatever else I needed for an experiment. And to the administrative staff in the program and graduate school, you make the lives of students so much easier, thank you! The collaborative nature of the department and school makes science a little bit easier and a lot more fun.

There are also too many members of the CRB and BCB program to thank for listening to presentations, enjoyable conversations, and encouragement. The students

who started in the program before me (Meredith, Dhananjay, Randi, Kelsey, and Courtney), thank you for your guidance early on. Sam, Asha, Brittany, Janani, Max, and Elia, somehow, we never had a dull lunch conversation, thank you for the fun and sanity conserving conversations and Starbucks runs. Max and Tara, I cannot imagine having gotten through grad school without you. You listened to my complaints, presentations, wacky ideas, helped me with statistic, and everything in between, I hope you know how much I appreciated it all.

I saved the best for last. To my mentor, Carmen you have inspired me from the very start. I knew almost instantly I wanted/needed to train with you. I still remember how excited I was after our conversations during my interview weekend. Your dedication to science and those you mentor is what I strive to emulate as I continue my journey to become an independent investigator. You have shown me what it takes to produce innovative and reproducible science from critically considering controls, techniques, and analysis to perfecting how I present my data and ideas. The foundation you have provided has made me the scientist I am today.

ADENYLYL CYCLASE TYPE 9: REGULATION AND CARDIAC FUNCTION

Tanya A. Baldwin, B.S.

Advisory Professor: Carmen W. Dessauer, Ph.D.

Abnormalities in cardiac stress signaling underlie a number of cardiovascular diseases (e.g. arrhythmias and heart failure). Cardiac stress signaling pathways normally integrate signals from the sympathetic nervous system to promote efficient contraction and relaxation under stress. Sympathetic control through β-adrenergic stimulation is propagated by adenylyl cyclase (AC). AC synthesizes cyclic AMP (cAMP), an important second messenger that initiates signaling pathways to modulate physiological and pathophysiological functions of the heart, including the activation of PKA and subsequent phosphorylation of ion channels, contractile machinery, and stress response proteins that enhance cardiac function. Alterations of cAMP signaling occur in the failing heart and contribute to impaired function. Of the AC isoforms present in adult cardiomyocytes (AC 4, 5, 6, and 9), AC9 is the most divergent in sequence and understudied. The work presented in this dissertation sought to evaluate the direct regulatory properties of AC9 and explores roles for AC9 in heart.

To clarify conflicting reports for AC9 regulation, proposed regulators were systematically evaluated, including G-proteins, protein kinases, and forskolin utilizing *in vitro* and cell based assays. Overall, I conclude that most G-proteins or protein kinases do not directly regulate AC9, except Gαs, *in vitro*. Although AC9 is forskolin insensitive alone, weak activation by forskolin in the presence of Gαs is possible. AC9 shows significant homodimerization and modest heterodimerization with AC5/6, which may account for the conflicting reports surrounding the regulation of this AC isoform.

To study the role of AC9 in heart, a mouse model of AC9 genetic deletion was utilized. Although deletion of AC9 reduces less than 3% of total AC activity in heart, Yotiao-associated AC activity is eliminated. $AC9^{-/-}$ mice exhibit no structural abnormalities but show a significant bradycardia and alterations in Doppler echocardiography indicative of grade 1 diastolic dysfunction with preserved ejection fraction. Identification of novel AC9 binding partners, including the small heat shock protein 20 (Hsp20) and Popeye domain containing (Popdc) proteins may contribute to the underlying mechanisms of $AC9^{-/-}$ phenotypes. Collectively, this work suggests that AC9 forms distinct macromolecular complexes that contribute to local cAMP pools important for driving physiological function of the heart.

Table of Contents

List of Illustrations

List of Tables

List of frequently used abbreviations

AC: adenylyl cyclase

$A_{2A}R$: adenosine 2A receptor

AKAP: A-kinase anchoring protein

β-gal: beta galactosidase

βAR: beta adrenergic receptor

BiFC: bimolecular fluorescence complementation

cADDis: cAMP Difference Detector *in situ*

CaM: calmodulin

CaMKII: calcium-calmodulin kinase II

cAMP: 3'-5' cyclic adenosine monophosphate

CaN: calcineurin

COS-7: Monkey (*Cercopithecus aethiops)* embryonic kidney cell line

D2L: dopamine D2 long receptor

DAMGO: [D-Ala^2, *N*-MePhe^4, Gly-ol]-enkephalin

DAPI: 49,6-diamidino-2- phenylindole

DMEM: Dulbecco's modified Eagle's medium

EPAC: exchange protein directly activated by cAMP

Fsk: forskolin

GFP: green fluorescent protein

GPCR: G-protein coupled receptor

HCN: hyperpolarization-activated cyclic nucleotide gated channel

HEK293: human embryonic kidney 293 cells

Hsp20: heat shock protein 20

FDFM: familial dyskinesia with facial myokymia

IBMX: 3-isobutyl-1-methylxanthine

KCNQ1: potassium voltage-gated channel subfamily Q member 1

LQTS: long QT syndrome

LTCC: L-type calcium channels

MPB: myelin basic protein

μOR: mu opioid receptor

PDE: phosphodiesterase

PKA: protein kinase A

PKC: protein kinase C

PKD: protein kinase D

PLA: proximity ligation assay

PLN: phospholamban

PMA: phorbol 12-myristate 13-acetate

Popdc (Pop): Popeye domain containing

PP1: protein phosphatase 1

RyR: ryanodine receptor

SAN: sinoatrial node

SST2: somatostatin receptor 2

TAC: transverse aortic constriction

TREK-1:TWIK-related K^+ channel 1

VC: C-terminal half of Venus

VN: N-terminal half of Venus

YFP: yellow fluorescent protein

Chapter 1

Introduction

The heart continuously balances the interplay of various signaling mechanisms in order to maintain homeostasis and to respond to stress. One pathway that contributes to cardiac physiology and stress is the cyclic adenosine monophosphate (cAMP) pathway. cAMP is a universal second messenger that integrates input from G-protein coupled receptors to coordinate subsequent intracellular signaling. Synthesis of cAMP from adenosine triphosphate (ATP) is controlled by the enzyme adenylyl cyclase (AC) (Rall and Sutherland, 1958). In the heart, cAMP acts downstream on a variety of effectors including protein kinase A (PKA), hyperpolarization-activated cyclic nucleotide gated channels (HCN), exchange protein directly activated by cAMP (EPAC), Popdc proteins, and a fraction of phosphodiesterase (PDEs). PKA is the best known and studied cAMP effector. PKA phosphorylation of intracellular targets coordinates a number of physiological outputs including contraction (Antos et al., 2001; Fink et al., 2001) and relaxation (Zhang et al., 1995). HCN channel regulation by cAMP maintains basal heart rate (Alig et al., 2009) while EPAC facilitates calcium handling and cardiac hypertrophy (Metrich et al., 2010). PDEs degrade cAMP, further defining the temporal regulation of the signal. The most recently discovered cAMP effector, Popdc, is important for heart rate dynamics through regulation of the potassium channel, TREK1 (Schindler and Brand, 2016).

The AC family is composed of nine membrane bound isoforms (AC 1-9) and one soluble isoform (sAC). All of the isoforms can be found in the heart with the exception of AC8 (Sadana and Dessauer, 2009; Willoughby and Cooper, 2007). Cardiac fibroblasts express AC's 2-7 (Ostrom et al., 2003), while in adult cardiac myocytes AC5 and AC6 are considered the major isoforms (Iwatsubo et al., 2004; Okumura et al.,

2003a). Lower levels of AC2, AC4 and AC9 are reported in myocytes (Li et al., 2012; Ping et al., 1997).

1.1 ACs and their role in cardiac function: KO phenotypes

AC5 and AC6 are closely related isoforms that share similar regulatory mechanisms, including inhibition by Gαi as the hallmark of this group; however, physiologically they appear to play distinct roles in cardiac function (Efendiev and Dessauer, 2011; Sadana and Dessauer, 2009). Additional modes of regulation for AC5/6 are extensively reviewed elsewhere (Dessauer et al., 2017). AC5 and AC6 are differentially expressed in development, with age, and in pressure overload models of cardiac hypertrophy. Additionally, an increase in AC5 protein is observed in neonatal hearts and models of heart disease (Hu et al., 2009; Scarpace et al., 1996). Another potential distinction between these two isoforms is their subcellular localization (Timofeyev et al., 2013).

Several overexpression and deletion studies have focused on roles of these isoforms in cardiac function. Two independent AC5 deletion ($AC5^{-/-}$) mouse lines have been generated. Overall, deletion of AC5 decreases total cAMP activity in cardiac membranes and isolated myocytes (~35-40%) under basal and stimulated (isoproterenol and forskolin) conditions (Okumura et al., 2003b; Tang et al., 2006). The two studies reported varying results for changes in cardiac function. Okumura et al. (Okumura et al., 2003b) observed a decrease in isoproterenol-stimulated left ventricular (LV) ejection fraction (LVEF) but no alterations in basal cardiac function (with intravenous isoproterenol). Conversely, Tang et al. (Tang et al., 2006) noted basal changes in contractile function of perfused isolated hearts in addition to a decreased sensitivity to β_1-adrenergic receptor agonist. The most notable finding of $AC5^{-/-}$ mice was the effect on parasympathetic regulation of cAMP. Inhibition of cAMP production by Gi-

coupled acetylcholine treatment was ablated and Ca^{2+} mediated inhibition was significantly reduced upon AC5 deletion (Okumura et al., 2003b). Physiologically, this corresponds to a reduction in LVEF and heart rate in response to muscarinic agonists and an attenuation of baroreflexes (Okumura et al., 2003b; Tang et al., 2006). Similarly, AC6 deletion results in a significant reduction of cAMP production in stimulated left ventricular homogenates or in cardiac myocytes (60-70%), with no changes to basal cAMP production (Tang et al., 2008). AC6 deletion revealed a number of unique contributions not observed in $AC5^{-/-}$, including impaired calcium handling which results in depressed LV function (Tang et al., 2008). Furthermore, levels of AC6, but not AC5, limit βAR signaling in heart (Gao et al., 1998; Tepe et al., 1999).

In addition to cardiac contractility, AC5 and AC6 play important roles with regard to cardiac stress. Deletion of AC5 is protective in a number of models of cardiac stress, including transverse aorta constriction, chronic isoproterenol infusion, age-related cardiomyopathy, and high fat diet, but not overexpression of Gq (Okumura et al., 2003b; Okumura et al., 2007; Timofeyev et al., 2010; Yan et al., 2007). While knockout of AC5 can be beneficial to heart, overexpression of AC6 in heart infers protection in response to myocardial ischemia or dilated cardiomyopathy (Lai et al., 2008; Roth et al., 2002; Roth et al., 1999), but not chronic pressure overload using transverse aortic constriction (Guellich et al., 2010). However, the protection provided upon AC6 overexpression is independent of its catalytic activity, as expression of catalytically inactive AC6 is also cardioprotective (Gao et al., 2017), but requires proper localization via the N-terminus of AC6 (Wu et al., 2017). In fact, expression of AC6 using adenoviral vectors for treatment of heart disease is currently in clinical trials (Hammond et al., 2016). Therefore, it is tempting to simplify the system and suggest that AC5 is largely

associated with stress responses while AC6 is necessary for calcium handling and contractility. For these reasons, there has been considerable interest in AC5-selective inhibitors for treatment of heart disease. However, deletion of AC6 can also be protective from chronic pressure overload in female, but not in male mice (Tang et al., 2010); therefore, roles for AC isoforms may depend on the type of heart disease model. AC inhibitors such as Ara-A (Vidarabine) do have benefits for treatment of myocardial ischemia when delivered after coronary artery reperfusion in mice (Bravo et al., 2016), however Ara-A and related AC inhibitors are not selective for AC5 over AC6, although they show considerable selectivity over other AC isoforms (Braeunig et al., 2013; Brand et al., 2013). Therefore, any benefits of Ara-A likely arise from inhibition of both AC isoforms. However, this could prove risky, as AC6 deletion increases mortality during sustained catecholamine stress (Tang et al., 2013).

Surprisingly, no polymorphisms that give rise to cardiovascular disease are known to occur in ACs (Ikoma et al., 2003). However, mutations in AC5 are linked to familial dyskinesia with facial myokymia (FDFM), a disease characterized by uncontrolled movement of limb and facial muscles (Chen et al., 2014; Chen et al., 2012). These patients may also have a predisposition to congestive heart failure (Chen et al., 2012). Two FDFM mutations occur in a newly appreciated region of AC5, a helical domain that is present immediately after the transmembrane domain and precedes the catalytic cyclase domain (Figure 1). In other nucleotidyl cyclases, this domain forms a tight hairpin to induce an active dimeric conformation of the catalytic domains (Vercellino et al., 2017). Thus, the helical domain may play a role in stability of the catalytic core or direct regulation of activity.

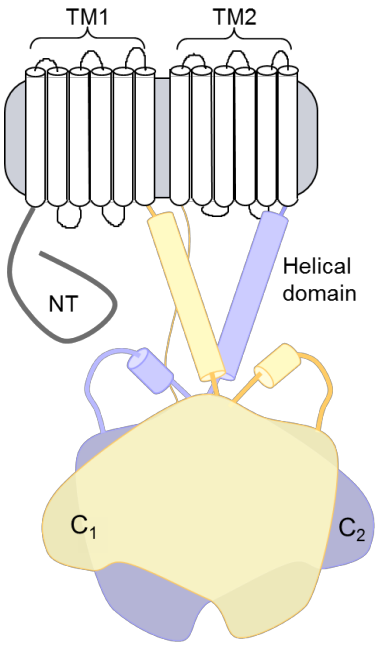

Figure 1. Topology of AC Isoforms. The structural topology of mammalian membranous ACs consists of an N-terminal (NT) domain followed by a repeating set of transmembrane (TM1/2) domains, helical dimerization, and cytoplasmic domains. The two cytoplasmic domains (C1 and C2) make up the catalytic core and the binding site for many regulatory proteins.

Roles for additional AC isoforms in cardiac function have been largely overlooked. AC1 was proposed to function as the calcium-stimulated AC in sinoatrial node that modulates the I_f pacemaker current (Mattick et al., 2007; Younes et al., 2008). However, AC1 knockout mice are not reported to have a heart rate defect and RNA sequencing detects higher expression of AC1 in right atrium versus sinoatrial node (Vedantham et al., 2015). Roles for AC2 and/or AC4 are unknown. Currently, a knockout of AC4 is unavailable and AC2 knockout mice display no cardiac phenotype, although RNA for AC2 is elevated in pediatric dilated cardiomyopathy subjects (Nakano et al., 2017). Cardiac functions for AC9 are discussed below.

1.2 The AKAP connection: Generating specificity for AC function

Tissue distribution and regulation provide one mode for how the AC isoforms contribute to distinct physiological functions (Dessauer et al., 2017; Sadana and Dessauer, 2009). Another mode of signal specificity comes from the formation of AC macromolecular complexes through the scaffolding family of A-kinase anchoring

proteins (AKAPs). AKAPs not only facilitate cellular localization of ACs but they also enhance temporal regulation of cAMP signaling. A number of AKAPs exist in heart including, AKAP15/18, AKAP79/150, Yotiao, mAKAP, AKAP-Lbc, and Gravin (Scott et al., 2013) (Figure 2). In the heart, the spatial and temporal regulation by AKAPs provides an important mechanism to facilitate stress response. The associations of ACs with AKAPs facilitate regulation of PKA, downstream effectors and ACs. This was shown in the dorsal root ganglion, where the activation of the transient receptor potential vanilloid 1 (TRPV1) channel by forskolin or prostaglandin E2 is facilitated by AKAP79-AC5-PKA-TRPV1 complex formation and shifts the response to lower concentrations of forskolin by ~100 fold. Disruption of this complex attenuates sensitization of the channel, as anchoring of both PKA and AC5 are required to elicit the maximal effect on TRPV1 current (Efendiev et al., 2013). Anchoring of PKA and ACs to AKAPs can also regulate AC activity. Association of AC5/6 with AKAP79/150 creates a negative feedback loop where cAMP production is inhibited by PKA phosphorylation of AC5/6 (Bauman et al., 2006). Although this complex and feedback mechanism was defined in the nervous system, modulation of TRPV1 in heart is suggested to influence cardiac response to disease and injury (Randhawa and Jaggi, 2017). Fine tuning of the signal is important for modulating a number of effectors contributing to physiological function.

AC localization is assessed primarily through functional roles of associated complex members enriched at various cardiomyocyte substructures (Figure 2). Association of both AC5 and AC6 with AKAP5 suggests localization at the t-tubule, based upon functional association with calcium-induced calcium release (Nichols et al., 2010). However, with respect to β adrenergic signaling, AC5 is enriched with β2 adrenergic receptors in t-tubules, whereas AC6 localizes outside of the t-tubule (Nikolaev et al.,

2010; Timofeyev et al., 2013). Disruption of cAMP compartmentalization is potentially an underlying mechanism of heart failure (Nikolaev et al., 2010). AC9 association with Yotiao and KCNQ1 suggest localization at intercalated discs, the sarcolemma, and t-tubules (Kurokawa et al., 2004). These AC-AKAP complexes are discussed next.

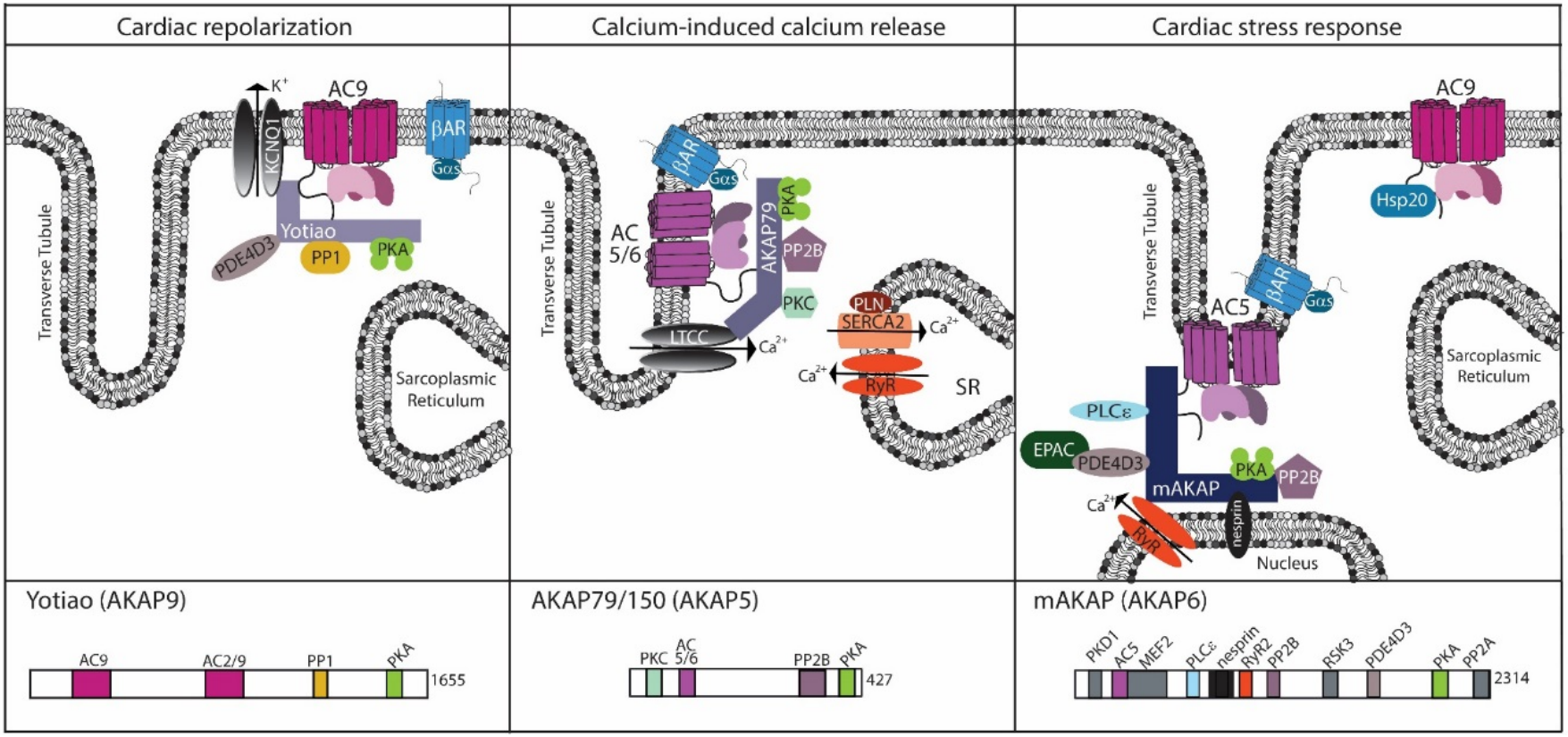

Figure 2. Cardiac AC complexes. AC-associated AKAP complexes localize to distinct locations within the cardiomyocyte and facilitate physiological function. For each AKAP, a subset of known binding partners and their interaction sites are represented. Model is based upon functional localization of AC complexes.

1.2.1 AKAP5

The AKAP5 family of orthologs are named for their size on SDS-PAGE in different species, e.g. human AKAP79, mouse AKAP150, and bovine AKAP75. AKAP79/150 can associate with AC 2, 3, 5, 6, 8, and 9 as evaluated in tissue culture models (Bauman et al., 2006; Efendiev et al., 2010). In heart, AKAP79 primarily interacts with AC5/6 (Nichols et al., 2010). The interaction site is located on the N-terminus of AC and in the second and third polybasic domain on AKAP79 (aa 77-153). In cells, AKAP79-scaffolded PKA phosphorylates AC5/6 to inhibit cAMP production (Bauman et al., 2006; Efendiev et al., 2010). This feedback loop allows for precisely timed activation and inactivation of the cAMP signal. Although AKAP79-anchored AC5/6 is inhibited by associated PKA, it is unclear how AKAP79 regulates AC2 activity in isolated plasma membranes.

AKAP79/150 has been studied in isolated cardiomyocytes from WT and AKAP150 knockouts. Deletion of AKAP150 significantly reduced stimulated calcium transients and calcium sparks in response to isoproterenol. Additionally, the phosphorylation of the ryanodine receptor (RyR) and phospholamban (PLN) were eliminated in cardiomyocytes from knockout mice. It was further shown that AKAP150 forms a complex with AC5/6, PKA, protein phosphatase type 2 (PP2B or calcineurin), $Ca_v1.2$, and caveolin 3 (CAV3). This complex is found on t-tubules, while disruption of complex formation upon AKAP150 deletion alters CAV3 and AC6 localization (Nichols et al., 2010).

AKAP150 has additional roles, independent of AC and PKA. AKAP150 localizes protein kinase C (PKC) and LTCC to the subsarcolema in atrial myocytes enabling regulation of calcium sparklets (Navedo et al., 2008). TRPV4 sparklets are also modulated by the AKAP150-PKC complex in a distance dependent manner; where a distance less than 200 nM between the TRPV4 and AKAP150-PKC is ideal for proper

regulation (Tajada et al., 2017). AKAP150 is also implicated in β_1AR recycling. Knockdown or knockout of AKAP150 in isolated myocytes inhibits recycling of β_1ARs back to the membrane after isoproterenol stimulation, but not internalization. Isolated AKAP150$^{-/-}$ cardiomyocytes have an enhanced contraction rate in response to isoproterenol and an increased cell size at basal and stimulated conditions. Based on these results it was postulated that AKAP150 is cardioprotective because the hypertrophy phenotype was enhanced in AKAP150$^{-/-}$ (Li et al., 2013b).

AKAP150 has been examined in a number of pathology models including myocardial infarction and pressure overload. AKAP150$^{-/-}$ mice were subjected to transverse aortic constriction surgery (TAC) to induce pressure overload, AKAP150 expression significantly decreased in conjunction with a significant increase in hypertrophy, fibrosis, and cell death. Physiologically, deletion of AKAP150 increased left ventricular end diastolic size and impaired fractional shortening after TAC compared to sham animals. Physiological changes were mirrored by alterations in calcium signaling. Phosphorylation of RyR and PLN in addition to calcium transients were impaired in response to isoproterenol (Li et al., 2017a). A model of myocardial infarction (MI) was also examined in AKAP150$^{-/-}$ mice. Alteration in cardiac signaling after MI is well documented. MI causes an increase in NFATc3 activation and associated K_v channel down regulation. AKAP150$^{-/-}$ cardiomyocytes displayed impaired NFAT translocation in response to phenylephrine, which was dependent on calcineurin activity, preventing down regulation of K_v channel currents (Nieves-Cintron et al., 2016). Cardiovascular disease is a co-morbidity associated with diabetes (Matheus et al., 2013). Unlike the other models, in a model of diabetes mellitus, knockdown of AKAP150 ameliorated glucotoxicity induced diastolic dysfunction in mice. In rat cardiomyocytes from diabetic

animals or treated with high glucose, AKAP150 expression is enhanced combined with increased active PKC at the plasma membrane. This, in turn, promotes activation of NFκB and Nox (Zeng et al., 2014), players in the reactive oxygen species pathway that underlie diabetes induced cardiovascular injury (Matheus et al., 2013). Thus, while AKAP150 may play a cardioprotective role in some pathology models, this is not always the case.

1.2.2 mAKAP (AKAP6)

Anchored to the nuclear envelope, the cardiac splice variant of muscle AKAP (mAKAPβ) interacts with AC5 to facilitate cardiac signaling (Kapiloff et al., 2009; Kapiloff et al., 1999). mAKAP is localized to the nuclear envelope through its interaction with nesprin (Pare et al., 2005b) while much lower levels of mAKAP are found at the sarcoplasmic reticulum (SR) (Ruehr et al., 2004). While mAKAP is intracellularly located primarily at the nuclear envelope and AC5 is membrane bound, it is thought that localization of AC5 to the t-tubules allows for this interaction due to the close proximity of the nucleus and t-tubules at sites within the cardiomyocyte (Escobar et al., 2011; Gao et al., 1997). AC5 interacts with mAKAP through a unique binding site on the N-terminus (245-340). Similar to AKAP79, PKA binding to the mAKAP complex creates a negative feedback loop to inhibit AC5 activity (Kapiloff et al., 2009).

A number of molecules implicated in hypertrophy are anchored by mAKAP, including protein phosphatases 2A and 2B (PP2A/2B), PDE4D3, hypoxia inducible factor 1α (HIF1α), phospholipase Cε, myocyte enhancer factor-2 (Vargas et al., 2012), and p90 ribosomal S6 kinase 3 (RSK3) (Dodge et al., 2001; Dodge-Kafka et al., 2010; Li et al., 2013a; Wong et al., 2008; Zhang et al., 2013). Other proteins are associated indirectly with mAKAP complexes, including EPAC1 and the ERK5 and MEK5 mitogen

activated protein kinases via interactions with PDE4D3 (Dodge-Kafka et al., 2005). The interaction of mAKAP and the RyR at the SR promotes phosphorylation and enhances calcium release (Ruehr et al., 2003), while RyR located within the nucleus promote hypertrophy as discussed below.

A role for mAKAP in pathological hypertrophy was first described in mAKAP knockdown myocytes (Pare et al., 2005a) and subsequently shown in mAKAP knockout mice where knockout mice subjected to TAC had reduced hypertrophy, cell death, and did not display TAC inducible gene expression (Kritzer et al., 2014). Further characterization of the mAKAP macromolecular complex highlights how multiple pathways converge on mAKAP to integrate hypertrophic signaling. The cAMP pathway is integrated through AC5-mAKAP-PDE4D3-EPAC binding to utilize and maintain local cAMP pools (Dodge et al., 2001; Dodge-Kafka et al., 2010; Dodge-Kafka et al., 2005; Kapiloff et al., 2009). Activated calcineurin is recruited to the complex and is required for nuclear translocation of NFAT (Li et al., 2010). PLCε binds to a complex containing mAKAP, Epac, PKD, and RyR2 contributing to PKD activity, and nuclear calcium levels (Zhang et al., 2011; Zhang et al., 2013).

1.2.3 Yotiao (AKAP9)

Yotiao is a 250 kDa splice variant of AKAP9 present in heart. Yotiao interacts with the alpha subunit (KCNQ1) of the slowly activating delayed rectifier K^+ current (I_{Ks}), a critical component for the late phase repolarization of the cardiac action potential in humans (Marx et al., 2002). I_{Ks} is made up of four alpha subunits and accessory beta subunits, KCNE1. Beta adrenergic control of I_{Ks} by PKA phosphorylation of KCNQ1 increases channel current to shorten the action potential and maintain diastolic intervals in response to an increase in heart rate. Mutations in KCNQ1 are associated with long

QT syndrome type 1 (LQT1), a potentially lethal hereditary arrhythmia. Not only do mutations in the KCNQ1 lead to this disease, but mutations within Yotiao (LQT11) and KCNE1 (LQT5) can also give rise to LQT syndrome (Chen et al., 2007; Duggal et al., 1998). A subset of these mutations in either Yotiao (S1570L) or KCNQ1 (G589D) disrupts the KCNQ1-Yotiao interaction, resulting in altered regulation of the I_{Ks} channel (Chen et al., 2007).

Yotiao creates a macromolecular complex between KCNQ1 and important regulators of KCNQ1 phosphorylation. Yotiao scaffolds both positive (PKA) and negative regulators, protein phosphatase 1 (PP1) and phosphodiesterase 4DE3 (PDE4D3), of KCNQ1 phosphorylation (Lin et al., 1998; Marx et al., 2002; Terrenoire et al., 2009; Westphal et al., 1999). Loss of this scaffold decreases cAMP dependent PKA phosphorylation of KCNQ1, eliminates functional response by I_{Ks}, and prolongs the action potential (Terrenoire et al., 2009). Yotiao is the key to maintaining a tightly regulated feedback loop for I_{Ks} dependent cardiac repolarization and heart rate. Although Yotiao facilitates cardiac repolarization, it cannot overcome channel mutations that alter the capacity for phosphorylation. For example, an A341V mutation in KCNQ1 acts as a dominant negative that reduces basal channel activity and KCNQ1 phosphorylation with no alteration in Yotiao binding (Heijman et al., 2012).

Of the AC isoforms that Yotiao scaffolds (AC 1, 2, 3 and 9) (Piggott et al., 2008), AC9 is the only one present in cardiomyocytes. Unlike the other AKAPs that interact with AC in heart, Yotiao does not scaffold the major cardiac isoforms AC5/6. While Yotiao binds to the N-terminus of AC9, there appears to be multiple sites of interaction of AC9 on Yotiao, with the primary site located within the first 808 amino acids and a second, weaker site that overlaps with the AC2 binding site on Yotiao (amino acids 808-

956). The interaction of AC9 with Yotiao and KCNQ1 was shown by immunoprecipitation of the complex from cells co-expressing all three proteins, a transgenic mouse line with cardiac expression of KCNQ1-KCNE1, and from guinea pig hearts, which endogenously express the complex. Co-expression of AC9 and Yotiao in CHO cells stably expressing KCNQ1-E1 sensitize PKA phosphorylation of KCNQ1 in response to isoproterenol compared to AC9 or Yotiao expression alone (Li et al., 2012). Yotiao inhibits AC2 and AC3 activity but the mechanism of inhibition is unknown; no inhibition of AC9 activity is observed (Piggott et al., 2008). Based on these results we postulate that the AC9-Yotiao-PKA-KCNQ1 macromolecular complex generates a local pool of cAMP that is critical for cardiac repolarization in humans.

1.3 Newly appreciated AC's in heart

1.3.1 AC9 KO phenotype

An in depth look at the role of AC9 in cardiomyocytes has not been forthcoming for a long time. This is likely due to the low level of expression of AC9 in cardiomyocytes, the fact that AC5/6 accounts for nearly all of total cAMP production (Sadana and Dessauer, 2009), and observations from FA Antoni showing deletion of AC9 through conventional targeting was embryonically lethal (Antoni, 2006). The interaction of AC9 with the Yotiao-I_{Ks} complex sparked renewed interest in examining its role in cardiac physiology (Li et al., 2012). Meanwhile, the Mutant Mouse Regional Resource Center, a NIH funded strain repository, generated a viable AC9 deletion mouse utilizing a gene trapping cassette. Examination of this AC9 deletion strain resulted in two distinct physiological phenotypes, bradycardia and diastolic dysfunction with preserved ejection fraction; no structural abnormalities were observed in AC9 $^{-/-}$ mice using echocardiograms (Li et al., 2017b). In addition, Yotiao-anchored AC9 activity is present

in the sinoatrial node, supporting a role for AC9 in heart rate. These results are detailed in Chapter 4.

1.3.2 AC9 regulation

Of the AC isoforms, AC9 is the most divergent in sequence and has been the least studied. Expression analysis shows that AC9 is widely expressed in the central nervous system, heart, and other tissues (Antoni et al., 1995; Hacker et al., 1998; Paterson et al., 2000; Sosunov et al., 2001b). While the regulatory mechanisms of the other isoforms have been well studied, studies of AC9 regulation have yielded conflicting results. Potential modes of AC9 regulation (Figure 3) include stimulation by Gαs, protein kinase C βII (PKCβII) (Liu et al., 2014), or calcium-calmodulin kinase II (CaMKII) (Cumbay and Watts, 2005) and inhibition by Gαi/o (Cumbay and Watts, 2004), novel PKC isoforms (Cumbay and Watts, 2004), or calcium/calcineurin (CaN) (Hacker et al., 1998).

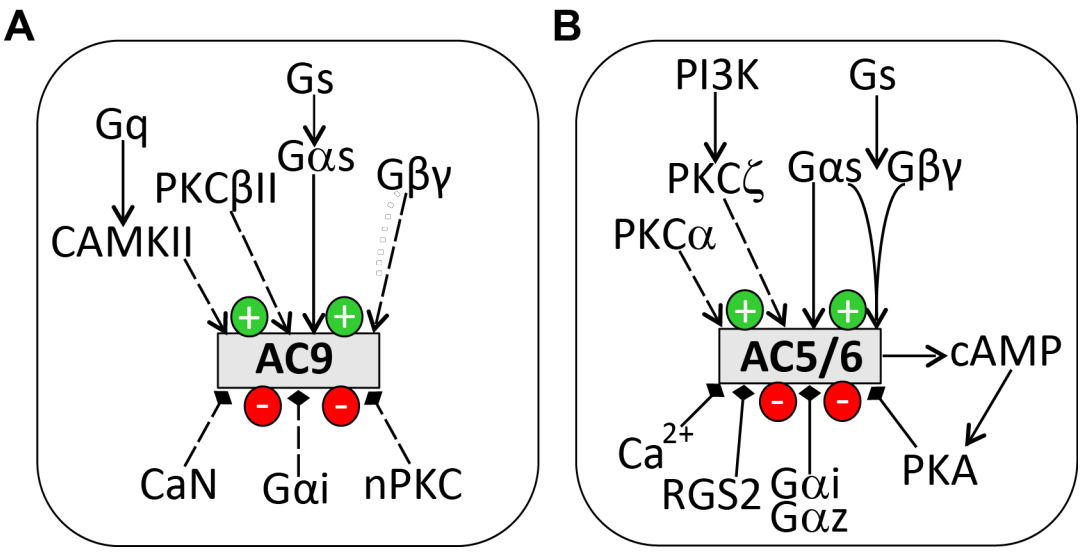

Figure 3. Modes of AC9 regulation versus AC5/6. (A) Proposed modes of AC9 regulation based upon whole cells studies. **(B)** Regulators of AC5/6 activity from whole cell and *in vitro* studies.

Determining the regulatory modalities for various AC isoforms is crucial to understand how the individual isoforms function physiologically. Ideally, the regulation of AC9 would

be examined in biochemical and tissue culture models, then be confirmed in cardiomyocytes, but due to the low levels of expression, examining AC9 regulation will prove difficult in this system.

1.3.2.1 G-protein regulation

Every membrane bound AC isoform is stimulated by Gαs (Sadana and Dessauer, 2009). Compared to AC6, AC9 has a right shifted Gαs dose response curve in Sf9 cells, showing a reduced sensitivity to Gαs (TA Baldwin, unpublished observations). This would potentially impact signaling, where a decreased sensitivity to Gαs reduces downstream signaling outputs, making AC9 even more dependent on complex formation to facilitate local pools of cAMP. Interestingly, all of the alterations in cardiac physiology observed in $AC9^{-/-}$ mice were at basal levels suggesting that AC9 may be more important for setting the basal tone in cardiac signaling (Li et al., 2017b). However, in cells AC9 requires Yotiao anchoring to sensitize the phosphorylation of KCNQ1 in response to isoproterenol (Li et al., 2012), emphasizing again the need for complex-dependent signaling.

The original cloning and characterization of human AC9 examined Gαi/o regulation of AC9 in HEK293 but did not detect inhibition of AC9 by endogenously expressed somatostatin receptors (Hacker et al., 1998). Subsequently, Gαi/o regulation of AC9 was reexamined in HEK293 cells upon transient expression of the dopamine receptor (D2L); cells treated with a D2L selective agonist, had a significant reduction in AC activity. Thus the researchers concluded that Gαi/o may inhibit AC9 (Cumbay and Watts, 2004). It is unclear whether the discrepancy between these two studies is due to the type of Gαi/o-coupled receptor, receptor preference for Gαi versus Gαo, or background activity of endogenously expressed AC6. Interestingly, AC9 does not contain the important

residues that are required for Gαi binding and inhibition of AC5 (Dessauer et al., 1998). Direct regulation of AC9 by Gαi is described in Chapter 3.

Gβγ is another common regulator of AC activity, inhibiting AC1, AC3, and AC8 or stimulating AC2, AC4, and AC5-7 (Dessauer et al., 2017; Sadana and Dessauer, 2009). AC9 regulation by Gβγ had been postulated based on neutrophil chemotaxis studies, but never tested in other cells (Liu et al., 2010). Still others have concluded that Gβγ does not regulate basal or Gαs-stimulated AC9 activity (Hacker et al., 1998; Premont et al., 1996). Despite not having a direct regulatory role, Gβγ binds the N-terminus of AC9 (Brand et al., 2015; Li et al., 2017b).

1.3.2.2 Kinase and phosphatase regulation

Gq regulation of AC9 through CaMKII and PKC was examined in HEK293 cells expressing AC9 stably with transient transfection of either the muscarinic receptor M_5 or the serotonin receptor, $5HT_{2A}$. Treatment of cells with the receptor agonists (M5, carbachol or $5HT_{2A}$, 5HT) potentiated AC9 activity in the presence of isoproterenol; expression of the constitutively active Gαq mutant (Q209L) showed similar results. Co-treatment with receptor agonists and the PKC inhibitor, bisindolylmaleimide, further potentiated activity suggesting that PKC acted as an inhibitor of AC9 activity. The authors also examined potentiation of AC9 activity by calcium/calmodulin (CaM) kinase (CaMK) through the M_5 receptor, by treating cells with carbachol in the presence of a CaM (W-7) or CaMKII (KN-93) inhibitor; both inhibitors reduced AC9 activity. Thus, Gq potentiation of AC activity occurs through activation of CaMKII. However, the authors could not determine whether AC9 is directly phosphorylated by these kinases or whether regulation was via an indirect mechanism (Cumbay and Watts, 2005).

AC9 is also important for neutrophil chemotaxis through activation of AC9 by PKCβII. Neutrophils express high levels of AC9 and have also been used to examine AC9 regulation. Knockdown of AC9 in a neutrophil cell line was shown to inhibit chemotaxis in response to fMLP caused by a decrease in cAMP in extending pseudopods (Liu et al., 2010). This mechanism was further dissected to show PKCβII knockdown recapitulated the AC9 knockdown phenotype. It was proposed that AC9 phosphorylation by PKCβII was the mechanism for increased cAMP in neutrophils leading to chemotaxis (Liu et al., 2014).

AC9 was originally cloned from mouse as a calcineurin inhibited isoform (Paterson et al., 1995). In HEK293 cells expressing mouse AC9, activity was inhibited by calcium in a concentration dependent manner that was restored by increasing treatments with the calcineurin inhibitors FK506 or cyclosporin A (Antoni et al., 1995; Paterson et al., 1995). Subsequent characterizations of human AC9 show conflicting results for calcineurin inhibition (Hacker et al., 1998; Paterson et al., 2000). The discrepancy was suggested to occur due to differences in variants of AC9 mRNA. Overall, it is unclear whether regulator differences reported for AC9 are due to different expression systems, species differences, or interaction with cell-specific proteins (including AKAPs).

1.4 Conclusions

Multiple distinct AC complexes exist in heart and are important regulators of cardiac physiology. While great strides have been made to understand the composition and roles of these complexes, there are still many questions left to answer. Pharmacological targeting of AC isoforms has been actively pursued, but obtaining isoform specificity is difficult, especially for AC5 and AC6. An alternative and widely considered approach is targeting specific protein-protein interactions within the cardiac AC complexes.

Targeting components of a complex could provide specificity unlike pan enzyme inhibitors, as these complexes frequently contain only a small percentage of the total protein in the cell. This was the idea behind disrupting the AC5-mAKAP complex, as mAKAP-localized cAMP signaling is involved in cardiac hypertrophy (Kapiloff et al., 2009). While disruption of this complex was proposed to have a beneficial effect on hypertrophy, the opposite effect was observed. In cardiomyocytes disruption of AC5-mAKAP binding lead to cellular hypertrophy though an increase in cAMP levels. As previously discussed AC5 binding to the mAKAP complex creates multiple feedback loops to inhibit cAMP production. These data show how important the fine tuning of cAMP signaling is and emphasizes the need for extensive studies when designing AKAP complex disruptors for therapeutic use. Finally, many ACs interact with up and or downstream effectors through AKAP-facilitated interactions. However, there is still the possibility that other AC-AKAP complexes have yet to be identified. Moving forward the possibility of AC complexes independent of AKAPs should also be considered.

The exploration of a role for AC9 in cardiac function has long been forthcoming. Based upon its interaction with Yotiao and the growing evidence for macromolecular complex dependent regulation of cAMP signaling, *I hypothesize that macromolecular complexes facilitate regulation of AC9 that underlies cardiac repolarization.* The goal of my dissertation work was two-fold, first to determine the direct regulator mechanism controlling AC9 enzymatic activity (Chapter 3) and second to examine the *in vivo* role of AC9 in cardiac function (Chapter 4).

Chapter 2

Materials and Methods

Note:

Figures and text are partially reprinted from Li, Y., T. A. Baldwin, Y. Wang, J. Subramaniam, A. G. Carbajal, C. S. Brand, S. R. Cunha, and C. W. Dessauer. 2017. Loss of type 9 adenylyl cyclase triggers reduced phosphorylation of Hsp20 and diastolic dysfunction. *Scientific Reports* 7: 5522.

2.1 Materials and antibodies.

All protocols utilizing animals were approved by the Institutional Animal Care and Use Committee (IACUC) at The University of Texas Health Science Center at Houston in accordance with the Animal Welfare Act and NIH guidelines.

Drugs used included forskolin (Sigma-Aldrich, St. Louis, MO), isoproterenol hydrochloride (Calbiochem, Darmstadt, Germany), DAMGO ([D-Ala^2, *N*-MePhe^4, Gly-ol]-enkephalin) (Bachem, Bubendorf, Switzerland), 49,6-diamidino-2- phenylindole phorbol (DAPI), 12-myristate 13-acetate (PMA) and IBMX (3-isobutyl-1-methylxanthine) (Sigma-Aldrich, St. Louis, MO).

Antibodies used for immunoprecipitation and western blotting are shown in Table 1. Rabbit polyclonal anti-AC9 was generated against human AC9 peptide KINPKQLSSNSHPKHPC conjugated to KLH. Affinity-purified antibody showed high selectivity for AC9 over AC3, 5, and 6 (data not shown). Antibodies used for Western blots were diluted in Tris-buffered saline/Tween 20.

Table 1. Antibodies used for western blotting, immunoprecipitation, and immunofluorescence.

Antibody	Supplier/Citation	Application	1° Dilution	2° Type
anti-AC5	(Bavencoffe et al., 2016)	WB	1:1000	Mouse
anti-AC5/6	Santa Cruz Biotechnology	WB	1:1000	Rabbit
anti-AC9 (N18)	Santa Cruz Biotechnology	WB	1:1000	Goat
anti-AC9	Described above	WB	1:1000	Rabbit
anti-AKAP150	EDM Millipore	WB	1:1000	Mouse
anti-AKAP150	Santa Cruz Biotechnology	IP	2 μg	Rabbit
anti-A.V. Monoclonal (JL-8) for GFP/YFP	Takara Biology	WB IP	1:1000 1:100	Mouse
anti-Bves(Popdc1)	Santa Cruz Biotechnology	WB	1:1000	Goat

anti-cmyc	NIH	WB IP	1:1000 1:100	Mouse
anti-DYKDDDDK tag	Cell Signaling Technologies	WB IP IF	1:1500 1:100 1:800	Mouse Alexa 567
anit-Flag	Sigma Aldrich	WB	1:1000	Mouse
anti-Flag M2 agarose affinity gel	Sigma-Aldrich	IP	15 μl beads	---
anti-HA	Roche	WB	1:1000	Mouse
anti-Hsp20 (Hsp20-11)	Santa Cruz Biotechnology	WB IP	1:1000 2 μg	Mouse
Normal mouse or rabbit IgG	Santa Cruz Biotechnology	IP controls		
Alexa Fluor 633 Phalloidin	Invitrogen	IF	1:2000	---
anti-phospho Hsp20 (S16)	Abcam	WB	1:1000	Rabbit
anti-phospho Troponin I (Ser23/24)	Cell Signaling Technologies	WB	1:1000	Rabbit
anti-phospho Phospholamban (Ser 16)	EDM Millipore	WB	1:1000	Rabbit
anti-Phospholamban (2D12)	ThermoFisher	WB	1:1000	Mouse
anti-sodium potassium ATPase[EP1845Y]	Abcam	WB	1:10,000	Rabbit
anti-Troponin I	Cell Signaling Technologies	WB	1:1000	Rabbit
anti-Yotiao	(Piggott et al., 2008)	WB IP IF	1:1000 2 μg 1:50	Rabbit Alexa 647

* Western blot (WB), IP (immunoprecipitation), IF (immunofluorescence). Secondary antibodies are diluted as follows mouse (1:30,000), rabbit (1:20,000), goat (1:5000), Alexa fluorophores (1:500).

2.2 Plasmids and viruses.

Human AC6, rat AC1, and rat AC2 baculoviruses were amplified and expressed in Sf9 cells as previously described (Chen-Goodspeed et al., 2005; Tang and Gilman, 1991; Tang et al., 1991). Human Flag–tagged AC9 (aa 1-1252; (Hacker et al., 1998)) was cloned into the SalI and NotI restriction sites of pFastBacDual to generate a baculovirus according to manufacturer's specifications (Invitrogen). A baculovirus

expressing β-galactosidase (β-gal) was used as a control. Eukaryotic expression vectors for human Flag-AC9 (full-length, AJ133123; (Paterson et al., 2000)), AC5, Flag-AC5, AC6, and YFP-AC6 in pcDNA3.1 were previously described (Brand et al., 2015; Kapiloff et al., 2009; Li et al., 2012; Sadana et al., 2009). A truncated eukaryotic expression vector for human Flag-AC9 (aa 1-1252, AF036927; (Hacker et al., 1998)) was also generated to compare the two clones; the truncated form has comparable Gαs-stimulated activity as full-length when expressed in HEK293 cells (data not shown). The HA-tagged mu opioid receptor (μOR) was a generous gift from Dr. Heather Carr (UTHealth). The BiFC expression construct for YN-AC5 was previously described (Brand et al., 2015). Two types of constructs were designed for AC9. For Myc-AC9-VN and HA-AC9-VC, VN and VC were cloned using PCR in frame with the C-terminus of full-length AC9, separated by a sequence encoding a 12 and 19 aa linker, respectively. Additional AC9-VN and AC9-VC constructs were generated that lacked an N-terminal tag and consisted of a C-terminal 7 aa linker (AAAGGGS) followed by VN or VC tags. All AC9-VN/VC constructs behaved similarly in assays. Human AC5-VN and AC5-VC were cloned by PCR, replacing YFP using KpnI/BamHI restriction sites in AC5-YFP (Efendiev et al., 2010). To generate AC6 BiFC clones, the stop codon was deleted and a KpnI site was inserted at the end of the coding region. VN and VC were then cloned in frame by PCR to the C-terminus of human AC6, separated by a sequence encoding a 10 and 9 aa linker, respectively. All clones were verified by DNA sequencing.

Myc-Yotiao-pcDNA3 was previously described (Piggott et al., 2008). Myc-tagged Hsp20 was purchased from Origene; V5-Hsp20 was a gift from Dr. George Baillie (University of Glasgow). A Flag-tag (MDYKDDDDK) plus two residue linker (GA) was inserted in frame at the N-terminus of human AC9 using nested PCR primers. The

resulting clone was sequenced, and the activity of the tagged protein verified upon expression in HEK293 cells and Sf9 cells. YFP-tagged AC9 was similarly created using Flag-AC9 pCDNA3 as the starting construct and replacing the Flag-tag with YFP. To create a catalytically inactive AC9, aspartate 399 was mutated to alanine using QuikChange II Site-Directed Mutagenesis Kit (Agilent Technologies). For adenoviral expression, GFP and YFP-tagged catalytically inactive (AC9-D399A, AC9d) were inserted into the KpnI/XbaI restriction sites of pShuttle-CMV vector. Recombinant adenoviruses were produced according to the manufacturer's instructions (AdEasy Adenoviral Vector Systems, Stratagene). Appropriate clones were selected by RT-PCR and sequenced. Note, although AC9d is expressed as YFP-tagged, YFP is typically cleaved when expressed by adenoviruses in cardiomyocytes and the full-length YFP-AC9d is never observed by WB.

The epidermal growth factor receptor-GFP and lysosomal associated protein 1-GFP plasmids were generous gifts from Drs. Yong Zhou and Mike Zhu (UTHealth), respectively. All of the Popdc-myc tagged constructs full length and truncations were generous gifts from Dr. Thomas Brand (Imperial College London) and previously described (Andree et al., 2000). Popdc1(or 2)-VN and -VC clones were constructed by replacement of the C-terminal myc tag in Popdc-myc with VN or VC by PCR. All clones were verified by sequencing

2.3 Proteins and Sf9 membranes.

Kinases used included CaMKIIα, a generous gift from Dr. M Neil Waxham (UTHealth), and PKCβII (SignalChem, British Columbia, Canada). Myelin basic protein (MBP) for control kinase assays is from Invitrogen (Carslbad, CA). Purified calmodulin (CaM) was a gift from Dr. John Putkey (UTHealth). Myristoylated Gαo expressed in

Escherichia coli was a generous gift from Dr. Greg G. Tall (University of Michigan). Gαo was activated with [^{35}S]GTPγS in the absence of Ric-8A (Tall et al., 2003). Gαs-H_6 and myristoylated Gαi were expressed in *Escherichia coli*, purified by nickel-NTA and ion exchange chromatography, and activated with [^{35}S]GTPγS (Dessauer et al., 1998). Gβ1, Gγ2, and H_6-tagged Gαi were used for expression and purification of non-tagged Gβ1γ2 from Sf9 cells (Kozasa and Gilman, 1995). To purify non-tagged Gαi1 and Gαi3 from Sf9 cells, proteins were co-expressed with H_6-tagged Gβ1 and Gγ2 and purified by nickel-NTA chromatography (Kozasa and Gilman, 1995). All G proteins were activated by [^{35}S]GTPγS; free GTPγS was subsequently removed by size-exclusion chromatography (Dessauer et al., 1998). Baculoviral expression of AC isoforms in Sf9 cells and subsequent plasma membrane preparation was performed as described previously (Chen-Goodspeed et al., 2005).

2.4 Cell culture, transfection, and membrane preparation.

COS-7 and human embryonic kidney 293 (HEK293) cells were maintained in Dulbecco's modified Eagle medium containing 10% fetal bovine serum at 37°C with 5% CO_2; cell lines were authenticated by short tandem repeat profiling (HEK293) or mitochondrial cytochrome c oxidase I DNA barcodes (COS-7) by ATCC. The day before transfection, the cells were seeded at 2.5 x 10^6 cells or 1.5 x 10^6 cells per 10-cm dish for HEK293 and COS-7 cells respectively. The cells were transfected with appropriate plasmids (10 μg of total DNA per 10-cm plate) using Lipofectamine 2000 (Invitrogen, Carlsbad, CA) (Efendiev et al., 2010; Piggott et al., 2008). The transfected cells were incubated for 4 to 6 hours before the media was replaced. HEK293 and COS-7 cells were harvested 40 to 48 hours after transfection for use in immunoprecipitation (Brand et al., 2015; Li et al., 2012) or preparation of cell membranes (Brand et al., 2013). To

prepare lysates for western blotting or immunoprecipitation, transfected cells were rinsed in cold phosphate buffered saline (PBS), lysed with buffer (50 mM HEPES (pH 7.4), 1 mM EDTA, 1 mM $MgCl_2$, 150 mM NaCl, 0.5% $C_{12}E_9$, and protease inhibitors), and homogenized with a 23-gauge syringe. Homogenate was cleared of cellular debris by centrifugation. An aliquot of total lysates was saved for AC assay or western blot prior to immunoprecipitation at 4° C for 1.5 hour with antibody followed by an additional 1.5 hours with protein A or G sepharose. Immunoprecipitation with Flag agarose was rotated at 4° C for 3 hours. Samples are washed twice in lysis buffer (0.05% $C_{12}E_9$) then resuspended in lysis buffer (0 mM NaCl, 0.04% $C_{12}E_9$).

To prepare cell membranes, cells were rinsed and harvested in cold (PBS), pelleted and resuspended in a buffered medium containing 20 mM HEPES pH 7.4, 1 mM EDTA, 2mM $MgCl_2$, 1 mM DTT, 250 mM sucrose, and protease inhibitors. Cells were Dounce homogenized, subjected to centrifugation at 500 x g to pellet nuclei, followed by centrifugation at 100,000 x g; membranes were resuspended in buffer without protease inhibitors. The resulting samples were immediately used for AC assays or frozen for future use.

Neonatal rat ventricular myocytes (NRVM) were isolated from 1- to 2-day-old Sprague-Dawley rat hearts as previously described (Wu et al., 2015). For biochemical assays medium was changed 24 hours after plating and 48-72 hrs post isolation NRVMs were infected with adenovirus (multiplicity of infection of 50-100) for 50 hrs prior to treatments. Experiments were carried out on at least three separate NRVM isolations. Isoproterenol was stored and diluted in AT buffer (100 mM ascorbate and 10 mM thiourea, pH 7.4). For imaging cardiomyocytes were separated from non-cardiomyocyte cells with a Percoll gradient as previously described (Lash and Jones, 1993). Briefly,

cells were resuspended in 1.082 g/mL Percoll. Gradient tubes were prepared in 15 mL conicals by adding increasing densities of Percoll (1.05g/mL, 1.062 g/mL, and 1.082 g/mL). Cardiomyocytes were added to the Percoll gradient tubes and centrifuged at 300 x g for 30 minutes at room temperature in a swing bucket centrifuge. Cardiomyocytes collect at the 1.082 g/mL layer. Cardiomyocytes are collected and washed twice. After final wash cell are resuspended in complete media (50% DMEM, 40% HAMS F10, 10% FBS + 1% Pen/Strep). Cell were plated on fibronectin coated glass bottom MatTek plates (P35G-1.5-14-C, MatTek Corporation, Ashland, MA) at a density of 100,000 cell/plate and medium was changed 24 hours after plating. 48 hours after plating cells are washes to remove debris and media replaced with DMEM + 2% FBS + 1% Pen/Strep. Between 72 and 90 hrs post isolation NRVMs were infected with adenovirus (multiplicity of infection of 50-100) for 60 hrs prior to fixing and staining.

2.5 AC9 shRNA and siRNA knockdown.

AC9 shRNA and control shRNA constructs were a generous gift from Dr. Carole Parent (University of Michigan Medical School) and previously described (Liu et al., 2010). AC9 (SASI_Hs01_00098729 and SASI_Hs01_00098727) and control (SIC001 siRNA universal negative control #1) siRNAs were purchased from Sigma-Aldrich (St. Louis, MO). Control and AC9 shRNA plasmids were packaged into lentiviruses using HEK293T cells. COS-7 cells were then transduced with shRNA-encoding lentivirus and stable knockdowns were generated by selection with 2 μg/ml puromycin (Liu et al., 2010). For siRNA knockdown, COS-7 cells were transiently transfected with control siRNA (600 pmol) or a mixture of two AC9 siRNAs (300 pmol of each) using Lipofectamine 2000, replacing media 4-6 hours post transfection. Cells were harvested for membrane assays 60 hours post-transfection.

2.6 Adenylyl cyclase membrane assays.

Membrane assays were performed as described previously (Dessauer, 2002). Briefly, membrane (Sf9, HEK293, COS7, or mouse spleen) preparations were incubated for 10 minutes at 30°C with an AC mix containing 5 mM $MgCl_2$, 200 μM Mg-ATP, [α-^{32}P]ATP and purified proteins or drugs. Reactions were terminated with a mix of 2.5% SDS, 50 mM ATP, and 1.75 mM cAMP. Each reaction was subjected to column chromatography to separate nucleotides and to isolate [^{32}P]cAMP produced during the reaction; [^{3}H]cAMP was used to monitor column recovery rates by scintillation counting.

For kinase-AC assays, kinase reactions preceded measurement of cAMP production. Proteins and membranes were diluted as follows: CaMKII (100 ng) was diluted in kinase buffer (10 mM HEPES pH 7.4, 200 mM KCl, 0.1% Tween-20, and 1 mg/ml BSA); Sf9 membranes in 20 mM HEPES pH 7.4 and 2 mM DTT; and calmodulin (CaM) in 5 mM MOPS pH 7.0 and 0.01 mg/ml BSA. In a 25 μl reaction, the kinase assay was initiated by the addition of 100 ng of CaMKII to 30 μg of Sf9 membranes, 1 μM CaM and 10X reaction mix (final concentration: 25 mM HEPES pH 7.4, 10 mM $MgCl_2$, 50 mM KCl, 2 mM $CaCl_2$, 400 μM DTT, 100 μM ATP). The reaction was incubated on ice for 10 minutes, then transferred to 30°C for 5 minutes. The assay of AC activity was initiated with 25 μl of AC mix (containing 100 μM Mg-ATP, [α-^{32}P]ATP +/- 100 nM Gαs) and incubated for an additional 10 minutes at 30°C. PKCβII reactions were similar in design. PKCβII and Sf9 membranes were diluted in 20 mM HEPES pH 7.4 and 2 mM DTT. In a 60 μl reaction, PKCβII (5 or 20 nM) was added to Sf9 membranes (15 μg AC2, 30 μg AC9 or β-gal), 100 μM $CaCl_2$, and 1 μM phorbol 12-myristate 13-acetate (PMA); reactions were initiated with activation buffer (final concentration: 20 mM HEPES pH 7.4, 5 mM $MgCl_2$, and 100 μM ATP) and placed at 30°C for 7 minutes. The subsequent

AC assay was initiated with 40 µl of AC mix, (containing 5 mM $MgCl_2$, 100 µM Mg-ATP, [α-^{32}P]ATP +/- 100 nM Gαs), and incubated for an additional 7 min at 30°C. PKCβII and CaMKIIα activity were confirmed by measuring [γ^{32}P] incorporation into myelin basic protein (MBP); control kinase assays substituted [γ-^{32}P]ATP for [α-^{32}P]ATP.

Preparation of heart extracts and measurement of AC activity were performed as previously described (Efendiev et al., 2010; Piggott et al., 2008). AC9 activity in WT hearts was estimated from increasing concentrations of the SQ22,536 inhibitor that displays >100 fold selectivity for AC5/6 over AC9 (Brand et al., 2013). At X concentration of SQ22,536, AC9 activity = (WT-KO)/%AC9 activity remaining at X concentration. The % AC9 activity remaining based upon SQ22,536 dose response curves generated with AC9 Sf9 membranes (Brand et al., 2013). Averages of 4 experiments, performed in duplicate or triplicate, using 10, 30, 100, and 300 µM concentrations of SQ22,536 were used for estimates; a 0.08-2.5% difference in activity is observed between WT and AC9KO heart membranes. Note, at zero SQ22,536 there is no detectable difference in activity. Immunoprecipitation of AKAP or Hsp20 complexes followed by western blotting or measurement of associated AC activity was performed as described (Li and Dessauer, 2015). AC activity was stimulated with the indicated reagents and cAMP was detected by enzyme immunoassay (Assay Designs) or using [γ^{32}P]ATP.

Throughout the paper, AC activity is primarily displayed as specific activity (nmol/min/mg) unless otherwise indicated. Otherwise, results are generally displayed after subtracting control background or as fold over basal, as noted in the figure.

2.7 Live-cell cAMP accumulation monitoring (cADDis and GloSensor).

COS-7 cells were transiently transfected with an empty vector, µOR, and AC9, or AC6; media was changed 4 hours post transfection. After 24 hrs, cells (0.05 x 10^6

cells/ well) were resuspended in DMEM plus 10 % FBS and 6 mM valproic acid, replated on a black, poly-l-lysine coated 96 well plate with clear bottom and incubated with 30 µl of the BacMam sensor (red upward cADDis; cAMP Difference Detector *in situ*, Montana Molecular, Bozeman, MT), according to manufacturer's guidelines. Fluorescent experiments were conducted 24 hours after addition of sensor with Tecan Infinite 200 Pro. Red fluorescence was excited at 560 nm, and emitted light was collected at 605 nM. Prior to fluorescent reads, cell media was replaced with phosphate buffered saline (PBS) for 20-30 minutes to acclimate. A baseline read was measured for 7.5 minutes prior to addition of drug, fluorescence was then monitored for an additional 15 minutes. Isoproterenol and DAMGO were prepared and diluted in AT buffer (0.1 mM ascorbic acid and 1 mM thiourea) for cell treatments. The average of the 7.5 minute baseline read for each well was subtracted from each point to account for variability between assays. Background subtracted fluorescence was averaged over 5-7 minutes post addition of drug (12-14 minutes after start of assay).

For measurement of basal cAMP accumulation, COS-7 cells were transiently transfected with 5 µg of the -20F GloSensor plasmid (Promega, Madison, WI) and with AC isoforms or control vectors on a 10 cm plate. 36 hours post transfection, cells were replated at a density of 0.05 x 10^6 cells per well on white, poly-l-lysine coated 96 well plates and assayed 4 hours later according to the manufacturer's protocol. Cells were pre-treated with 1 mM IBMX for 10 minutes followed by a 5 minute baseline read. Baseline reads were averaged over the 5 minutes.

2.8 Preparation of spleen membranes and splenocytes.

Isolation of membranes from wild-type and AC9 knockout mice was performed as previously described (Piggott et al., 2008; Efendiev et al., 2010). Briefly, fresh or

frozen spleens were washed in ice-cold PBS and quartered. Tissue was resuspended and homogenized with a polytron homogenizer followed by dounce homogenizing in a buffered medium containing 10 mM HEPES pH 7.4, 5 mM EDTA, 300 mM sucrose, and protease inhibitors. The homogenate was centrifuged at 2000 x g to remove cell nuclei, the supernatant from the first spin was then centrifuged at 100,000 x g to collect membranes. Collected membranes were resuspended in a buffer containing 50 mM HEPES pH 7.4, 1 mM EDTA, and 300 mM sucrose. The resulting samples were immediately used for AC assays.

For preparation of splenocytes, spleens were removed from wild-type and AC9 knockout mice and placed on ice in PBS. Tissue was homogenized in MACS buffer (0.5% BSA and 2 mM EDTA in PBS), filtered through a 40 μm strainer, and cells collected by centrifugation (300 x g for 5 minutes). Cells were resuspended in Hybri-Max buffer (Sigma-Aldrich, St. Louis, MO) for 4 min to lyse red blood cells. The reaction was neutralized with excess MACS buffer, centrifuged and resuspended in MACS buffer for counting. Collected splenocytes were then centrifuged and resuspended in RPMI 1640 media with 25 mM HEPES pH 7.4 and immediately used for cAMP accumulation assays. Splenocytes were treated with 1 mM IBMX at 37°C for 20 minutes before addition of vehicle or 1 μM isoproterenol. Reactions were stopped by two-fold dilution with 0.2 N HCl. Cell particulates were removed by centrifugation and cAMP in the supernatant was detected by enzyme immunoassay (Enzo Life Sciences, Farmingdale, NY, catalog # ADI-900-066).

Splenocytes used for profiling were isolated as described above and resuspended in 2 mL of freezing media (40% FBS, 10% DMSO, 50% DMEM) and aliquoted into four cryovial per sample. Samples were frozen at -80°C for 4 hours then

placed in liquid nitrogen. Samples were shipped to Dr. Mark Ormiston's lab (Queen's University, Ontario, Canada) for profiling.

2.9 Bimolecular Fluorescence Complementation (BiFC).

COS-7 cells were transiently transfected as indicated in 12-well plates with VN- or VC-tagged AC9, AC5, or AC6. Approximately 40-48 hours post transfection, cells were stained with DAPI (49,6-diamidino-2- phenylindole; 10 mg/ml) for 1 hour at 37°C. Cells were then scrapped in PBS and transferred to a black 96-well plate with clear, flat bottom (Corning Inc, Coring, NY). Venus and DAPI signals were measured with a multi-well plate reader, Infinite 200 Pro (Tecan, Mannedorf, Switzerland) at room temperature. Venus intensity was measured at an excitation wavelength of 506 and emission wavelengths of 536-542 nm (2-nm step measurements). DAPI intensity was measured at wavelengths of 358 nm (excitation) and 461 nm (emission). Peak signals from 540-542 nm emissions were averaged and normalized to DAPI signal to account for differences in cell number. Background fluorescence from control samples expressing pCDNA3 and/or only VN- or VC-tagged protein was subtracted.

2.11 Generation of AC9 Gene-Targeted Mice.

The mouse strain used for this research project, B6;129S5-*Adcy9Gt(neo)159Lex*/Mmucd, identification number 011682-UCD, was obtained from the Mutant Mouse Regional Resource Center, a NIH funded strain repository, and was donated to the MMRRC by Lexicon, Inc. The insertion of the gene trap vector was generated in strain 129/SvEvBrd-derived embryonic stem cells (International Mouse Knockout et al., 2007). The retroviral insertion (5174 bp) occurred in the intron between exons 1 and 2. The chimeric mice were bred to C57BL/6J mice to generate F1

heterozygous animals. Mice were backcrossed with C57BL/6J mice for 7-9 generations. Age matched or wild-type C57BL/6J littermate controls were used as described.

2.12 Genotyping and RT-PCR.

Primers used to detect gene trap insertion (WT #1 and KO #3; 494 bp) or WT animals (WT #1 and #2; 280 bp) were as follows: KO #3, GGCCAAGAACAGATGGAACAG; WT #1, TCCCTAGCCATTCCTAGCAAAGC; WT #2, CAGTTCACCTTTTCCATACCCCTAG. Primers used for real-time PCR are from (Landa et al., 2005), except AC9. Primer sequences for AC9 are as follows (see Fig 1): AC9-1 Fwd CGGTCTCCCACAGATGAGAT; AC9-1 Rev, TCTGGGGACAGAAACTGAGG; AC9-2 Fwd, CTTTGATAACCTTAAGACTTGC; AC9-2 Rev, CAGGAGCTGGAGCGATCATA. Real-time PCR was performed and analyzed as described (Bavencoffe et al., 2016), using GAPDH as a control template.

2.13 Western blotting from heart lysates

For analysis of PKA phosphorylation in heart, WT and $AC9^{-/-}$ mice were injected with saline or isoproterenol (2 µg/g body weight, IP). Animals were sacrificed 4 min later and heart tissue was harvested. Cardiac extracts were prepared in the presence of phosphatase inhibitors. Equal protein supernatants were subjected to Western blot analysis as described in figure legends.

2.14 Proximity Ligation Assay.

In situ PLA was performed using a Duolink kit (Sigma-Aldrich, cat. DUO92101) following the manufacturer's protocol. HEK293 cells were cultured on clear bottom 96 well plates (Greiner Bio-One), transfected with the required plasmids and fixed with 4% PFA. After washing the plate 3 times with PBS, the cells were blocked (1% BSA + 0.075% Triton X100) for 1 h at room temperature and then incubated with primary

antibodies overnight. Antibodies included: mouse anti-HSP20 (SC-51955, SantaCruz, 1:500), mouse anti-GFP (632381, Living colors, 1:500), rabbit anti-GFP (SC-8334, SantaCruz, 1:1000), mouse anti-Gβγ (SC-378, SantaCruz, 1:1000), and mouse anti-cmyc (9E10, NIH, 1:1000). After removal of primary antibodies, the samples were incubated with anti-mouse PLUS and anti-rabbit MINUS PLA probes for 1 h at 37 °C. Subsequent steps of ligation and elongation were according to the manufacturer's protocol. After the last wash, cells were stained with DAPI (1 μg/ml) and imaged using an epifluorescence high content imaging microscope with a 20X objective (Cell Insight CX5 High Content Screening platform, ThermoFisher). Data analysis was performed using FACS analysis software (FlowJo, USA). To prevent false positives, cells with saturating YFP fluorescence or less than 4 positive signals (dots) per cell were not considered in the analysis.

2.15 Echocardiography.

AC9 knockout and WT mice (3-7 months) were anesthetized in a chamber under 2.5% isoflurane. After sedation, mice were transferred to a heated platform and fixed in the prone position for electrocardiogram recordings and cardiac imaging. Anesthesia was administered via a nose cone at 1-1.5% isoflurane during recordings. Cardiac imaging was utilized to assess left ventricular (LV) diastolic function and other key cardiac parameters. Initial analysis of LV diastolic function was evaluated with pulsed-wave Doppler (PWD) (20MHz, Doppler Signaling Processing Workstation (DSPW), Indus Instruments, Webster, USA) of the mitral valve (MV) inflow (Reddy et al., 2005). Key parameters of the mitral valve flow profile including, early (E) and late (A) filling velocities, aortic ejection time (AET), isovolumetric relaxation time (IVRT), and

isovolumetric contraction time (IVCT) were determined from recordings with DSPW. The ratio of the E/A velocities was used to assess changes in LV filling.

Further evaluation of LV diastolic function and key cardiac function used high resolution ultrasound (40MHz; Vevo 3100, Visual Sonics Inc., Toronto, Canada). All analyses were performed in VevoLab (VisualSonic). LV volume and mass, ejection fraction (EF), and fractional shortening (FS) were calculated from recordings of the short axis using M-mode imaging. Additional measurements from M-mode imaging included the thickness of the LV anterior and posterior wall (LVAW and LVPW) during both systole and diastole as well as the velocity of contraction. Diastolic function was assessed with both PWD and tissue Doppler imaging (TDI), visualized in apical four-chamber view. IVCT, IVRT, AET, E and A velocities, myocardial performance index (MPI), and E/A ratios were determined from PWD recordings. TDI from the septal side of the mitral annulus were used to assess the early (E') and late (A') velocities of the mitral annulus and the ratio of E'/A', A'/E', and MV E/E'. All measurements were averaged from 5 cardiac cycles for each parameter. Note, differences in MV E/A and E'/A' ratios are likely underestimates since the A' and MV A measurements were not always possible on WT mice with very fast heart rates where the early wave is dominant; this was never an issue with $AC9^{-/-}$ mice.

2.11 Fluorescence and immunofluorescence imaging

HEK293 cells expressing YFP- or CFP- tagged proteins were fixed with 2% PFA in PBS for 20 minutes at RT and washed twice with PBS then mounted on slides. Images were acquired 48 hours post transfection with a TE 2000 microscope (Nikon, Tokyo, Japan) with a DG4 xenon light source and CoolSNAP camera (Roper Scientific,

Trenton, NJ). YFP (excitation 500/20 nm, emission 535/30 nM) and CFP (excitation 436/20 nm, emission 465/30 nM) images were collected.

Approximately 60 hours post infection cardiomyocytes are washed with RT PBS and fixed with 2% PFA in PBS at RT for 20 minutes. Cells were permeabilized with 0.1% TritionX-100 for 10 minutes blocked with 3% fish oil in PBS for at least an hour at room temperature, then incubated with primary antibody diluted in PBS with 0.075% TritonX-100 and 3% fish oil overnight at 4° C. Primary antibodies used are described in Table 1. Images were obtained with a Nikon A1R confocal (Nikon, Melville, NY) with a 40x oil, 1.49 numerical aperture objective.

2.12 Statistical Analysis.

Individual experiments were performed in duplicate or triplicate and repeated a minimum of n=3. Experiments are expressed as mean ± standard error of the mean (SEM), except where noted. Sample differences were determined with paired or unpaired t-tests for comparisons between two groups. Comparisons between single groups were determined with a Kruskal-Wallis One Way Analysis of Variance on Ranks followed by Dunn's Method Test. Comparisons between multiple groups were determined using two-way analysis of variance (ANOVA followed by Bonferroni's Multiple Comparison Test. Significant p values are expressed as follows: (*) denotes a p value of < 0.05, (**) < 0.01, and (***) < 0.001. Analysis was performed with Excel or Sigma Plot statistical analysis software.

Chapter 3

Regulatory mechanisms of AC9 enzymatic activity

3.1 Introduction

Of the ten mammalian AC isoforms, AC9 is the most divergent in sequence, and it is also the most understudied. Expression analysis shows that AC9 is widely expressed in the central nervous system, heart, and other tissues (Berndt et al., 2013; Li et al., 2017b; Paterson et al., 2000; Premont et al., 1996; Sosunov et al., 2001a). Although AC9 knockout mice were initially reported to be embryonically lethal (Antoni, 2006), mice lacking AC9 protein expression are viable despite a preweaning subviable homozygous phenotype with incomplete penetrance (Li et al., 2017b). Knockdown and gene-trapping studies provide clear *in vivo* roles for AC9 in neutrophil chemotaxis (Liu et al., 2010; Liu et al., 2014) and cardiac function (Li et al., 2017b) (discussed in Chapter 4). Additionally, polymorphism of the ADCY9 gene is associated with risks for asthma, and mood and body weight disorders (Berndt et al., 2013; Small et al., 2003).

While the regulatory mechanisms of many AC isoforms are defined (reviewed extensively elsewhere (Dessauer et al., 2017)), studies of AC9 regulation have yielded conflicting results. Currently, models of AC9 regulation include stimulation by Gαs, protein kinase C βII (PKCβII) (Liu et al., 2014), or calcium-calmodulin kinase II (CaMKII) (Cumbay and Watts, 2005) and inhibition by Gαi/o (Cumbay and Watts, 2004), novel PKC isoforms (Cumbay and Watts, 2004), or calcium/calcineurin (CaN) (Antoni et al., 1998). Conversely, the original cloning of human AC9 characterized it as insensitive to inhibition by Gαi and CaN (Hacker et al., 1998).

3.2 Results

To investigate direct regulatory properties of AC9, Flag-AC9 was expressed in Sf9 cells and membranes purified; expression was confirmed via western blotting against the FLAG tag and AC9 (Figure 4A). In order to ensure the N-terminal Flag tag

did not alter AC9 activity, membranes from HEK293 cells expressing pcDNA3, non-tagged, and Flag-tagged AC9 were assayed with 300 nM Gαs. No significant difference was observed where AC activity fold over control (pcDNA3) were 7.7 +/- 2.0 and 7.7 +/- 0.8 for AC9 and Flag AC9, respectively.

3.2.1 AC9 is conditionally stimulated by forskolin.

AC9 is the only member of the AC isoform group IV, characterized by forskolin insensitivity (Hacker et al., 1998; Paterson et al., 1995). Although AC9 is insensitive to forskolin stimulation alone, conditional stimulation has not been tested. *In vitro* AC assays were performed with membranes from Sf9 or HEK cells expressing Flag-AC9. AC9 activity was examined in the presence of increasing amounts of activated Gαs with vehicle (DMSO) or forskolin. β-gal- or pcDNA3-expressing membranes served as negative controls for Sf9 and HEK293 membranes, respectively. AC9-containing Sf9 membranes treated with forskolin in the presence of high concentrations of Gαs were weakly, activated compared to membranes treated with Gαs alone (Figure 4B). The same weak conditional activation was observed in HEK293 membranes at high concentrations of Gαs (Figure 4C). Background AC activity in HEK293 membranes is shown (Figure 4D).

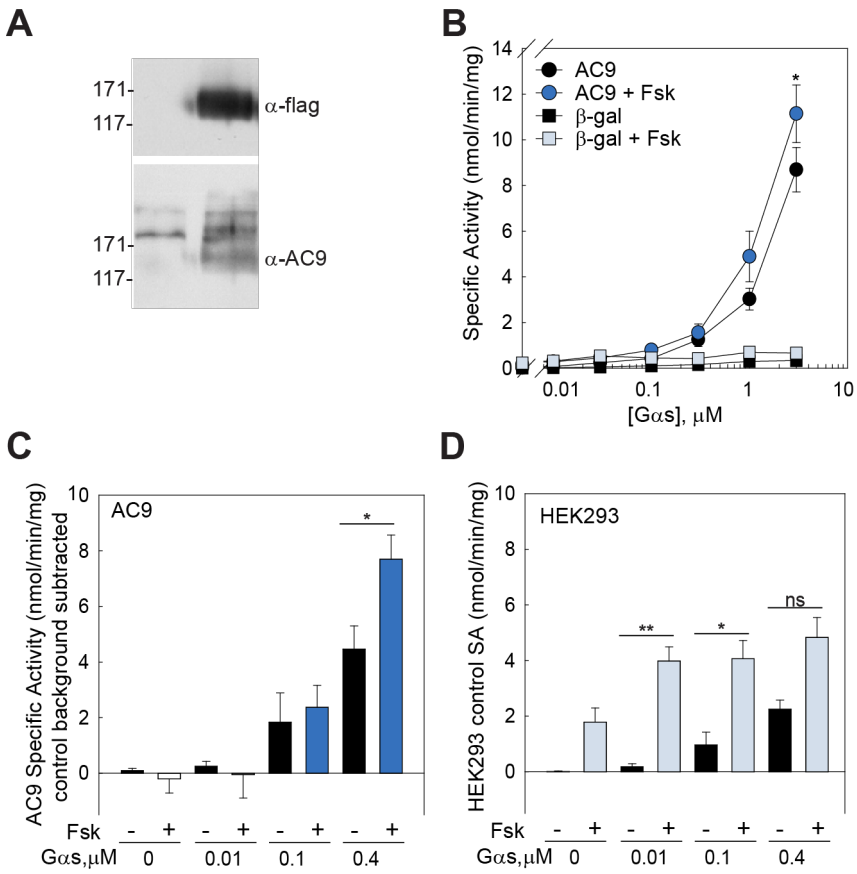

Figure 4. AC9 is conditionally activated by forskolin. (A) Western blot using α-FLAG (top) and goat α-AC9 (bottom) for membranes from Sf9 cells expressing vector control (β-gal) or human AC9. Dose-response curves of Gαs stimulation of **(B)** AC9 and β-gal Sf9 membranes in the presence or absence of 50 μM forskolin and **(C)** membranes from HEK293 cells expressing AC9 in the presence or absence of 100 μM forskolin (activity from control membranes (D) was subtracted). **(D)** AC activity of membranes isolated from HEK293 cells expressing pcDNA3 (background AC activity). Statistics: Paired t-test of experimental means comparing the vehicle and forskolin stimulated groups at each concentration indicated; n = 3-4 with experiments performed in duplicate; *P < 0.05, **P<0.01.

3.2.2 AC9 regulation by Gαs and Gβγ subunits.

It was often noted previously that significantly greater concentrations of Gαs were required to activate AC9 in immunoprecipitation-AC assays than to activate other AC isoforms (Efendiev et al., 2010; Piggott et al., 2008). To gain further insight into how

Gαs-stimulation of AC9 activity compared to other well characterized isoforms, Gαs dose-response curves (1 nM – 1 μM) were generated for membranes from Sf9 cells expressing AC9, AC6, and β-gal. While dose-response curves for Gαs-activation of AC6 were comparable to previously published results (EC50 = 100 nM for AC6; (Chen-Goodspeed et al., 2005)), the Gαs dose response curve for AC9 appears right-shifted (EC50 > 300 nM; Figure 5A). For β-gal membranes EC50=175 nM.

Gβγ either inhibits (AC 1, 3, 8) or conditionally stimulates (AC 2, 4-7) all other membrane bound AC isoforms (Diel et al., 2006; Gao and Gilman, 1991; Gao et al., 2007; Steiner et al., 2006; Tang and Gilman, 1991; Yoshimura et al., 1996). To determine whether AC9 was sensitive to Gβγ, Gαs dose-response curves were performed in the presence or absence of 100 nM $G\beta_1\gamma_2$ (Figure 5B). Gβγ had no direct effect on AC9 activity at any Gαs concentration.

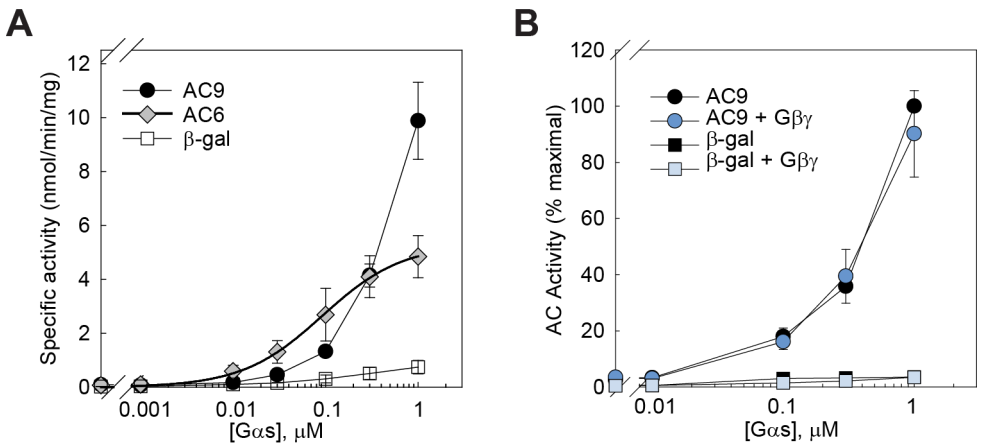

Figure 5. AC9 is less sensitive to Gαs compared to AC6 and insensitive to Gβγ. **(A)** Dose-response curves of Gαs stimulation of membranes from Sf9 cells expressing AC9, AC6, or β-gal. **(B)** Dose-response curves of Gαs stimulation of Sf9 membranes expressing AC9 or β-gal in the presence and absence of 100 nM Gβγ. Statistics: Paired t-test of experiment means comparing the vehicle and Gas or Gβγ stimulated groups at each concentration indicated; n = 3.

3.2.3 AC9 is insensitive to direct regulation by Gαi/o *in vitro*.

AC9 inhibition by dopamine (D2L)-coupled Gαi/o (Cumbay and Watts, 2004) and AC9 insensitivity to somatostatin-coupled Gαi/o (Hacker et al., 1998) have been reported. Sequence alignments of the Gαi binding site for AC5 and AC6 with AC9 reveal no homology of key Gαi binding residues (Dessauer et al., 1998) (Figure 6A). Because the degree of inhibition of AC5 and AC6 by Gαi is dependent on Gαs concentrations (Chen-Goodspeed et al., 2005), myristoylated Gαi (purified from *E. coli*) was tested for its ability at 300 nM to inhibit AC9 in the presence of varying concentrations of Gαs (Figure 3B) or a fixed concentration of activated Gαs (300 nM) in the presence of increasing Gαi (Figure 6C). Regardless of Gαs or Gαi concentrations, no inhibition of AC9 was observed, despite significant inhibition of AC6 activity by Gαi in the same assays (Figure 6D). Gαi is dually modified in mammalian cells by myristoylation of the N-terminal glycine and palmitoylation of the neighboring cysteine residue. Co-expression of N-myristoyl transferase with Gαi in *E. coli* results in myristoylated Gαi that lacks palmitoylation (Linder et al., 1991), while Sf9 expression gives rise to both myristoylation and palmitoylation of Gαi (Linder et al., 1993). To rule out the requirement for palmitoylation of Gαi and/or differences in Gi/o family members, $G\alpha i_1$ (*E.coli* or Sf9), $G\alpha i_3$ (Sf9), and Gαo (*E.coli)* were also tested. No inhibition of AC9 activity was observed (Figure 6D) when incubated with $G\alpha i_1$ or $G\alpha i_3$, despite observed inhibition to AC6 activity (Figure 6D). Gαo likewise did not alter basal or Gαs-stimulated AC9 activity, although AC1 activity was inhibited by Gαo, as previously shown (Figure 6E; (Taussig et al., 1994)).

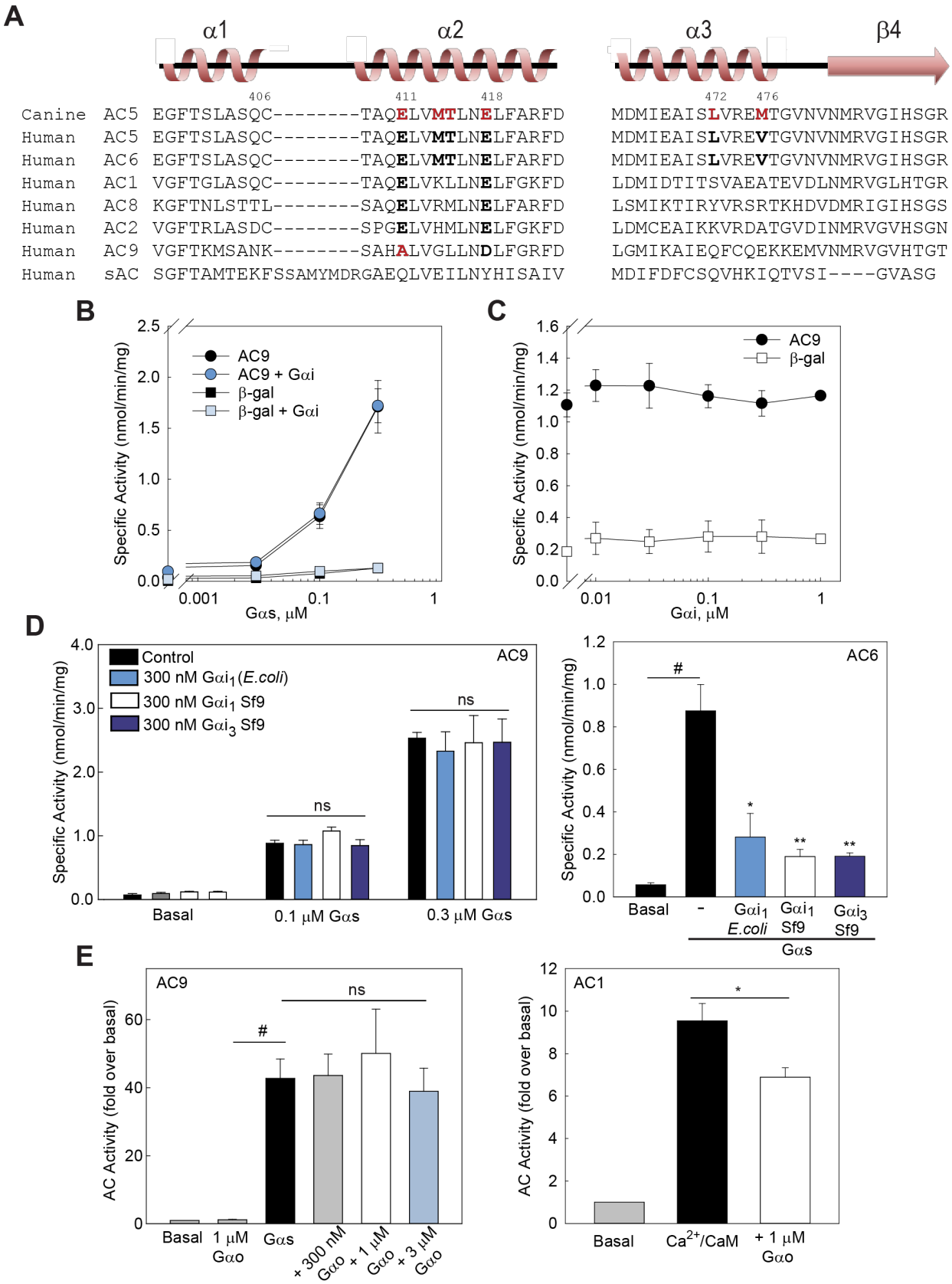
A
α1
α2
α3
β4
406
411
418
472
476
Canine AC5 EGFTSLASQC--------TAQELVMTLNELFARFD MDMIEAISLVREMTGVNVNMRVGIHSGR
Human AC5 EGFTSLASQC--------TAQELVMTLNELFARFD MDMIEAISLVREVTGVNVNMRVGIHSGR
Human AC6 EGFTSLASQC--------TAQELVMTLNELFARFD MDMIEAISLVREVTGVNVNMRVGIHSGR
Human AC1 VGFTGLASQC--------TAQELVKLLNELFGKFD LDMIDTITSVAEATEVDLNMRVGLHTGR
Human AC8 KGFTNLSTTL--------SAQELVRMLNELFARFD LSMIKTIRYVRSRTKHDVDMRIGIHSGS
Human AC2 VGFTRLASDC--------SPGELVHMLNELFGKFD LDMCEAIKKVRDATGVDINMRVGVHSGN
Human AC9 VGFTKMSANK--------SAHALVGLLNDLFGRFD LGMIKAIEQFCQEKKEMVNMRVGVHTGT
Human sAC SGFTAMTEKFSSAMYMDRGAEQLVEILNYHISAIV MDIFDFCSQVHKIQTVSI----GVASG
B
Specific Activity (nmol/min/mg)
AC9
AC9 + Gαi
β-gal
β-gal + Gαi
Gαs, μM
C
Specific Activity (nmol/min/mg)
AC9
β-gal
Gαi, μM
D
Specific Activity (nmol/min/mg)
Control
300 nM Gαi1 (E.coli)
300 nM Gαi1 Sf9
300 nM Gαi3 Sf9
AC9
ns
ns
Basal
0.1 μM Gαs
0.3 μM Gαs
AC6
#
*
**
**
Basal
-
Gαi1 E.coli
Gαi1 Sf9
Gαi3 Sf9
Gαs
E
AC Activity (fold over basal)
AC9
#
ns
Basal
1 μM Gαo
Gαs
+ 300 nM Gαo
+ 1 μM Gαo
+ 3 μM Gαo
AC1
*
Basal
Ca2+/CaM
+ 1 μM Gαo

Figure 6. AC9 is not directly regulated by Gαi/o in vitro. (A) Structure-based alignment of amino acids that correspond to the Gαi binding site in AC5. Based on alignment from Dessauer et al., 1998 **(B)** Gαs dose-response curves for AC9 and β-gal Sf9 membranes in the presence and absence of 300 nM Gαi. **(C)** Gαi dose-response curves for AC9 and β-gal Sf9 membranes in the presence of 300 nM Gαs. **(D)** *E. coli* versus Sf9 purified Gαi isoforms. AC9 Sf9 membranes were stimulated with 300 nM Gαs in the presence or absence of 300 nM $G\alpha i_1$ (*E.coli* or Sf9) or $G\alpha i_3$. AC6 membranes with 50 nM Gαs +/- 300 nM Gαi proteins served as a positive control. **(E)** Gαo regulation of AC9 Sf9 membranes stimulated with 300 nM Gαs; AC1 membranes stimulated with 100μM Ca^{2+}/ 300 nM CaM with 1 μM Gαo served as a positive control. Statistics: Paired t test of experiment means comparing the vehicle and Gαi/o groups at each concentration indicated; n = 3-4 with experiments performed in duplicate or triplicate; * or $^{\#}$ $P < 0.05$, ** $P<0.01$.

3.2.4 AC9 is insensitive to CaMKII and PKCβII *in vitro*.

CamKII and PKCβII have previously been reported to regulate AC9 in cellular assays (Cumbay and Watts, 2005; Liu et al., 2014). To assess whether these kinases act directly on AC9, kinase-AC assays were performed. AC9 activity was measured in the presence calcium/calmodulin (Ca^{2+}/CaM), non-stimulated CaMKII, or Ca^{2+}/CaM-activated CaMKII (Figure 7A). CaMKII activity was confirmed by evaluating phosphorylation of MBP (Figure 7A, inset). Despite significant CaMKII activity in the assays, no significant change in AC9 activity was observed. PKCβII assays were performed in a similar manner to CaMKII assays. Gαs-stimulated AC9, AC2, and control membranes were assayed in the presence of the phorbol ester, PMA, and activated PKCβII (PMA + PKCβII). PKCβII activity was confirmed by an *in vitro* kinase assay measuring MBP phosphorylation (Figure 7B inset). Although PKCβII did not activate AC9, it significantly stimulated AC2, as previously reported (Figure 7B; (Zimmermann and Taussig, 1996)).

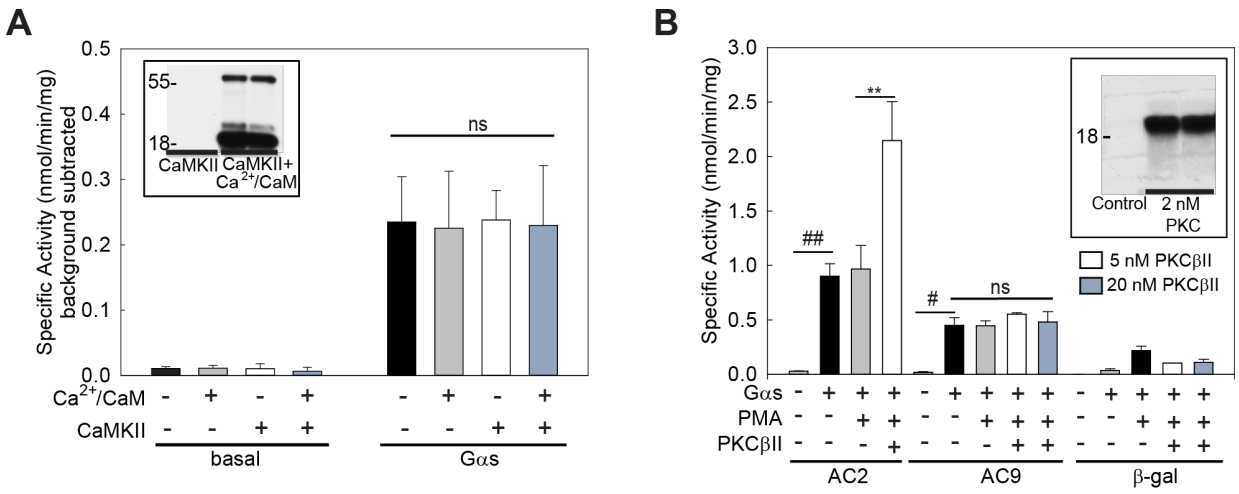

Figure 7. Neither CaMKII nor PKCβII directly regulate AC9. (A) AC9 membranes at basal or stimulated with 100 nM Gαs in the presence or absence of 200 μM Ca^{2+}/ 4 μM calmodulin (Ca^{2+}/CaM), 100 ng CaMKII, or Ca^{2+}/CaM + CaMKII. Inset, ^{32}P labeling of MBP by CaMKII, performed in duplicate. **(B)** AC2, AC9 and β-gal membranes were stimulated with 100 nM Gαs in the presence or absence of 1 μM PMA or PMA plus purified PKCβII. Inset, ^{32}P labeling of MBP by PKCβII, performed in duplicate. Statistics: Paired t test comparing vehicle and kinase groups; n = 3 with experiments performed in duplicate, * or $^{\#}$ $P<0.05$, ** or $^{\#\#}$ $P<0.01$.

3.2.5 AC9 is not inhibited by Gαi in COS-7 cells.

Previous work examining AC9 regulation was performed using whole cells assays in HEK293 cells. However, these cells express a significant amount of endogenous Gi/o-inhibitable AC activity that complicates analysis (Lefkimmiatis et al., 2009). In order to test whether Gαi/o inhibition of AC9 could be observed in other cell lines, cAMP accumulation assays were performed using the cAMP sensor, cADDis (cAMP Difference Detector *in situ*; (Tewson et al., 2016)) in COS-7 cells. Live cell cAMP accumulation was monitored in COS-7 cells transiently transfected with the Gi/o-coupled mu opioid receptor (μOR), in the absence or presence of AC6 or AC9. Cells were treated with isoproterenol plus or minus the μOR agonist, DAMGO (Figure 8A and 8B).

Compared to isoproterenol treatment, the addition of DAMGO did not alter cAMP levels in COS-7 cells expressing the μOR alone, consistent with previous reports that COS-7 cells express largely AC9 (Figure 8C-D) and AC7 (Premont, 1994). As expected, cells expressing AC6 showed a significant decrease in isoproterenol-stimulated cAMP accumulation when treated with DAMGO. DAMGO had no effect on isoproterenol-stimulated cAMP accumulation in cells expressing AC9 (Figure 8A and 8B).

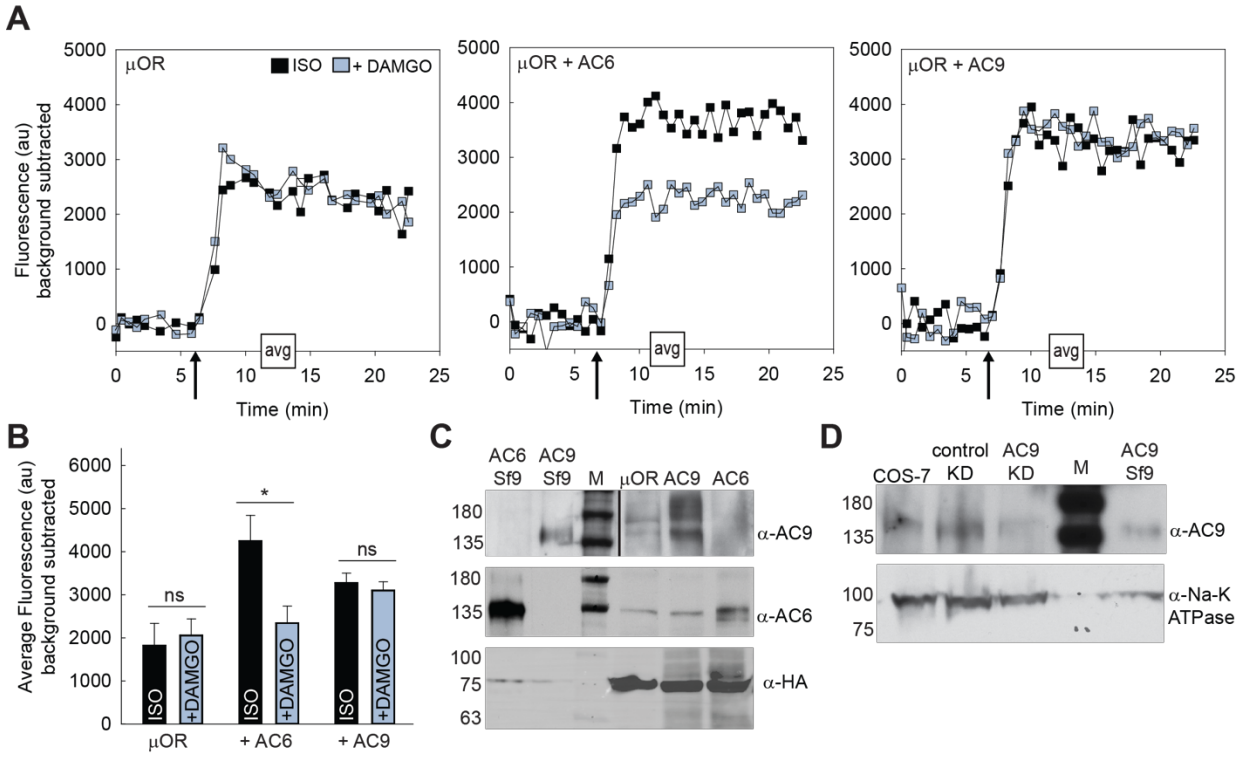

Figure 8. Regulation of endogenous and overexpressed AC9 in COS-7 cells. (A) Representative traces of cells expressing the mu opioid receptor (HA-μOR) +/- AC6 or AC9 treated with 1 μM isoproterenol (ISO; black squares) +/- 10 μM DAMGO. Arrows indicate addition of drugs (ISO/DAMGO). **(B)** Quantitation of individual cell traces. Data were averaged (avg) from 12-14 minute time points of ISO (1 μM) and ISO + 10 μM DAMGO. **(C)** Western blots of COS-7 cell whole cell lysates, confirming expression of endogenous or exogenous AC9 (top: rabbit anti-AC9), AC6 (middle), and HA- μOR (bottom). **(D)** Confirmation of endogenous AC9 protein by western blot of membranes isolated from COS-7 cells, or cells expressing an AC9 siRNA or control siRNA. AC9 Sf9 membranes serve as a positive antibody control. The Na-K ATPase served as a loading

control for COS-7 cells. Statistics: t test of experimental means comparing ISO and ISO + DAMGO; n = 3-5 with experiments performed in duplicate; *P < 0.05.

3.2.6 AC9 expression alters basal cellular levels of cAMP.

To examine endogenous AC9 basal activity, we utilized sh and siRNA knockdown of AC9 in COS-7 cells. Knockdown of AC9 was confirmed by western blot and AC activity assays in membranes isolated from cells expressing a control or AC9 shRNA/siRNA. Knockdown of AC9 resulted in a 39 +/- 3% reduction in AC9 protein (Figure 8D) and a significant reduction in Gαs (39+/-13%) and forskolin (37+/-15%) stimulated AC activity (Figure 9A). Overall changes in low basal AC activity are difficult to detect in membrane preparations, therefore the cAMP GloSensor was utilized to measure basal cAMP levels. The GloSensor plasmid was transiently transfected into COS-7 cells expressing control shRNA, AC9 shRNA, or AC9 overexpression plasmid (OVE). Knockdown of AC9 significantly reduced basal cAMP levels, whereas overexpression of AC9 enhanced basal cAMP levels compared to control shRNA (Figure 9B).

AC9 is generally expressed at low levels in most tissues (Hacker et al., 1998). For example, in heart, AC9 represents less than 3% of total AC activity (Li et al., 2017b). Surprisingly, knockout of AC9 significantly reduced AC activity in spleen membranes by 54 +/- 4% and 47 +/- 9% for Gαs- and forskolin-stimulation, respectively compared to wild type mice (Figure 9C). The considerable contribution of AC9 to total spleen AC activity presented a unique opportunity to examine endogenous AC9 regulation by Gαi. However, wild-type spleen membranes show only modest inhibition by 300 nM Gαi (19 +/- 2%); the degree of Gαi inhibition was not significantly altered in spleen membranes from $AC9^{-/-}$.

To further reveal contributions from AC9, membranes were treated with the P-site inhibitor Ara-A which shows preferential inhibition of AC 1, 3, 4, 5, and 6 versus AC9 (Brand et al., 2013). In membranes treated with 300 nM Ara-A, Gαs-stimulated AC activity in AC9$^{-/-}$ membranes was reduced by 70 +/- 9% compared to wild-type, while forskolin-stimulated activity was only reduced by 41 +/- 7% (Figure 9C). Although differences in basal activity between wild-type and AC9$^{-/-}$ spleen membranes did not reach significance, basal whole cell cAMP accumulation in splenocytes isolated from AC9$^{-/-}$ compared to wild-type was significantly reduced in cells treated with IBMX (Figure 9D). Similarly, cAMP accumulation was also reduced in splenocytes from AC9$^{-/-}$ treated with IBMX and isoproterenol (Figure 9E), supporting a significant contribution from AC9 in basal and Gαs-stimulated AC activity in spleen.

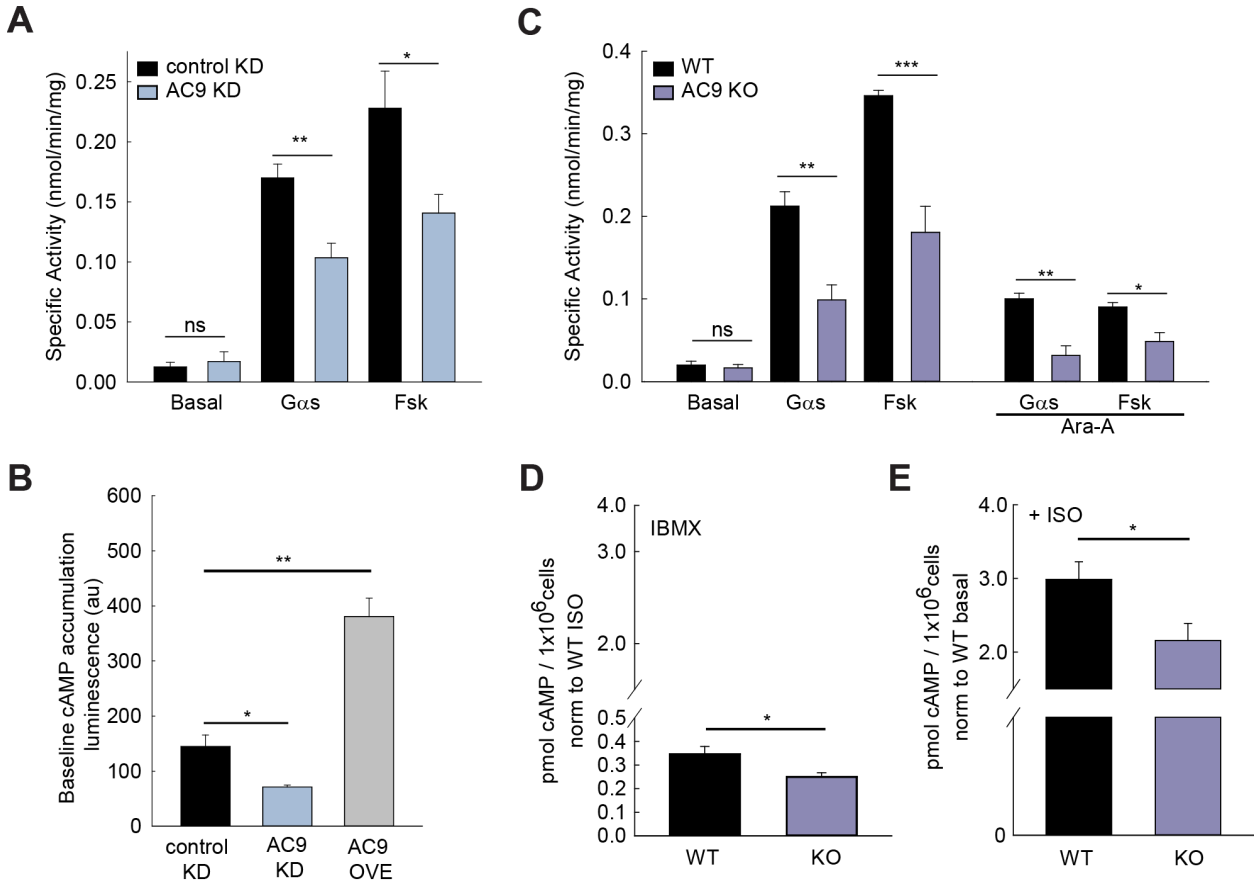

Figure 9. Basal AC activity is dependent on AC9 in COS-7 cells and splenocytes. **(A)** AC assay of membranes from COS-7 cells stably expressing control or AC9 shRNA/siRNA stimulated with 400 nM Gαs or 50 μM forskolin. **(B)** Whole cell basal cAMP accumulation was measured in COS7 cells expressing NS shRNA, AC9 shRNA, or overexpressing (OVE) AC9 using a GloSensor bioluminescent cAMP reporter. Cells were pre-treated with 1 mM IBMX for 10 minutes. **(C)** AC assay of WT and AC9KO spleen membranes stimulated with 400 nM Gαs or 50 μM forskolin in the presence or absence of the P-site inhibitor, Ara-A (300 nM). **(D-E)** Whole cell cAMP accumulation of mouse splenocytes isolated from WT and AC9KO mice treated with 1 mM IBMX +/- 1 μM ISO. Statistics: unpaired t-test of means comparing the indicated groups; n = 3-4 with experiments performed in duplicate; *P < 0.05, **P<0.01, ***P<0.001.

3.2.7 Subsets of splenocyte cell populations are not altered in AC9 knockout

The spleen hosts a variety of cells that are either resident to the organ or recruited there for innate and adaptive immune processes (Bronte and Pittet, 2013). Given our findings that knockout of AC9 decreased of Gαs-stimulated cAMP production in isolated membranes and reduced basal and isoproterenol stimulated cAMP accumulation in splenocytes, we were curious whether AC9 knockout altered the composition of cell population present in the spleen. To test this, isolated splenocytes were profiled with flow cytometry. Alterations in lymphocyte populations were broken down into B cell, T cell (CD4+ or CD8+), natural killer (NK), and natural killer t-cells (NKT) (Figure 10A-H).

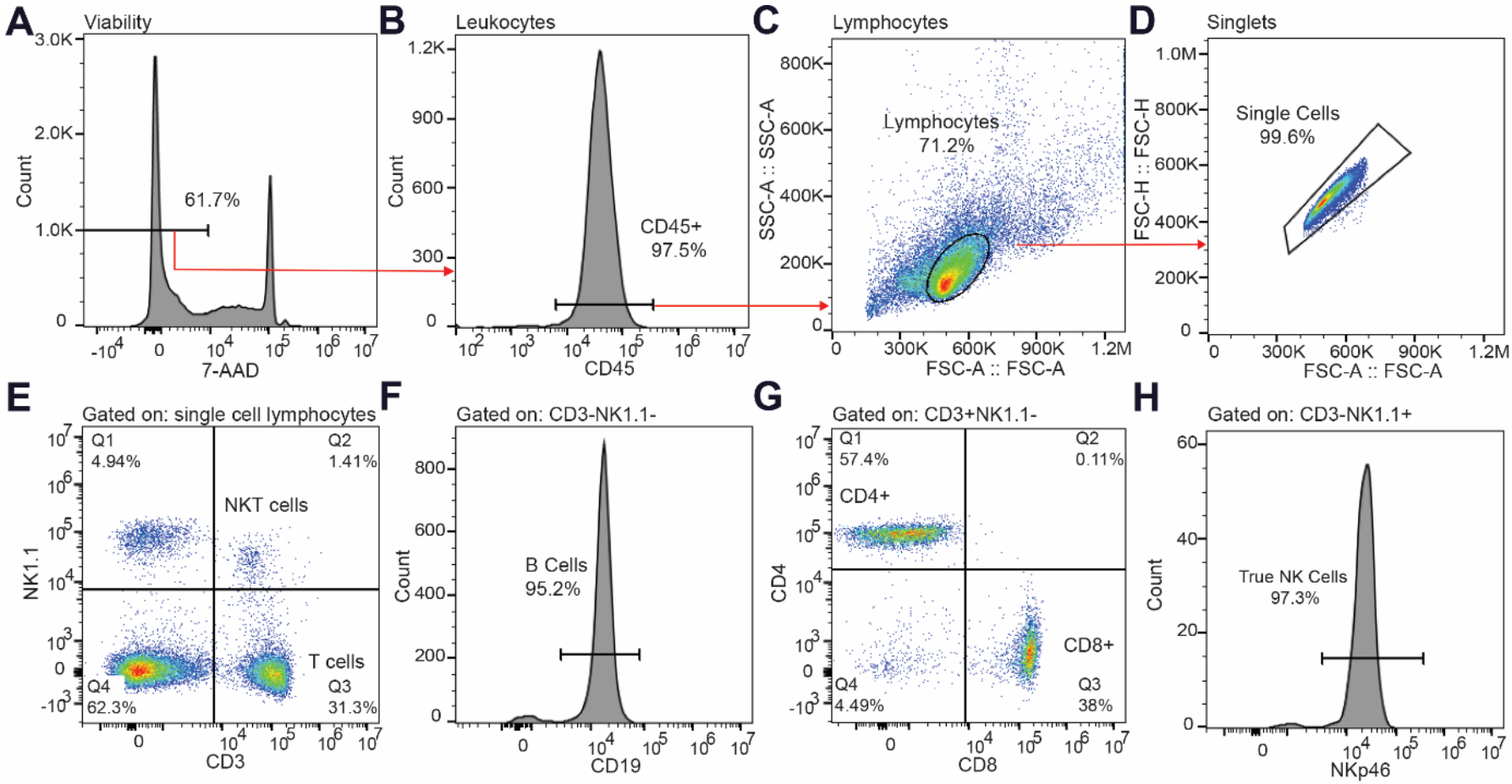
A
Viability
Count
7-AAD
61.7%
B
Leukocytes
Count
CD45
CD45+
97.5%
C
Lymphocytes
SSC-A :: SSC-A
FSC-A :: FSC-A
Lymphocytes
71.2%
D
Singlets
FSC-H :: FSC-H
FSC-A :: FSC-A
Single Cells
99.6%
E
Gated on: single cell lymphocytes
NK1.1
CD3
Q1
4.94%
Q2
1.41%
NKT cells
T cells
Q4
62.3%
Q3
31.3%
F
Gated on: CD3-NK1.1-
Count
CD19
B Cells
95.2%
G
Gated on: CD3+NK1.1-
CD4
CD8
Q1
57.4%
Q2
0.11%
CD4+
CD8+
Q4
4.49%
Q3
38%
H
Gated on: CD3-NK1.1+
Count
NKp46
True NK Cells
97.3%

Figure 10. Gating strategy for profiling of splenocyte cell populations. The gating strategy and markers used for sorting subtypes of lymphocytes are described. **(A)** Histogram of cells stained with the membrane impermeant dye 7-aminoactinomyocyin D (7-ADD) separates viable and dead cells. **(B)** Histogram of CD45+ cells to assess leukocytes from the viable population. **(C)** Leukocytes are subjected to forward scatter area (FSC-A) and side scatter area (SSC-A) to select for lymphocytes. **(D)** Lymphocytes are evaluated with FSC-A and FSC-H (forward scatter height) to ensure the cells are singlets for flow sorting. **(E)** NK1.1 and CD3 are used to sort lymphocytes into subpopulations with natural killer t-cells in quadrant 2 (Q2) and T-cells in quadrant 3 (Q3) **(F)** Histogram of B-cell population selected with CD19 **(G)** CD4 and CD8 antibodies are used to separate subpopulations of T-cells **(H)** Histogram of natural killer t-cells marked with NKp46.

The percentage of viable cells, lymphocytes, and subtypes were compared between WT and AC9$^{-/-}$ splenocytes (Figure 11A-G). No significant difference was detected between subtypes. Although the spread of NK cell percentages historically observed in both WT mice from Mark Ostrom's lab (Queens University) and WT mice from our lab was collapsed in AC9$^{-/-}$ mice. It is possible that with more replicates this might be significant if the current trends hold.

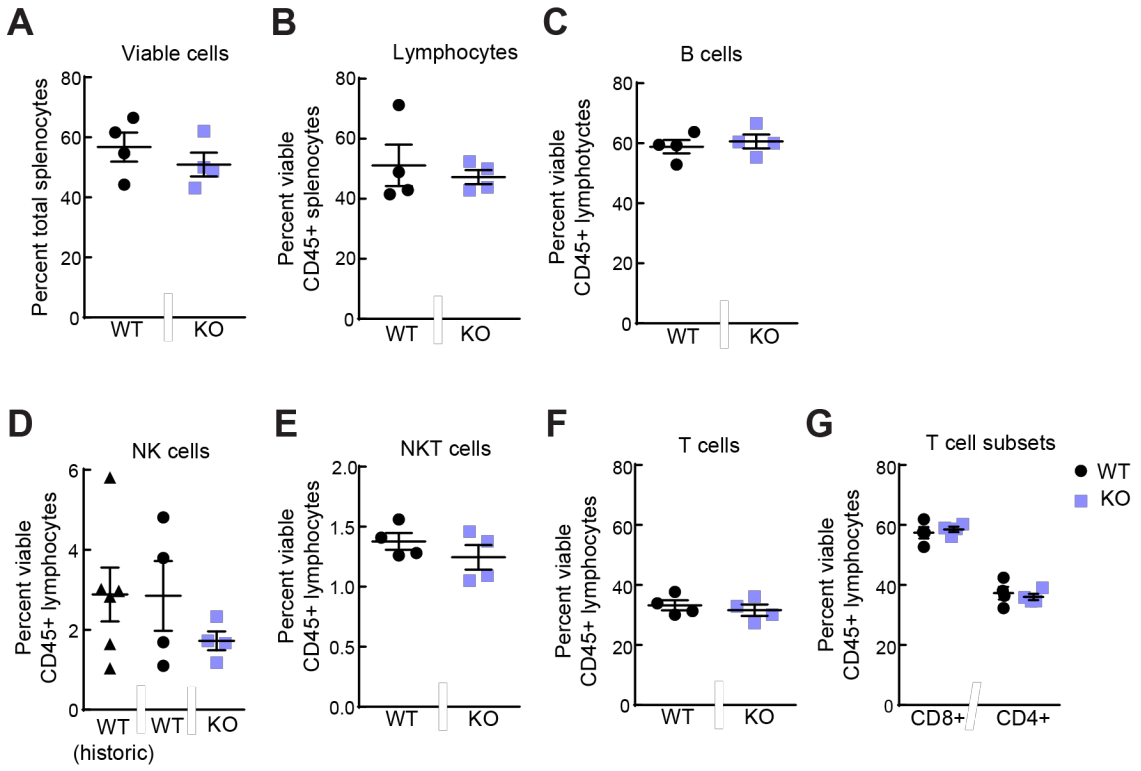

Figure 11. Comparison of splenocyte cell populations isolated from WT and AC9 knockout mice. (A) Percentage of total viable splenocytes. **(B)** Percentage of CD45+ positive splenocytes. **(C-G)** Percentage of cell types based on percentage of viable CD45+ lymphocytes. **(D)** WT (historic) is data gathered for percent NK cells from Mark Ostrom's lab (Queen's University). **(G)** Total T cells from panel F are separated into CD8+ and CD4+ subsets.

3.2.8 AC9 can homo- and heterodimerize.

To explore why some cell lines show inhibition of overexpressed AC9 by Gi/o-coupled receptors, but not others, we examined whether AC9 could form heterodimers with other AC isoforms, particularly AC5 and AC6 which show strong Gαi-inhibition. Homo- and heterodimerization of AC9 was examined in COS-7 cells using Bimolecular Fluorescence Complementation (BiFC) with AC isoforms tagged with N- and C-terminal halves of the fluorescent protein Venus (VN and VC, respectively). No fluorescence was detected upon expression of the individual AC9-VN or AC9-VC constructs. Co-

expression of AC9-VN and AC9-VC resulted in strong reconstitution of fluorescence, indicating significant interaction and homodimerization between AC9 proteins (Ejendal et al., 2013). However, only modest homodimerization was detected for AC5 and no BiFC interaction between similarly tagged AC6 proteins was observed (Figure 12A).

The ability of AC9 to heterodimerize with AC5 and AC6 was also examined by BiFC. AC9 interaction with AC5 and AC6 was observed in a configuration dependent manner, as not all tested configurations resulted in significant interaction (Figure 7B). Significant heterodimerization was detected with AC5/6-VN and AC9-VC constructs. However, no significant fluorescence signals were obtained for AC9-VN and N-terminal tagged AC5. AC5 and AC6 heterodimerization was not observed in any configuration (Figure 12B). AC9-AC5 and AC9-AC6 heterodimerization was confirmed by co-immunoprecipitation in COS-7 cells (Figure 12C-D). Flag-tagged AC9 +/- non-tagged AC5 or AC6 were co-expressed and complexes isolated using Flag-agarose. AC5 and AC6 were both detected in immunoprecipitates of Flag-AC9. Neither AC5 nor AC6 were pulled-down in the absence of Flag-AC9 expression. Immunoprecipitations of Flag-AC5 and YFP-AC6 were used as positive controls (Figure 12C and 12D, respectively).

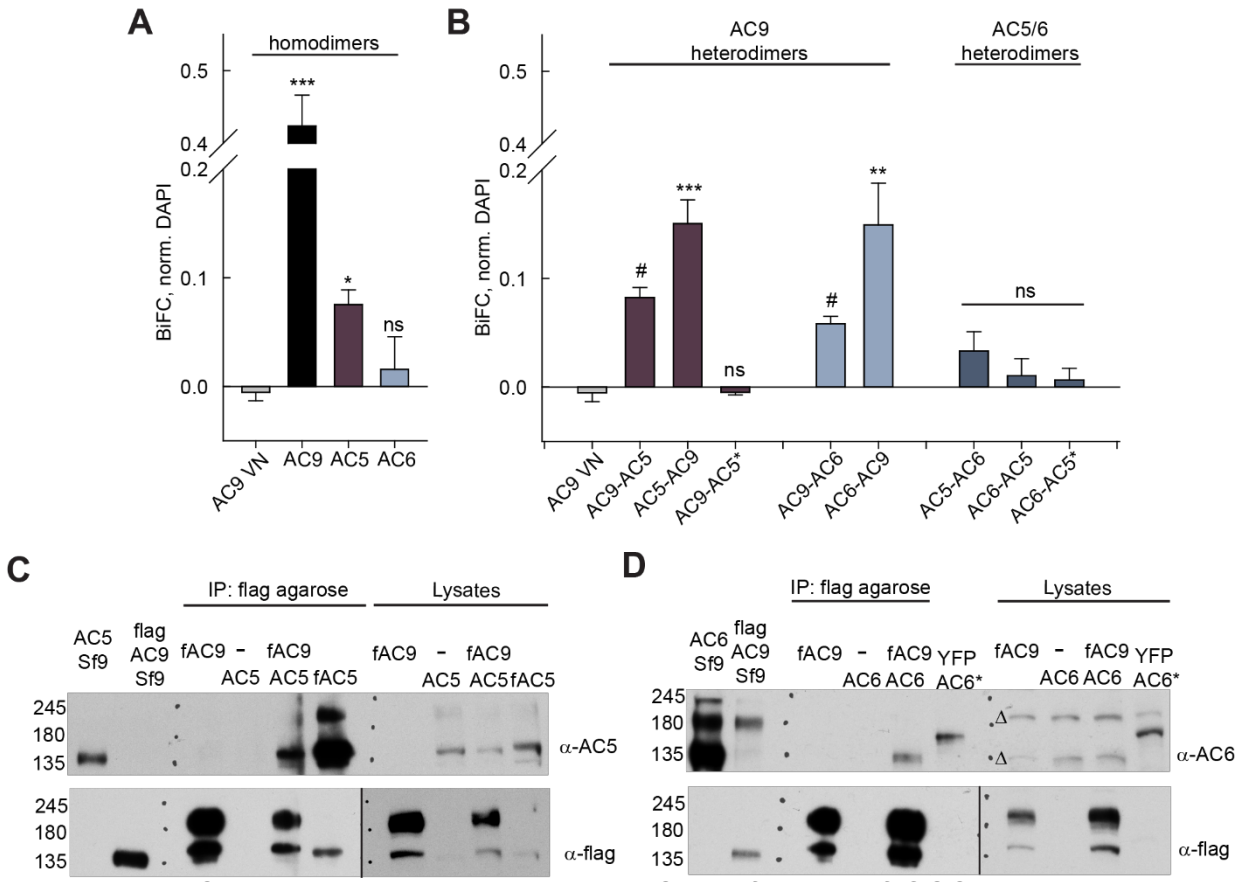

Figure 12. AC9 homo- and heterodimers. Quantification of COS7 cells expressing BiFC constructs for AC9, AC5, and AC6. The N-terminus (VN) or C-terminus (VC) of Venus is fused to the C-terminus of each AC isoform, except where noted. **(A)** Homodimers express both AC-VN and AC-VC. **(B)** Heterodimer formation utilized AC-VN (first one listed) with AC-VC from a second isoform. For example, AC5-AC9 corresponds to co-transfection of AC5-VN and AC9-VC. AC5* is N-terminally tagged. **(C-D)** Cells transiently transfected with **(C)** Flag AC9 (fAC9) +/- AC5 or **(D)** fAC9 +/- AC6 were subjected to immunoprecipitation with Flag agarose and western blotted for Flag, AC5, or AC6. As positive controls, Flag-AC5 (fAC5) and YFP-AC6 were immunoprecipitated with Flag-agarose or anti-GFP. ΔIndicates non-specific band. Statistics: Kruskal-Wallis One Way Analysis of Variance on Ranks followed by Dunn's Method Test comparing AC9 VN to each group indicated; n = 3-5 with experiments performed in duplicate; *P < 0.05, **P<0.01, ***P<0.001. #, P<0.001 for AC9/AC5 and P=0.01 for AC9/AC6 by t-test compared to AC9VN control; although not significance by ANOVA.

3.3 Summary

I have further investigated the mechanism of AC9 regulation by G-proteins and kinases, concluding that AC9 is directly regulated by Gαs and conditionally activated by forskolin; other modes of proposed regulation occur either indirectly or possibly require additional scaffolding proteins to facilitate regulation. I also show that AC9 contributes to basal cAMP production because knockdown or genetic elimination of endogenous AC9 reduces basal AC activity in COS-7 cells and splenocytes, respectively. Importantly, while AC9 is not directly inhibited by Gαi/o, it can heterodimerize with Gαi/o-regulated isoforms, AC5 and AC6.

Chapter 4

Contributions of AC9 to cardiac function

Note: Figures and text are partially reprinted from Li, Y., T. A. Baldwin, Y. Wang, J. Subramaniam, A. G. Carbajal, C. S. Brand, S. R. Cunha, and C. W. Dessauer. 2017. Loss of type 9 adenylyl cyclase triggers reduced phosphorylation of Hsp20 and diastolic dysfunction. *Scientific Reports* 7: 5522.

4.1 Introduction

We have previously shown that AC9, an understudied largely forskolin-insensitive AC isoform, is expressed in adult mouse cardiomyocytes and forms complexes in heart with Yotiao, an A-kinase anchoring protein (AKAP) (Li et al., 2012; Piggott et al., 2008). AKAPs are important scaffolds that direct the localization, regulation, and integration of cAMP-dependent PKA signaling with downstream targets. Dysregulation of AKAP organized complexes can lead to cardiac remodeling and development of heart failure (Efendiev and Dessauer, 2011; Scott et al., 2013). For example, mAKAP (AKAP6) scaffolds AC5 to regulate cardiac stress responses while AKAP79 (AKAP5) scaffolds AC5/6 and L-type calcium channels (Dessauer, 2009; Efendiev and Dessauer, 2011). Association of AC with AKAP complexes serves to sensitize bound PKA substrates to the effects of cAMP, by up to two orders of magnitude (Efendiev et al., 2013; Li et al., 2012).

In heart, AC9 is the only AC isoform to associate with Yotiao and the Yotiao-I_{Ks} channel complex (Li et al., 2012). The I_{Ks} channel results from the co-assembly of two subunits KCNQ1 and KCNE1. PKA phosphorylation of the anchored KCNQ1 channel subunit increases I_{Ks} current and shortens the action potential duration to allow sufficient diastolic intervals upon increased heart rate. Mutations in either KCNQ1 or Yotiao that disrupt their interaction give rise to Long-QT syndrome (LQT1, LQT11; a potentially lethal heritable arrhythmia syndrome) (Ackerman and Mohler, 2010). AC9 association with Yotiao-KCNQ1 facilitates KCNQ1 phosphorylation by PKA (Li et al., 2012). In humans, we suggest that AC9 is important for repolarization of heart. However, since a functional I_{Ks} is largely absent in adult mice, additional potential roles for AC9 in heart are unknown.

4.2 Results

4.2.1 AC9 and Yotiao co-localize in cardiomyocytes.

In cardiomyocytes KCNQ1 is detectable at intercalated disks, t-tubules, and sarcolemma (Nicolas et al., 2008). AC9-Yotiao-KCNQ1 complexes have been isolated from overexpression and endogenous systems by immunoprecipitation (Li et al., 2012). To examine where AC9-Yotiao co-localize Flag-AC9-D399A (Flag-AC9d) and cmyc-Yotiao I have co-expressed these proteins in neonatal rat cardiomyocytes by adenoviral infection (Figure 13). Distinctively, AC9 and Yotiao co-localize at the sarcolemma. AC9 and Yotiao also appear diffusely within the cardiomyocyte, with occasional co-localization. It is possible that AC9 and Yotiao also localize to t-tubules and but these structures are not present in neonatal cardiomyocytes (Delcarpio et al., 1989).

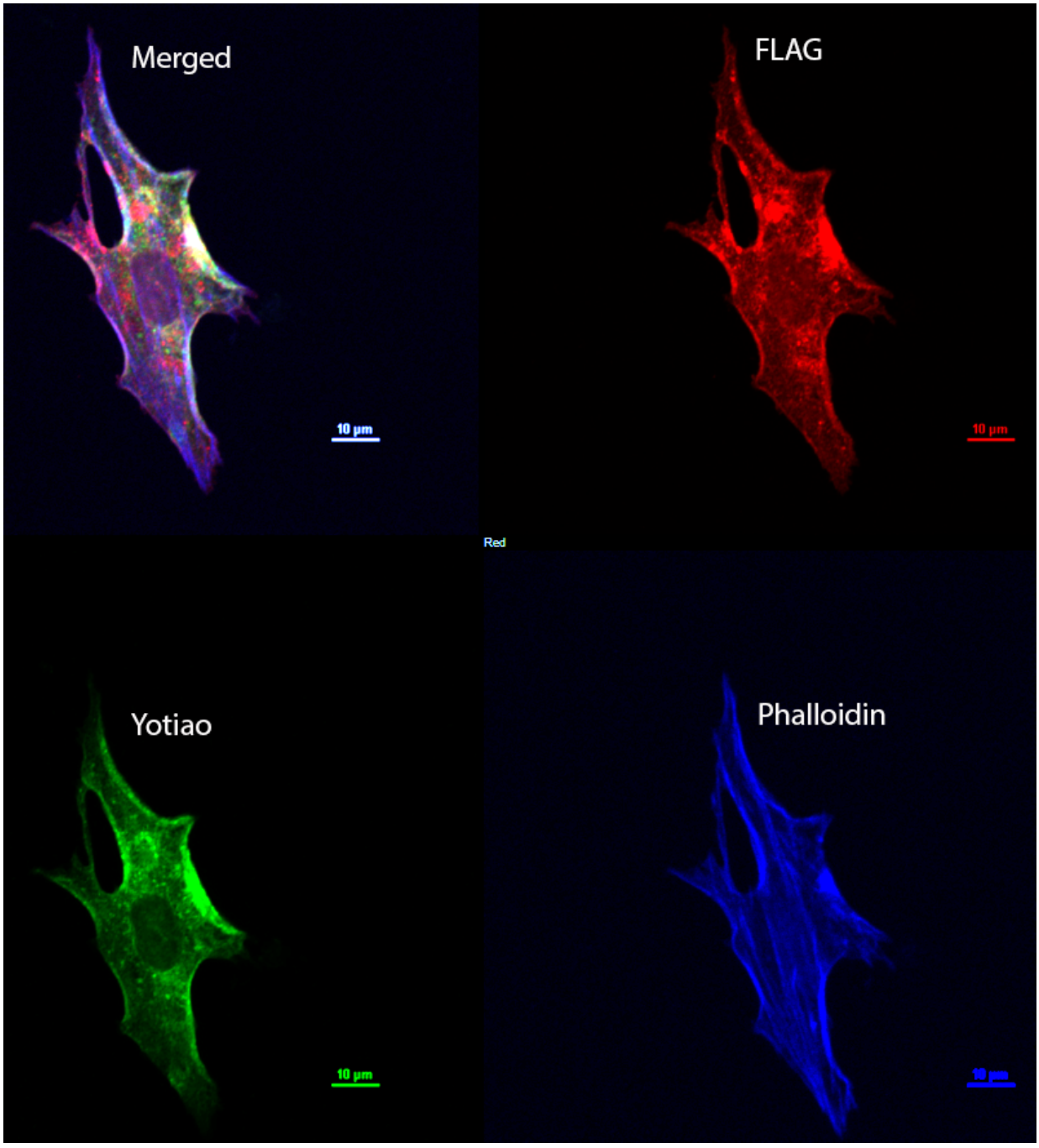

Figure 13. Colocalization of AC9 and Yotiao in rat neonatal cardiomyocytes.
RNCMs were infected with catalytically inactive Flag AC9-D399A (FLAG AC9d) and cmyc-Yotiao adenoviruses for 60 hours. Cells were stained with FLAG (red), Yotiao (green), and phalloidin (blue). The composite image is shown in the top left corner followed by separate channel images. The scale bars in each image represent 10 μM.

4.2.2 Genetic ablation of AC9 results in preweaning subviability.

AC9 is ubiquitously expressed but physiological roles for AC9 have been largely ignored. To investigate the *in vivo* function of AC9, we utilized a gene-trap strain of AC9 obtained from the Mutant Mouse Regional Resource Center, a NIH strain repository. The AC9$^{-/-}$ strain was created by Lexicon, Inc. using a retroviral insertion between exon 1 and 2 (Figure 14A). The mouse genotypes were determined by PCR assay (Figure 14B). AC9 protein is not detectable by western blotting in heart tissue homogenates and available antibodies against AC9 do not work well for immunoprecipitation. Therefore, to confirm the lack of AC9 protein expression, we probed the Yotiao-AC9 complex which forms a tight complex in mouse and guinea pig heart (Li et al., 2012). AC9 protein is detectable in immunoprecipitates of Yotiao from wild type (WT) hearts but not AC9$^{-/-}$ (Figure 14C). Multiple isoforms of AC were expressed in mouse adult cardiomyocytes, including AC 3, 4, 5, 6, and 9 (Li et al., 2012); quantitative PCR of these AC isoforms from WT and AC9$^{-/-}$ shows a 35 +/- 9% decrease in AC3 RNA and complete loss of AC9 but no significant difference in other AC isoforms (Figure 14D).

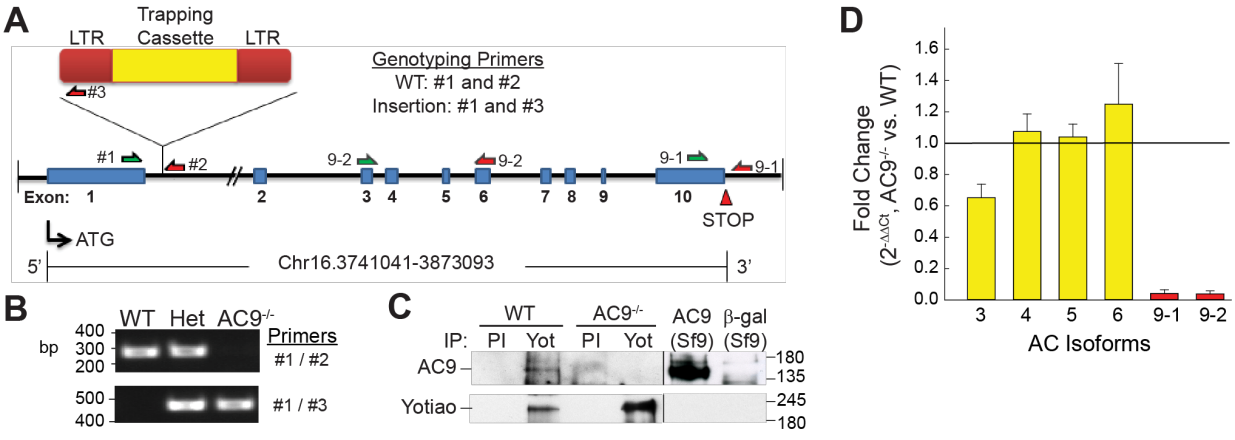

Figure 14. Design and verification of the AC9$^{-/-}$ mouse model. (A) Schematic of AC9 gene-trap strategy and genotyping primers. Intron distances are not drawn to scale. **(B)**

PCR analysis of genotyping: lanes 1, 2, and 3 represent wild-type (WT), $AC9^{+/-}$ (Het) and $AC9^{-/-}$, respectively. **(C)** AC9 protein levels were detected by immunoprecipitation of pre-immune (PI) or Yotiao complexes from WT and AC9 KO heart extracts followed by western blotting (WB) with anti-AC9 antibody. AC9 protein is not detectable in total heart extracts by WB (n=5). **(D)** Real time PCR of cardiac AC isoforms in $AC9^{-/-}$ heart, normalized to WT expression levels (n=3; mice 1 month of age). Loss of AC9 mRNA was confirmed with primer sets 9-1 and 9-2. Experiments performed by Yan Wang and Yong Li, PhD.

Unpublished observations by FA Antoni suggested that conventional targeted deletion of AC9 results in early embryonic lethality in mice (Antoni, 2006). Although viable, we noted abnormal genotype frequencies for heterozygous mating pairs after backcrossing to C57BL/6J (18% WT, 75% Het, 7% KO; n=68, P=0.002). The preweaning subviable homozygous phenotype with incomplete penetrance is also reported for another $Adcy9^{-/-}$ strain (Adcy9tm1b(EUCOMM)Wtsi) created as part of the International Knockout Mouse Consortium (International Mouse Knockout et al., 2007).

4.2.3 Deletion of AC9 results in loss of Yotiao-associated AC but insignificant changes in total AC activity.

AC9 mRNA and/or protein has previously been detected in both cardiac fibroblasts and myocytes (Li et al., 2012; Ostrom et al., 2003), however the degree to which AC9 contributes to total AC activity is unknown. Initial measurements of basal and Gαs-stimulated AC activity showed no difference between cardiac membranes isolated from WT versus $AC9^{-/-}$ mice (Figure 15A). To potentially unmask AC activity stemming from AC9, we used a P-site inhibitor that displays >100 fold selectivity for AC5/6 over AC9 (Figure 15B) (Brand et al., 2013). No significant difference in total AC activity is observed, even at SQ 22,536 concentrations that inhibit 70-90% of AC5/6, but only 20-30% of AC9 (30-100 μM). From this data, we estimate that AC9 represents less than

3% of total heart AC activity. In order to detect AC9 activity, we examined its association with specific AKAP complexes (Li et al., 2012; Piggott et al., 2008). Heart extracts subjected to immunoprecipitation of Yotiao show significant AC activity that is brought down with Yotiao in the immunoprecipitate; associated activity is lost in AC9$^{-/-}$ (Figure 15C). This is consistent with our previous findings that AC9 is the only AC isoform associated with Yotiao in heart. Although AC9 can also bind AKAP79/150 (Efendiev et al., 2010), it does not significantly contribute to the AC activity associated with AKAP79/150 in heart (Figure 15D).

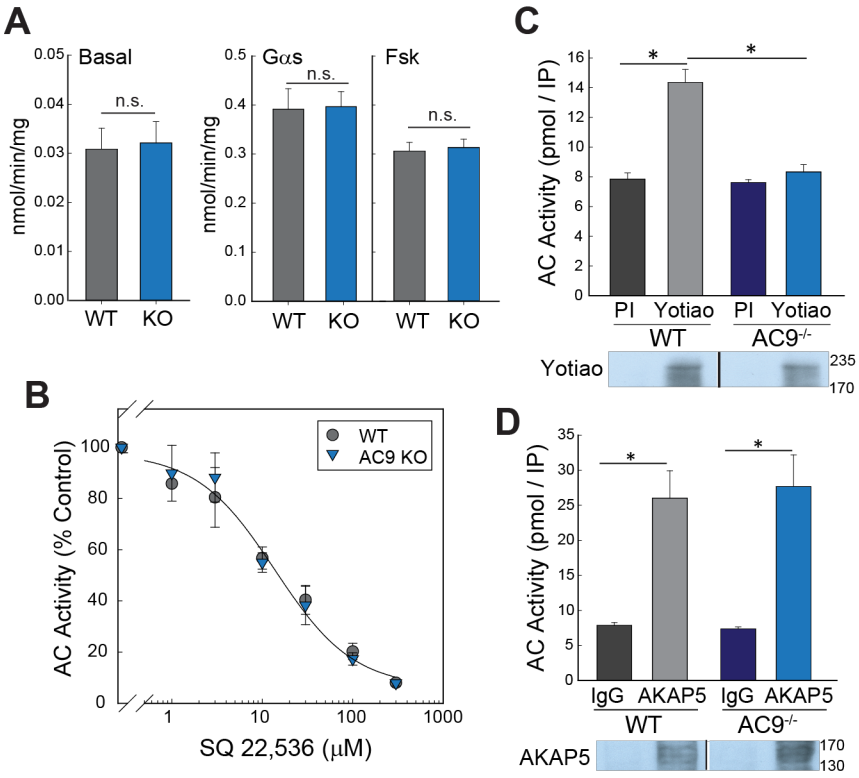

Figure 15. AC9 activity and AKAP association in heart. (**A, B)** Membranes were prepared from 6 week WT versus AC9$^{-/-}$ heart. **(A)** AC activity was measured under basal conditions and upon stimulation with 300 nM Gαs or 50 μM forskolin (n=4, performed in duplicate or triplicate). **(B)** AC activity was measured in the presence of increasing concentrations of SQ22,536 in the presence of 300 nM Gαs (n = 3, performed in duplicate). **(C, D)** Heart extracts from WT or AC9$^{-/-}$ mice were subjected to immunoprecipitation (IP) with pre-immune (control) or anti-Yotiao **(C)** and control IgG or

anti-AKAP5 **(D)**. AKAP-associated AC activity was stimulated with 300 nM Gαs and measured (n=3-4). Data are shown as mean +/- SD. A portion of the IP's from C and D were subjected to Western blot analysis for the appropriate AKAP. Note, preliminary experiments for A and B were performed by Cameron S. Brand and completed by myself. Experiments for Figure C and D were performed by Yong Li, PhD.

4.2.4 Reduced heart rate in the absence of AC9.

Functional analysis of WT and AC9$^{-/-}$ mice revealed a significant reduction of heart rate under isoflurane in both male and female mice for the two age groups examined (Table 2). Body weight was unchanged in male (21.1 +/- 0.2 versus 21.6 +/- 0.3, 6 months) and female mice (15.3 +/- 0.2 versus 15.6 +/- 0.2, 4 months).

Table 2. Deletion of AC9 gives rise to bradycardia.

Sex	Age (mo)	Average Heart Rate (bpm)		p-value
		WT	AC9$^{-/-}$	
Male/Female	1-2	433 +/- 5 (n=13/6)	409 +/- 7 (n=12/6)	0.008
Male	5-7	445 +/- 6 (n=10)	400 +/- 7 (n=11)	0.0002

No structural abnormalities were noted and myocardial performance index (0.9 +/- 0.1 vs 0.9 +/- 0.1), ejection fraction (53 +/- 3 vs 51 +/- 4) and percent fractional shortening (27 +/- 2 vs 26 +/- 3) were all unchanged, as assessed by M mode imaging of mice 3-7 months (Table 3).

Table 3. Cardiac parameters for WT and AC9$^{-/-}$ mice.

Parameter[#]	WT	AC9$^{-/-}$	P value
Mitral flow doppler			
Peak velocity, E' (mm/s)	20 +/- 1	15 +/- 1	0.004
Peak velocity, A' (mm/s)	16.5 +/- 0.6	16.3 +/- 0.5	n.s.
Aortic ejection time (AET, ms)	51 +/- 2	52 +/- 1	n.s.
Isovolumic Relaxation Time (ms)	24 +/- 2	27 +/- 2	n.s.
Isovolumic Contraction Time (ms)	20 +/- 1	20 +/- 1	n.s.
Mitral valve A (cm/s)	41 +/- 2	43 +/- 2	n.s.
Mitral valve E (cm/s)	64 +/- 2	54 +/- 2	0.005
A'/E'	0.88 +/- 0.05	1.2 +/- 0.1	0.04
MV E/A	1.57 +/- 0.08	1.27 +/- 0.07	0.01
MV E/E'	33 +/- 1	38 +/- 3	n.s., 0.1
Myocardial Performance Index (MPI)	0.9 +/- 0.1	0.9 +/- 0.1	n.s.
M-mode Echocardiography			
LV anterior wall, diastole (mm)	0.69 +/- 0.06	0.72 +/- 0.05	n.s.
LV anterior wall, systole (mm)	0.87 +/- 0.08	1.01 +/- 0.08	n.s.
LV internal diastolic diameter (mm)	3.6 +/- 0.1	3.6 +/- 0.1	n.s.
LV internal systolic diameter (mm)	2.6 +/- 0.1	2.7 +/- 0.1	n.s.
LV posterior diastolic wall (mm)	0.76 +/- 0.08	0.69 +/- 0.04	n.s.
LV posterior systolic wall (mm)	0.93 +/- 0.07	1.13 +/- 0.07	n.s., 0.06
EF (%)	53 +/- 3	50 +/- 5	n.s.
FS (%)	27 +/- 2	26 +/- 3	n.s.
LV Mass, corrected (mg)	71 +/- 13	70 +/- 7	n.s.
End diastolic volume (μL)	55 +/- 4	57 +/- 4	n.s.
End diastolic Volume (μL)	26 +/- 3	28 +/- 3	n.s.

[#], Mean +/- SE is given for male animals 3-7 months.

4.2.5 Global PKA phosphorylation is unaltered but Hsp20 phosphorylation is decreased in AC9$^{-/-}$.

In order to determine if AC9 deletion alters cAMP signaling, we used intraperitoneal injection of saline or isoproterenol in WT and AC9$^{-/-}$ mice to evaluate changes in phosphorylation of PKA targets. Global changes in PKA phosphorylation at baseline or after isoproterenol injection are not detected (Figure 16A), suggesting that AC9 does not significantly alter sympathetic responses. However, we detect a large

decrease in the basal phosphorylation state of Hsp20 in the absence of beta-adrenergic stimulation (Figure 16B).

To determine if AC9 is present in Hsp20-containing complexes, we used a proximity ligation assay (PLA) in HEK293 cells (Figure 16C). The high selectivity of PLA relies on double recognition of a protein complex by two oligonucleotide-conjugated secondary antibodies. Oligonucleotides in close proximity allows for rolling circle amplification that can be visualized (Figure 16C, red dots). YFP-AC9 and Hsp20 display a significant signal by PLA as compared to YFP alone. Gβγ binds to the N-terminus of AC9 and serves as a positive control (Brand et al., 2015).

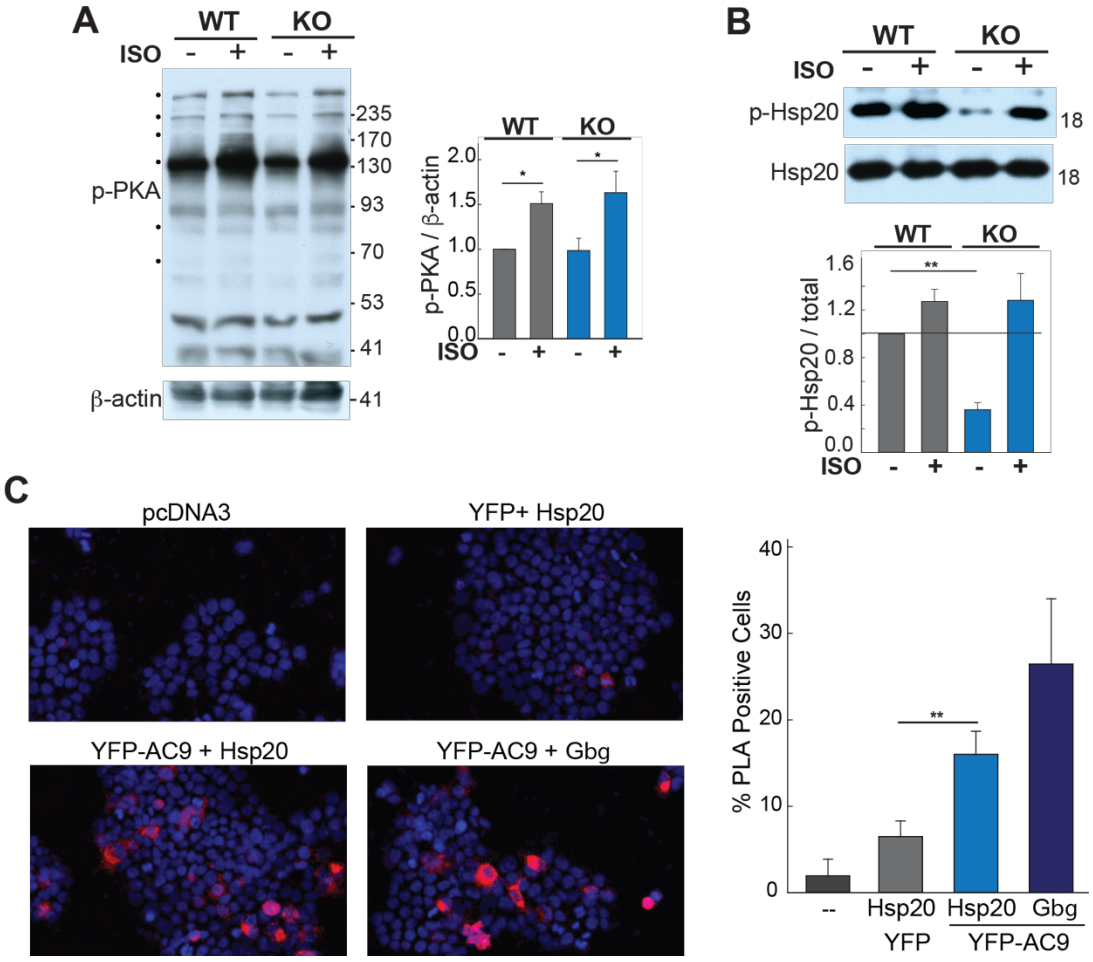

Figure 16. Basal PKA phosphorylation of Hsp20 is reduced in AC9$^{-/-}$; AC9 interacts with Hsp20. Equal protein supernatants were subjected to WB analysis with **(A)** anti-p-

PKA substrate, **(B)** anti-p-Hsp20. Quantitation of phospho-PKA was normalized to beta-actin levels (A) while the corresponding total protein was quantitated by WB (n=5-7) and the ratio of phosphoprotein to total was quantitated for p-Hsp20 (B) . Graphs for quantitation of the ratio of phosphorylated to non-phosphorylated protein are shown to the right for each panel. **, P<0.01 t-test on raw intensity values. **(C)** Proximity ligation assay for Hsp20 and Flag-tagged AC9. HEK293 cells were transfected with the indicated plasmids. Representative images are shown. PLA signals were quantified by high content microscopy (positive cells defined as 4 signals or "dots" per cell; ~2000 cells imaged per condition). *, P<0.05 t-test, n=3. Data for panels A and B were performed by Yong Li, PhD. Panel C was produced in collaboration with Anibal Garza Carbajal, PhD.

AC9 binding to an Hsp20 complex should regulate local cAMP production and subsequent Hsp20 phosphorylation. If this is the case, displacing AC9 with a catalytically inactive enzyme would lead to reduced local cAMP and Hsp20 phosphorylation. Mutation of D399 to alanine deletes a key metal-binding residue in the active site of AC9, reducing Gαs-stimulated activity by >90% (Figure 17C). Adenoviral expression of AC9d in rat neonatal cardiomyocytes significantly decreased isoproterenol-stimulation of Hsp20 (by 77 +/- 6%), as compared to non-infected or GFP-infected cells (Figure 17A). This is consistent with decreased Hsp20 phosphorylation and Hsp20-associated AC activity in $AC9^{-/-}$ heart. Hsp20 is a known PKA target (Beall et al., 1999; Fan et al., 2005a) and inhibition of PKA activity by H89 blocks isoproterenol-stimulated phosphorylation of Hsp20 in rat neonatal cardiomyocytes (Figure 17B). Loss of AC9 activity in AC9d is confirmed by AC activity assay in Sf9 membranes expressing WT or AC9d mutant (Figure 17C).

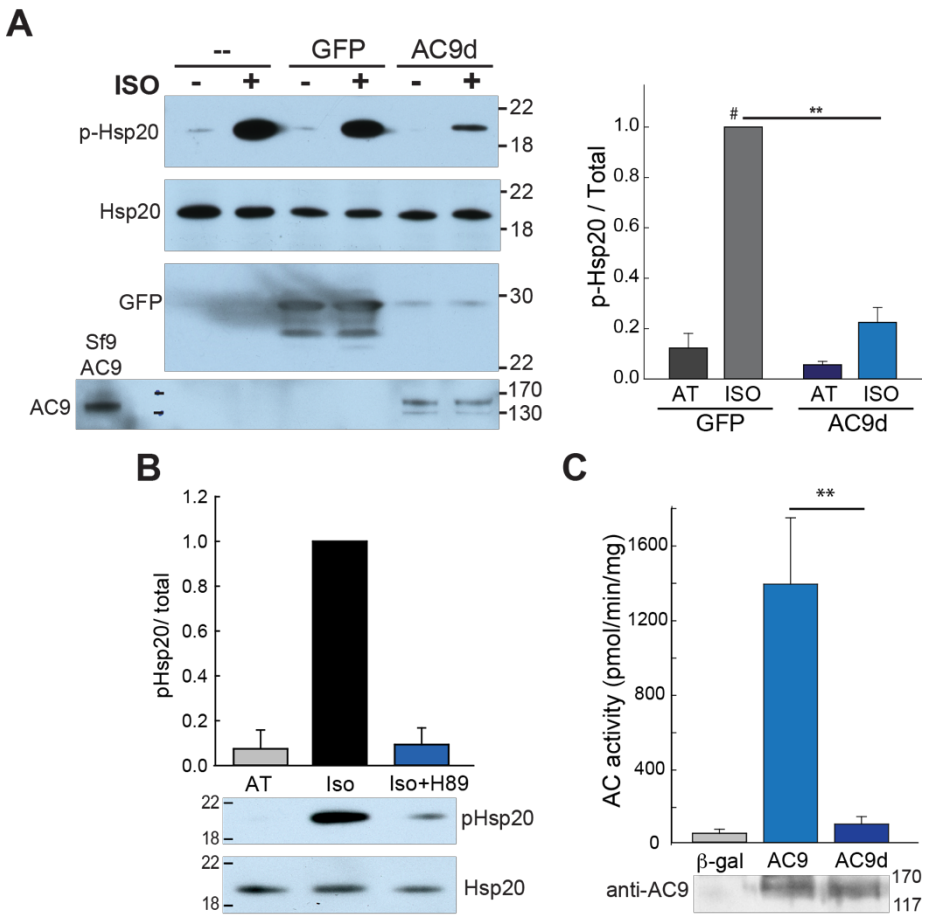

Figure 17. Expression of catalytically inactive AC9 decreases isoproterenol-stimulated phosphorylation of Hsp20 in rat neonatal cardiac myocytes.

(A) RNCMs were infected with GFP control or catalytically inactive AC9-D399A (AC9d) adenoviruses for 50 hr. Cells were treated with vehicle (AT) or isoproterenol (1 μM) for 5 min prior to cell lysis. The ratio of p-Hsp20 to total Hsp20 was quantitated by WB. #,** P<0.01 t-test, n=4. **(B)** Inhibition of PKA abolishes isoproterenol stimulated phosphorylation of Hsp20. Rat neonatal cardiomyocytes were pretreated in the absence or presence of 10 M of the PKA inhibitor H89 for 10 min followed by vehicle (AT) or isoproterenol (1 M) for 5 min. Cells were lysed and subjected to WB analysis for phosphorylation of Hsp20 (n=3). **(C)** Mutation of D399A in AC9 has dramatically reduced catalytic activity. Membranes were prepared from Sf9 cells expressing gal, AC9, or AC9D399A. AC activity was measured upon stimulation with 300 nM GTPSGs (n=3). WB of membrane proteins is shown.

4.2.6 Protective role for AC9 against diastolic dysfunction.

The decrease in baseline Hsp20 phosphorylation in AC9$^{-/-}$ suggests a potential loss of the cardioprotective effects of PKA phosphorylated Hsp20 (Edwards et al., 2012b; Nicolaou et al., 2008; Qian et al., 2009). Therefore, we measured overall left ventricular function using pulsed-wave Doppler echocardiography of early (E) and late (A) blood flow velocities through the mitral valve combined with tissue Doppler imaging of the mitral valve annulus (E' and A' velocity). Of the four phases of diastolic relaxation, isovolumetric relaxation, early ventricular filling, diastasis, and atrial contraction, the early filling phase (E wave) appears significantly reduced in AC9$^{-/-}$ mice (Table 3 and Figure 18). This was confirmed by tissue Doppler, measuring the early diastolic mitral annular velocity (E') which is preload independent. Trends towards increased filling pressures (E/e') are observed but never reach significance.

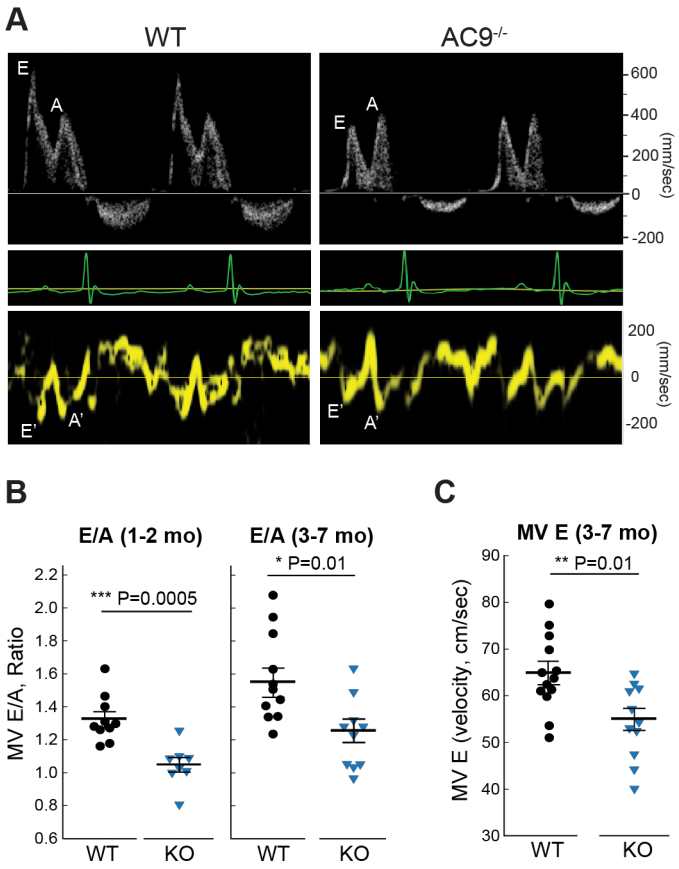

Figure 18. Cardiac parameters for WT and AC9$^{-/-}$ mice. (A) Pulsed-wave and tissue Doppler recordings for female WT and AC9$^{-/-}$ littermates (3 month) showing the relative amplitudes of the early ventricular filling (E wave) and the late filling caused by atrial contraction (A wave) (ECGs are shown below for each animal). **(B)** Quantitation of E/A ratio at 1-2 (n=10 WT and 8 AC9$^{-/-}$; males, P=0.0005) or 3-7 months (n=11 WT and 11 AC9$^{-/-}$; males and females, P=0.005). **(C)** Quantitation of mitral valve E wave at 3-7 months (n=13 WT and 11 AC9$^{-/-}$, P=0.005). Mean +/- SE.

4.3 Summary

AC9 is the most divergent in sequence of the nine mammalian transmembrane AC isoforms, is relatively insensitive to forskolin activation and remains the least characterized. It was originally cloned as a calcineurin-inhibitable AC isoform (Paterson et al., 1995), although it is unclear if calcineurin and other reported cellular regulators have direct or indirect mechanisms of action (Dessauer et al., 2017). AC9 mRNA is ubiquitously expressed, particularly in the hippocampus (Antoni et al., 1998), and the knockout of AC9 was thought to be embryonic lethal (Antoni, 2006). Therefore, physiological roles for AC9 have been largely ignored. Despite a preweaning subviability, AC9$^{-/-}$ mice show no obvious size or structural abnormalities. However, AC9 expression is important for human neutrophil chemotaxis (Liu et al., 2010), while ADCY9 gene polymorphisms are linked to asthma, mood disorders, and body weight (Berndt et al., 2013; Small et al., 2003; Toyota et al., 2002). In heart, AC9 mRNA and/or protein has been detected in both cardiomyocytes and fibroblasts, although, our estimates using P-site inhibitors suggest that AC9 represents less than 3% of total heart AC activity. Despite the low levels of AC9, Yotiao-associated AC activity is abolished in the knockout while AKAP79-associated AC activity is unchanged. Although AKAP79 can bind to AC9 in cell culture experiments, AKAP79 scaffolds the highly expressed AC5/6 isoforms in

heart (Efendiev et al., 2010; Nichols et al., 2010). The association with Yotiao is consistent with a role for AC9 in regulation of I_{Ks} channels and potentially long QT syndrome, for which mutations of I_{Ks} and Yotiao are well known (Ackerman and Mohler, 2010).

Chapter 5

Adenylyl cyclase and Popdc interactions

Note: This section details preliminary studies examining AC-Popdc interactions. Most results have been replicated two or more times. Any results replicated once are indicated in the figure legend.

5.1 Introduction

The bradycardia phenotype observed in AC9$^{-/-}$ mice suggests a role for AC9 in the sinoatrial node. Yotiao-AC9 complexes are detectable in the sinoatrial node, the left ventricle, and the right atria by immunoprecipitation assays evaluating AC associated activity with Yotiao (Li et al., 2017b). In an effort to examine the molecular mechanism underlying AC9 involvement in heart rate control we examine the interaction of AC9 with a novel cAMP effector involved in heart rate control, Popeye domain containing (Popdc) proteins.

5.1.1 A novel cAMP effector: Popdc

Protein kinase A (PKA) is the most prominent effector of cAMP; others are briefly discussed in the introduction. Popdc proteins represent a novel class of cAMP effectors. Although the POPDC genes (Andree et al., 2000; Reese et al., 1999) were discovered shortly after EPAC (de Rooji et al., 1998; Kawasaki et al., 1998), there were only recently appreciated as cAMP effectors (Froese et al., 2012; Schindler et al., 2016b). The Popdc family consists of Popdc1 (Bves (blood vessel epicardial substrate), Popdc2, and Popdc3. Popdc1-3 are highly conserved in vertebrates while most invertebrates express two genes; Drosophila uniquely have only one Popdc gene (Brand et al., 2014). The Popdc proteins are highly expressed in skeletal muscle and the heart (Andree et al., 2000), and in numerous other tissues: lung, gastrointestinal tract, bladder, uterus, epithelial cells, and neurons (Andree et al., 2000; Froese and Brand, 2008; Smith and Bader, 2006). Popdc1/2 are highly expressed in the sinoatrial and atrioventricular nodes (Froese et al., 2012). In cardiac myocytes and tissue, Popdc localizes to the sarcolemma, in addition to other structures, including intercalated discs, costameres, t-

tubules, and caveole (Alcalay et al., 2013). Popdc1 has also been reported to localize at the nuclear envelope (Korfali et al., 2012) and nucleoplasm (Brand, 2018).

Structurally, Popdc proteins consist of three trans-membrane spans, an extracellular N-terminal domain with two N-glycosylation sites (Knight et al., 2003), and a cytosolic C-terminal domain which contains the Popeye domain responsible for binding cAMP (Figure 19A/B) (Andree et al., 2002; Knight et al., 2003). Popdc1 can homodimerize (Knight et al., 2003; Vasavada et al., 2004) though interactions in the c-terminus of the Popeye domain (Kawaguchi et al., 2008) and other unidentified sites (Russ et al., 2011).

The Popeye domain is highly conserved among the Popdc family. Where the homology of the c-terminal portion of the protein is ~92% (Osler et al., 2006). The cAMP binding capacity of the Popeye domain was not identified immediately; while the predicted secondary structure of the cyclic nucleotide binding domain is similar to that of PKA, the sequence of the putative phosphate binding cassette (PBC) is not akin to other cAMP effectors (Figure 19A). The DSPE motif of the PBC is highly conserved from worm to humans (Schindler et al., 2016b). Popdc binding affinity to cAMP has an IC_{50} of ~118.4 nM and is 50-fold more selective for cAMP over cGMP which has an IC_{50} of ~5.27 µM (Froese et al., 2012).

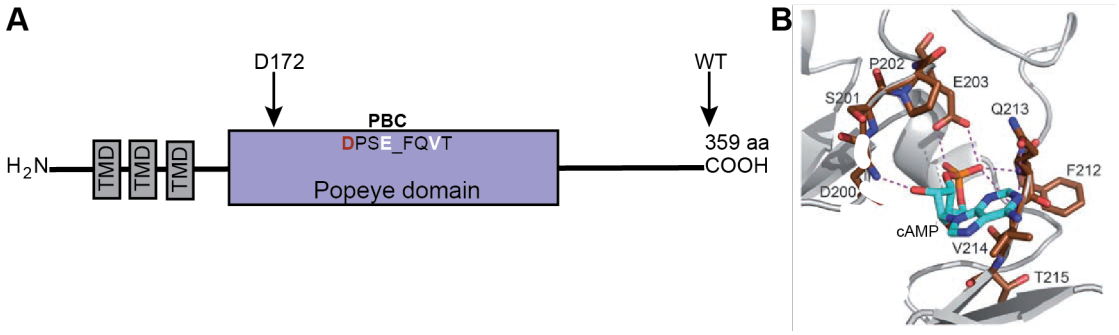

Figure 19. Popdc schematics. (A) Linear schematic of Popdc1 and C-terminal truncation highlighting the PBC (D200-T218) where residues in red eliminate cAMP

binding and in white result in intermediate binding when mutated to alanine. (B) 3-D model of the cAMP binding domain (Froese et al., 2012), displayed under license id: 4458970824151.

5.1.1 Popdc physiological functions

Popdc1/Bves was discovered by independent groups looking to identify novel genes involved in heart development (Andree et al., 2000; Reese et al., 1999). Since then, Popdc proteins have been shown to interact with a number of different proteins (overview of select interactions: Table 4) and connected to various roles in cell biology and physiology.

Table 4. Popdc protein interactions

Protein	Evidence	Function of Pop	Reference
TREK-1*	GST-PD, Co-IP, Co-IF, FRET, TEVC	Controls membrane trafficking	(Froese et al., 2012)
Caveolin-3	Co-IP, Co-IF	Size and number of caveolae	(Alcalay et al., 2013)
Dystrophin	Co-IP, Co-IF	Unknown	(Schindler et al., 2016a)
Dysferlin	Co-IP, Co-IF	Unknown	(Schindler et al., 2016a)
VAMP2,VAMP3	Y2H, GST-PD, Co-IF	Vesicular transport and fusion	(Hager et al., 2010)
NDRG4	Y2H, GST-PD, Co-IP, Co-IF	Vesicular trafficking	(Benesh et al., 2013)
ZO1	GST-PD, Co-IF, IG-EM	Epithelial integrity	(Osler et al., 2006)

*Binding modulated by cAMP.

Abbreviations. GST-PD (glutathione-s-transferase-pull down), Co-IP (coimmunoprecipitation), Co-IF (co-immunofluorescence), FRET (Forester resonance energy transfer), TEVC (two electrode voltage clamp), Y2H (yeast two hybrid), IG-EM (immunogold electron microscopy), VAMP (vesicle-associated membrane protein),

NDRG4 (n-myc downstream regulated gene 4), ZO1 (zonula occludens-1). Modified from: Schindler, R. F., and T. Brand. 2016. The Popeye domain containing protein family-A novel class of cAMP effectors with important functions in multiple tissues. Prog Biophys Mol Biol 120: 28-36. Publication is leased under CC BY-NC-ND license (http://creativecommons.org/licenses/by-nc-nd/4.0/).

Genetic deletion of Popdc1 or Popdc2 in mouse leads to an age dependent stress induced bradycardia in response to mental stress, exercise, or isoproterenol stimulation. While the I_f current in isolated SAN cells was unaffected by deletion of either Popdc, co-expression of Popdc1/2 with the two pore potassium channel TREK-1 enhanced channel activity and membrane localization of the channel. Popdc1 directly interacts with TREK-1; interestingly this interaction is modulated by cAMP. The binding of cAMP to Popdc disrupts binding to TREK-1 and reduces TREK-1 plasma membranes localization (Froese et al., 2012).

Recently, a familial mutation in Popdc1^{S201F} was linked to limb-girdle muscular dystrophy (LGMD) and cardiac arrhythmias. Patients develop a severe AV block with mild development of skeletal muscle disease. In skeletal muscle biopsies, patients with this mutation show significantly reduced Popdc1 and Popdc2 trafficking to the membrane. The identified mutation is located in the conserved DSPE motif of the PBC in the Popeye domain and alters cAMP binding. Popdc1 binding to cAMP is reduced by 50% and Popdc dependent enhancement of TREK-1 membrane localization is impaired. Homozygous expression of Popdc1^{S201F} in zebrafish recapitulated phenotypes similar to those observed in patients (Schindler et al., 2016a). Knockdown of Popdc1 or Popdc2 in zebrafish shows similar phenotypes (Kirchmaier et al., 2012; Schindler et al., 2016b).

5.2 Results

5.2.1 Interaction of AC and Popdc

Looking for proteins involved in heart rate control we came across the Popdc family. Popdc1/2 are highly expressed in the sinoatrial node, exhibit stress induced bradycardia, and are novel cAMP effectors. Additionally, AC9 and AC3 have been linked with Popdc2 in a large-scale human interactome screen (Huttlin et al., 2015). To test whether AC and Popdc interacted Flag tagged AC9 (or non-tagged AC3) was co-expressed +/- Popdc1-myc or Podpc2-myc in HEK293 cells. Complexes were isolated via the myc tag and associated AC activity was measured (Figure 20A). From the activity assays it appeared that AC9 interacted with Popdc1 but not Popdc2, while AC3 did not interact with either isoform. However, when immunoprecipitations were evaluated via western blot, significant amounts of AC3 (Figure 20D) and AC9 protein (20C) were detected in both Popdc1 and Popdc2 pull downs. It appears that while Popdc1/2 can pulldown AC3 there is dramatic inhibition of AC3 associated activity. While Popdc1 pulls down AC9 and maintains associated activity, Popdc2 pulls down AC9 and inhibits activity. In these assays, that have been used to identify numerous AC-AKAP interactions, a lack of associated activity typically corresponds to a lack of interaction (Efendiev et al., 2010; Kapiloff et al., 2009; Li et al., 2012; Piggott et al., 2008). A corresponding inhibition of AC activity was observed in total lysates upon co-expression of AC9 with Popdc2 or AC3 with Popdc1/2 (Figure 20B).

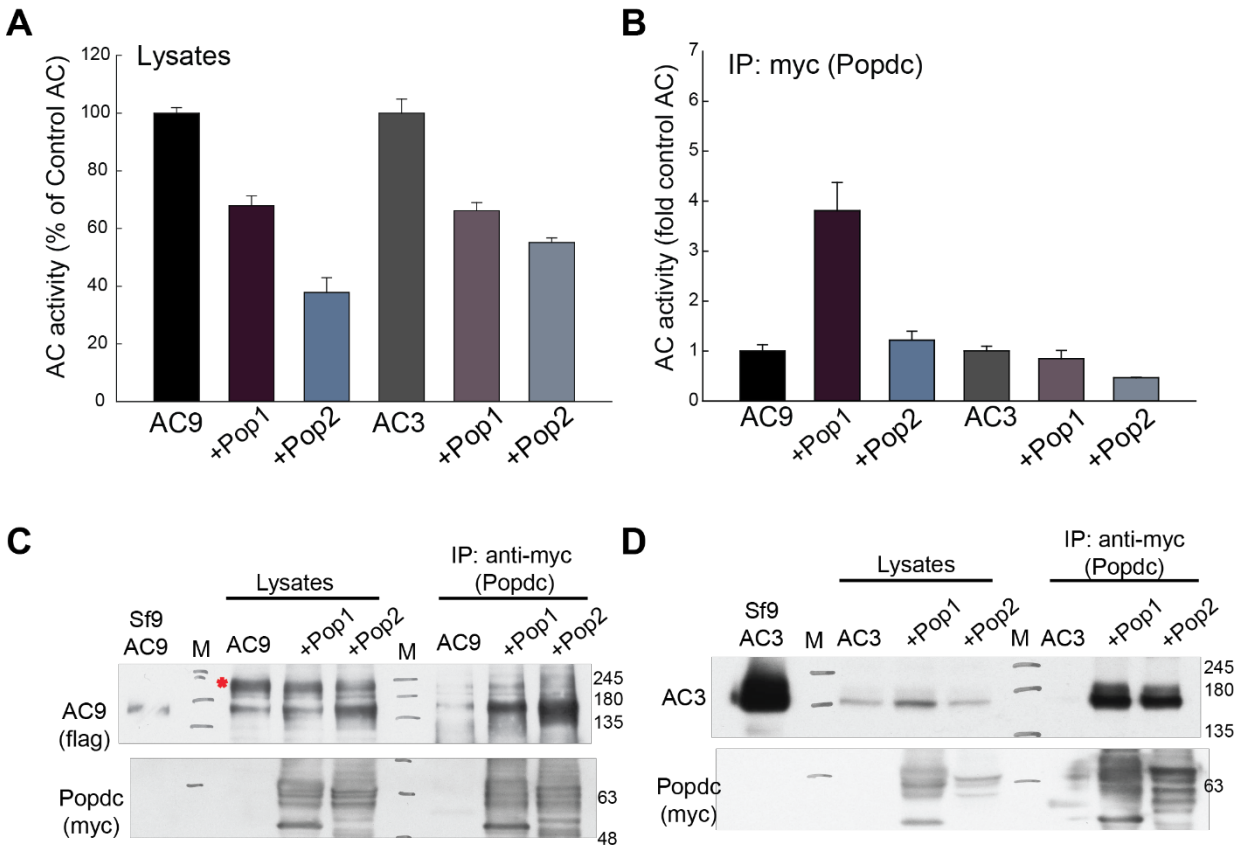

Figure 20. Popdc interacts with AC3 and AC9. (A) HEK293 cells expressing Flag AC9 or AC3 +/- myc tagged Popdc 1 or 2. Cell lysates were subjected to immunoprecipitation of myc and assayed for AC activity with 300 nM Gαs-GTPγS. **(B)** Total AC activity of cell lysates. **(C-D)** Western blot of lysates and IPs from IP-AC assay, blotting for myc (Popdc), FLAG (AC9), or AC3. Membranes isolated from Sf9 cells expressing Flag AC9 or AC3 serve as positive controls. * indicates a non-specific or alternative form of AC9 only present in lysates. Note, Popdc protein runs as multiple bands (48-65 kDa; confirmed in KO) with altered sizes/patterns in different tissues likely due to changes in glycosylation patterns (Schindler et al., 2016a).

AC9 and Popdc1/2 interactions were confirmed by performing reverse immunoprecipitations. Popdc1/2-myc +/- Flag AC9 were expressed in HEK293 cells and complexes were isolated with Flag-agarose. Popdc1 and Popdc2 were both detected in immunoprecipitates of Flag-AC9 (Figure 21).

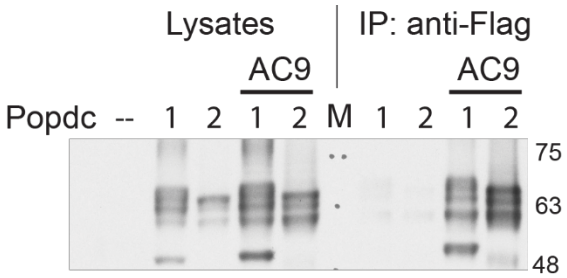

Figure 21. AC9 pulls down Popdc1/2. Lysates from HEK293 cells expressing Popdc 1 or 2 +/- FLAG AC9 were subjected to immunoprecipitation with FLAG-agarose and western blotted for top: myc (Popdc) or bottom: Flag (AC9).

AC9-Popdc1/2 interactions are also detectable in COS-7 cells in BiFC experiments (Figure 22). No fluorescence was detected upon expression of the individual Popdc1-VN or AC9-VN constructs. Co-expression of AC9-VN and Popdc1-VC or Popdc2-VC resulted in variable reconstitution of fluorescence. Expression of AC9-VN with AC9-VC serves as a positive control. Interaction of AC9 and Popdc1 although variable showed significant interaction.

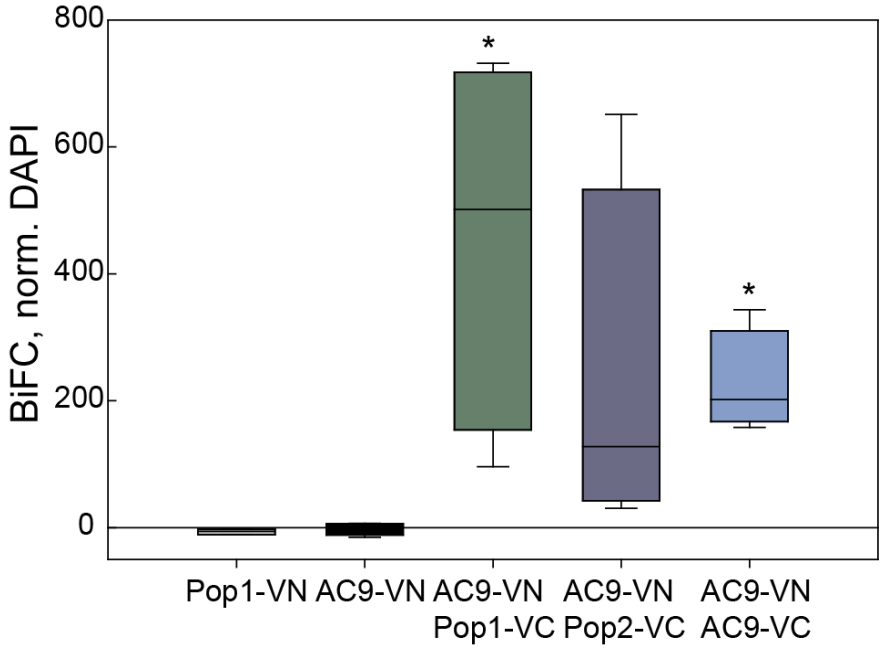

Figure 22. AC9-Popdc1 interaction. Quantification of COS7 cells expressing BiFC constructs for AC9, Popdc1, and Popdc2. The N-terminus (VN) or C-terminus (VC) of Venus is fused to the C-terminus of each protein. The first protein listed is tagged with VN and the second VC. Experiments performed by Simi Rahman.

The list of Popdc protein interactions is quite numerous (Schindler and Brand, 2016). To ensure that Popdc-AC interactions were specific and Popdc did not interact with any membrane bound protein we tested whether Popdc1 would pulldown other membrane bound proteins including the epidermal growth factor receptor (EGFR) which localizes to the plasma membrane or lysosomal associated membrane protein 1 (LAMP1) which localizes to the lysosomal membrane. Popdc1 was co-expressed with or without YFP-AC9, EGFR-GFP, or LAMP1-GFP. Complexes were immunoprecipitated with cmyc and western blotted (Figure 23). Only AC9 was present in Popdc1 pull downs.

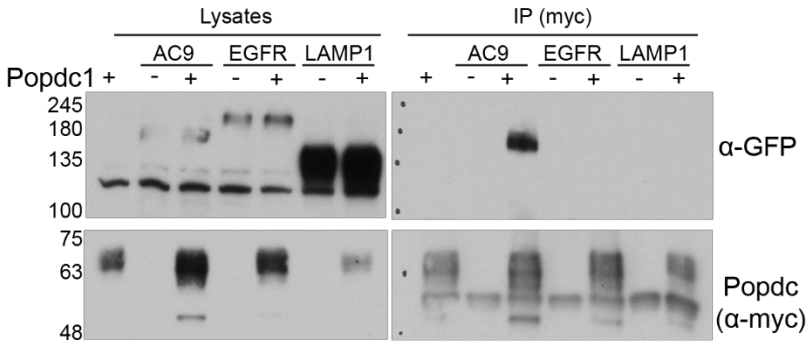

Figure 23. Popdc-AC9 interactions are specific. Immunoprecipitation of myc from HEK293 cells expressing myc-Popdc1 +/- YFP-AC9, EGFR-GFP, or LAMP1-GFP. Lysates and IPs were subjected to western blotting for GFP (top) and myc (bottom), n=1.

Of the proteins that interact with Popdc, binding to TREK-1 is modulated by cAMP binding (Froese et al., 2012). Popdc bound to cAMP prevents interaction with TREK-1 and reduces channel current by reducing channel expression on the membrane. To test whether Popdc binding to cAMP influenced AC interaction with Popdc or associated activity, cells were transfected with AC9 +/- Popdc1 or Popdc2 and treated with vehicle (DMSO) or forskolin for 30 minutes before lysis. Cells treated with forskolin were lysed in the presence of 1 μM exogenous cAMP. Complexes were immunoprecipitated with myc then associated AC activity and protein was measured. While cAMP does not alter AC9-Popdc binding, inhibition of AC associated activity is increased by both Popdc1 and Podc2 in lysates and IP. AC9 activity in lysates is not altered with 1 μM exogenous cAMP (Figure 24 A/B).

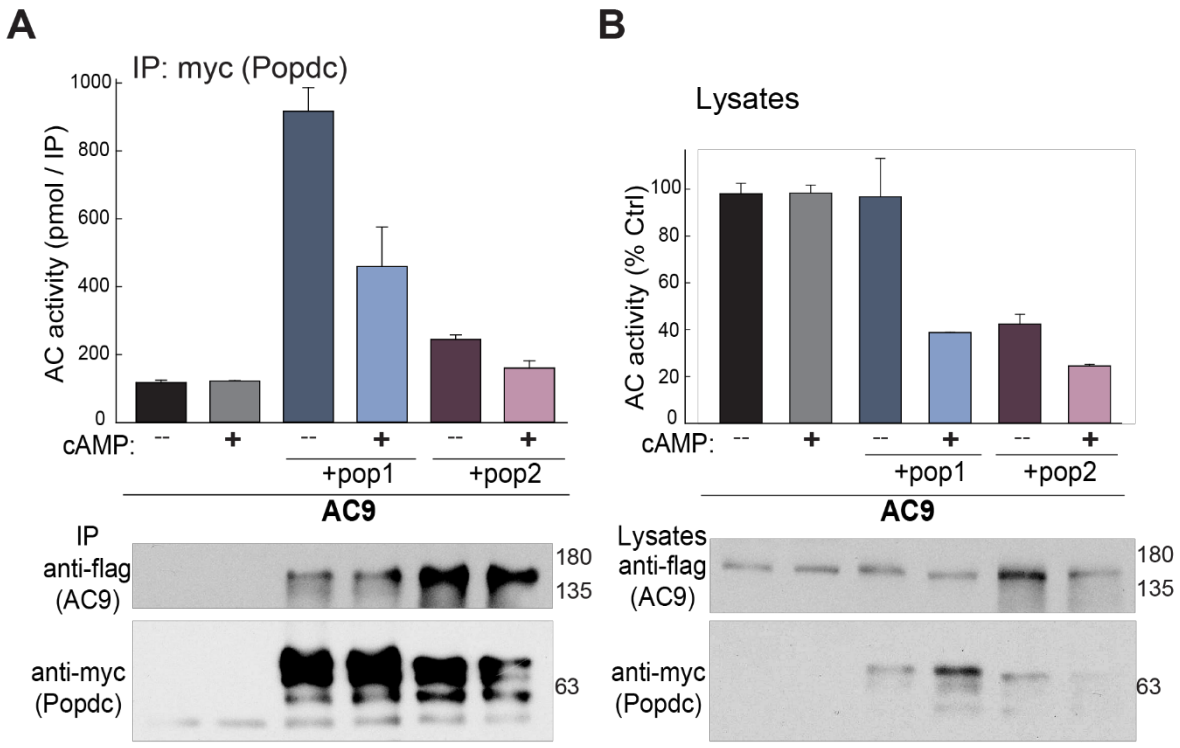

Figure 24. Popdc binding to cAMP inhibits AC9 activity. (A) AC activity and western blots of IP-AC assays of HEK293 cells expressing Flag AC9 +/- Popdc 1 or 2. Cells were stimulated for 30 minutes with forskolin prior to IP with 1 μM cAMP. **(B)** Total lysate AC activity and protein levels before immunoprecipitation.

To begin to narrow down the site of AC-Popdc interaction, a c-terminal truncation mutant was tested that deletes most of the Popeye domain, Popdc1Δ172 (Figure 19A). HEK293 cells were transfected with AC9 +/- WT Popdc1-myc or Popdc1Δ172-myc and complexes were isolated. AC activity associated with Popdc1 was reduced in complexes pulled down with Popdc1Δ172-myc, with no altered protein interaction (Figure 25 A/B). In lysates AC9 activity was inhibited to a similar extent with co-expression of either WT or Popdc1Δ172 (Figure 25 C). AC9 interaction with Popdc1Δ172 was confirmed in whole cells using proximity ligation assay (PLA). A vector control (pcDNA3) and Popdc-myc expressed with myristoylated YFP were used as negative controls and show no PLA

signal. Whereas a positive PLA signal is observed by expression of YFP-AC9 with Popdc1 WT or Δ172 (Figure 25 D).

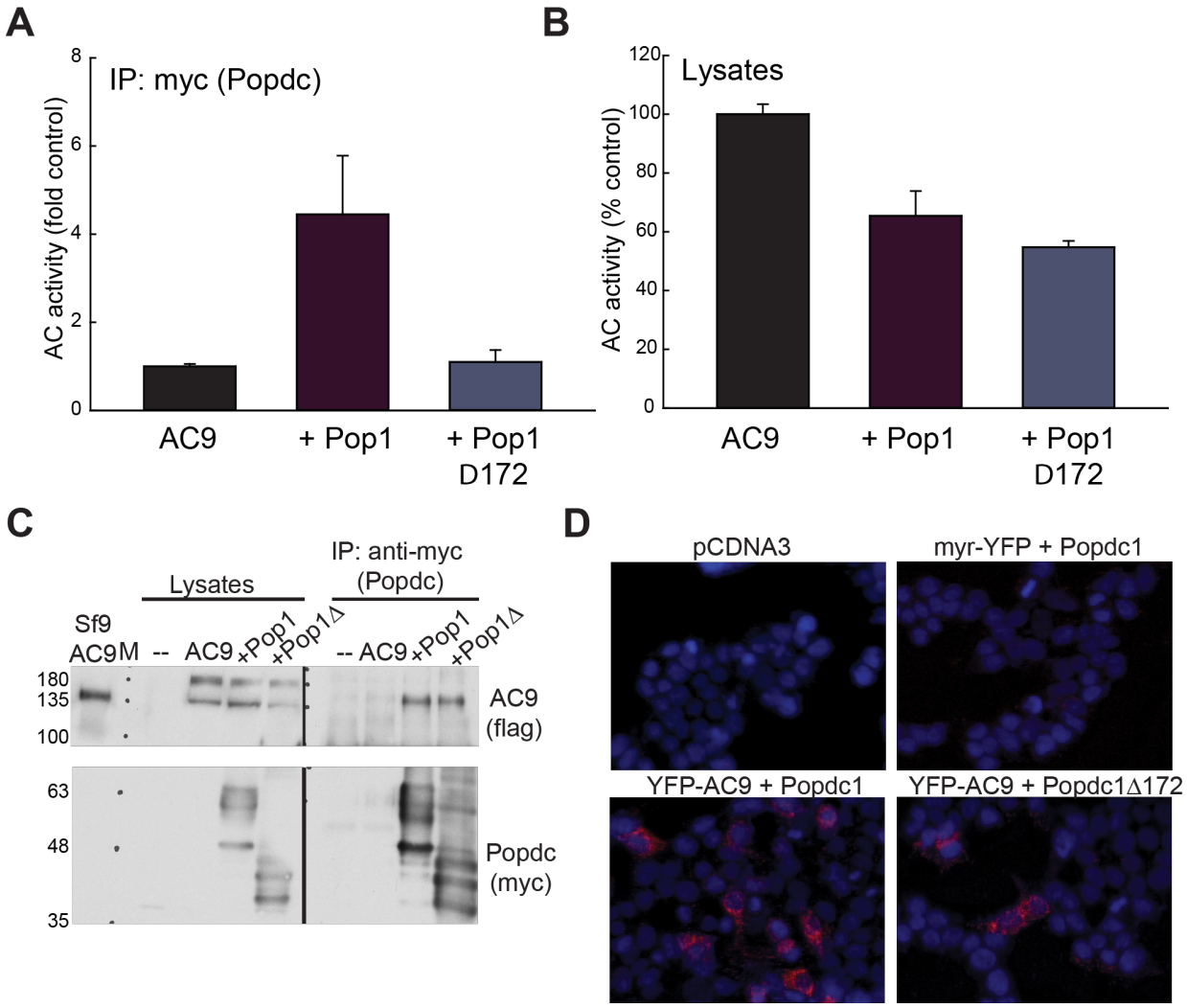

Figure 25. AC9 interacts with Popdc1Δ172. (A) IP-AC assay of Flag AC9 +/- Popdc1 or Popc1Δ172 truncation mutant (PopΔ). **(B)** AC activity from lysates of IP-AC assay. **(C)** Western blot of lysates and IP-AC assay. **(D)** Proximity ligation assay using anit-YFP and anti-myc (Popdc) in HEK-293 cells. PLA signal (red), DAPI (blue).

Popdc regulation of TREK-1 membrane localization and activity is likely the underlying cause of the stressed induced bradycardia observed in Popdc1 or Popdc2 knockout mice (Froese et al., 2012). The importance of TREK for maintaining normal

SAN excitability was recently shown, a cardiac specific knockout of TREK-1 exhibited bradycardia and reduced background potassium current (Unudurthi et al., 2016). To determine whether AC9 could associate with the TREK-1-Popdc complex, Popdc1 was immunoprecipitated from cells co-expressing with TREK-1 and AC5 or AC9. Popdc1 brought down both AC9 and AC5 in addition to TREK-1 (Figure 26 A). Neither AC5/9 or TREK-1 were observed in immunoprecipitates when Popdc1 was not expressed. Similarly, IP of TREK-1 brings down AC9 and endogenous Popdc1, while overexpression of Popdc enhances AC9 binding with TREK-1 (Figure 26 B). Compared to Popdc1, neither endogenous or exogenous AKAP79 interacts well with TREK-1; although TREK-1 has been shown to interact with AKAP79 (Sandoz et al., 2006). Co-localization of Popdc-TREK-1 and AC9-TREK-1 is observed in HEK293 cells (Figure 26 C).

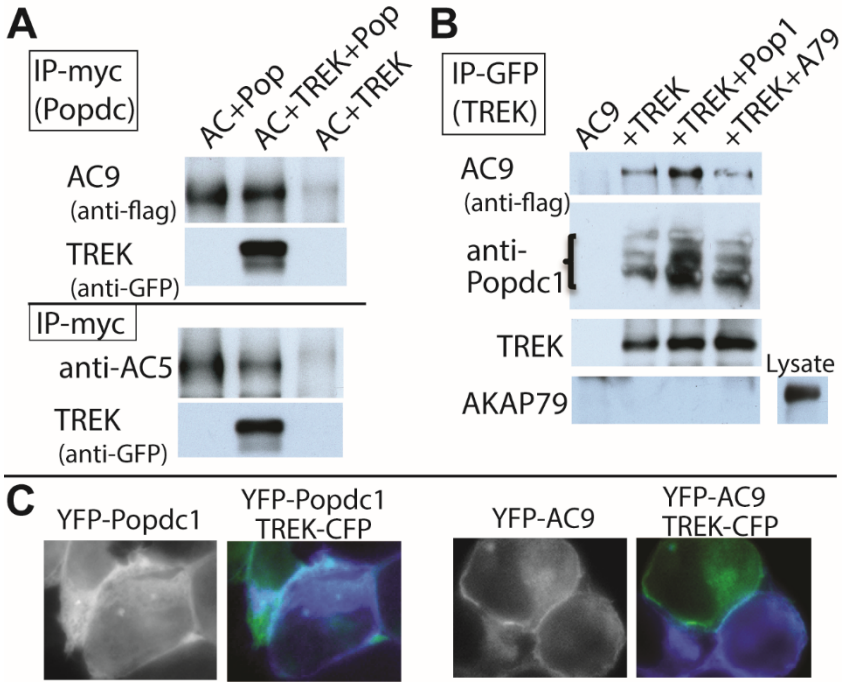

Figure 26. TREK-Popdc1-AC9 complex. (A) Expression of AC9 or AC5 +/- TREK-1 and Popdc1. IP/WB with myc-Popdc1. **(B)** IP of GFP-TREK-1 pulls down AC9 and

endogenous or overexpressed Popdc1, but not AKAP79. **(C)** Co-localization of TREK-CFP and YFP- Popdc (left) or TREK-CFP and YFP-AC9 (right), n=1.

5.3 Summary

While AKAPs are the best studied AC scaffolds, in our efforts to understand the molecular mechanism of bradycardia in $AC9^{-/-}$ mice we have identified a novel AC scaffold and regulator, Popdc. To date this is the first description of AC-Popdc interaction. We show that Popdc1 and Popdc2 interact with both AC3 and AC9 by immunoprecipitation, PLA, and BiFC. Dependent on isoform (both Popdc and AC), interaction of Popdc with AC can potently inhibit AC activity. This occurs in a cAMP dependent manner, where IP of the Popdc1-AC9 complex has reduced AC activity when exogenous cAMP was included in the lysis and IP steps. AC9 interacts with a truncation mutant of Popdc1 that lacks most of the Popeye domain and the C-terminus. This suggests that the interaction of Popdc1 with AC9 occurs via the transmembrane domains or initial portion of the Popeye domain; two distinct binding sites may also be possible.

The underlying mechanism of Popdc heart rate regulation is thought to be driven by interaction with TREK-1. Both AC9 and AC5 can associate with a Popdc1-TREK complex when exogenously expressed in HEK293 cells and immunoprecipitated. Co-localization of AC9 and TREK at the plasma membrane can also be detected in HEK293 cells.

Chapter 6

Concluding remarks and future directions

6.1 Summary of conclusions

Regulation of the enzyme adenylyl cyclase occurs on multiple levels. Broadly, physiological contributions of AC are regulated by tissue distribution. Specifically, enzymatic activity is regulated by heterotrimeric G-proteins, kinases, phosphatases, and calcium. Scaffolds add an additional layer of regulation, contributing to localization, indirect or direct regulation of enzymatic activity, and subsequent activation of downstream cAMP effectors. Although studies from my laboratory and others have provided insights into the possible physiological roles of AC9 (Berndt et al., 2013; Li et al., 2017b; Liu et al., 2010; Mahadeo et al., 2007; Small et al., 2003; Toyota et al., 2002), further elucidation of AC9 regulation is essential for a comprehensive understanding of how this enzyme functions and is controlled *in vivo*.

I first evaluated the direct regulation of AC9, showing that many proposed regulators work indirectly suggesting an alternative mechanism of AC heterodimerization to explain previous findings. Next I examined roles for AC9 in cardiac physiology and signaling are examined. Genetic deletion of AC9 in mice reduces total cardiac cAMP by ~3% yet it results in two cardiac phenotypes; diastolic dysfunction and bradycardia. These phenotypes likely arise from distinct mechanisms dependent on unique AC9-containing macromolecular complexes. Lastly, I examined a novel AC interacting partner, Popdc. This interaction represents a possible mechanism for the AC9 bradycardia phenotype. My findings also suggest that Popdc is a novel scaffold and negative regulator of AC activity.

6.2 AC9 regulation

Although no splice variants of AC9 are reported, proteolytic alterations of AC9 give rise to two main forms observed in both rodent and human heart (Palvolgyi et al.,

2018). The extended C-terminus of the larger form (~170 kDa) is reported to auto-inhibit AC9; this is lacking in the smaller form (~130 kDa) (Palvolgyi et al., 2018). To complicate regulation analysis, two main human clones have been utilized previously in studies of AC9 regulation. A truncated form of AC9 that lacks the last 75 aa of C2b domain (aa 1-1252; predicted molecular mass 144.2 kDa) was used to examine Gαi/o, CaMKII, and nPKC regulation (Cumbay and Watts, 2004; Cumbay and Watts, 2005; Hacker et al., 1998). Others have examined full-length AC9 (aa 1-1327; predicted molecular mass 147.7 kDa) for calcineurin and PKCβII regulation (Antoni et al., 1998; Liu et al., 2014; Paterson et al., 2000). My study utilized both forms: the truncated version for Sf9 expression and full-length for mammalian cell expression, however I did not observe a reduction in Gαs-stimulated activity for the full-length when expressed in HEK293 cells (data not shown).

There are a number of potential reasons for the conflicting reports surrounding AC9 regulation. Previous studies lack consistency in cell type, using a variety of cell types from HEK293 or neutrophil cell lines, to isolated mouse neutrophils. In particular the conflict surrounding Gαi regulation may be due to the use of different Gαi/o coupled receptors where use of the SST2 receptor showed no inhibition of AC9 activity (Hacker et al., 1998) while use of the D2L receptor showed AC9 inhibition (Cumbay and Watts, 2004). Adding to this, HEK293 cells endogenously express AC isoforms that are inhibited by Gαi, AC1,5, and 6 (Lefkimmiatis et al., 2009). These reasons prompted the evaluation of AC9 regulation using isolated membrane and purified proteins.

6.2.1 Conditional regulation of AC9 by forskolin

The plant diterpene, forskolin, is a potent activator of all the membrane bound ACs except AC9. Forskolin is regularly used as an experimental tool to examine

physiological and pathophysiological roles of AC. Forskolin acts by stabilizing the interaction of the C1 and C2 domains of AC by an order of magnitude resulting in a 60-fold increase of V_{max} (Sunahara et al., 1997) without altering the K_m of ATP (Dessauer et al., 1997). Mammalian AC9 has long been categorized as the only membrane-bound AC isoform that is forskolin insensitive (Hacker et al., 1998; Premont et al., 1996). Interestingly the Drosophila homolog of AC9 is sensitive to forskolin activation (Iourgenko et al., 1997). A point mutation in the C_2 domain of mouse AC9, 9C2-Y1082L, restores sensitivity to forskolin at suboptimal concentrations of Gαs. Mutation of the corresponding residue in the C_2 domain of AC2, 2C2-L912Y, eliminates forskolin activation (Yan et al., 1998). While forskolin is unable to stimulate basal human AC9 activity (Hacker et al., 1998), it can weakly activate AC9 in the presence of Gαs. Synergistic activation by Gαs, observed with other isoforms, likely promotes forskolin binding, despite alterations in the forskolin binding pocket of AC9 (Yan et al., 1998). The conditional activation of AC9 by forskolin is modest at best. This would discourage the pan use of forskolin alone as significant contributions by AC9 could be overlooked. Although this may be true, homo- and heterodimerization of AC9 (discussed below) could complicate the simplicity of this idea.

6.2.2 AC9 is not directly regulated by most G-proteins or kinases.

Like all other transmembrane AC isoforms, AC9 is directly activated by Gαs. However, the Gαs dose-response curve for AC9 is right shifted in comparison with other ACs (Chen-Goodspeed et al., 2005; Dessauer et al., 2017). Gαs interacts with the loop between the α1' and α2' helices of the C2 domain (Tesmer et al., 1997) (Figure 27). A possible explanation for the observed shift in Gαs dose-response curve is the shorter

loop between these two helices, which is two amino acids shorter in human AC9 compared to human or rat AC2.

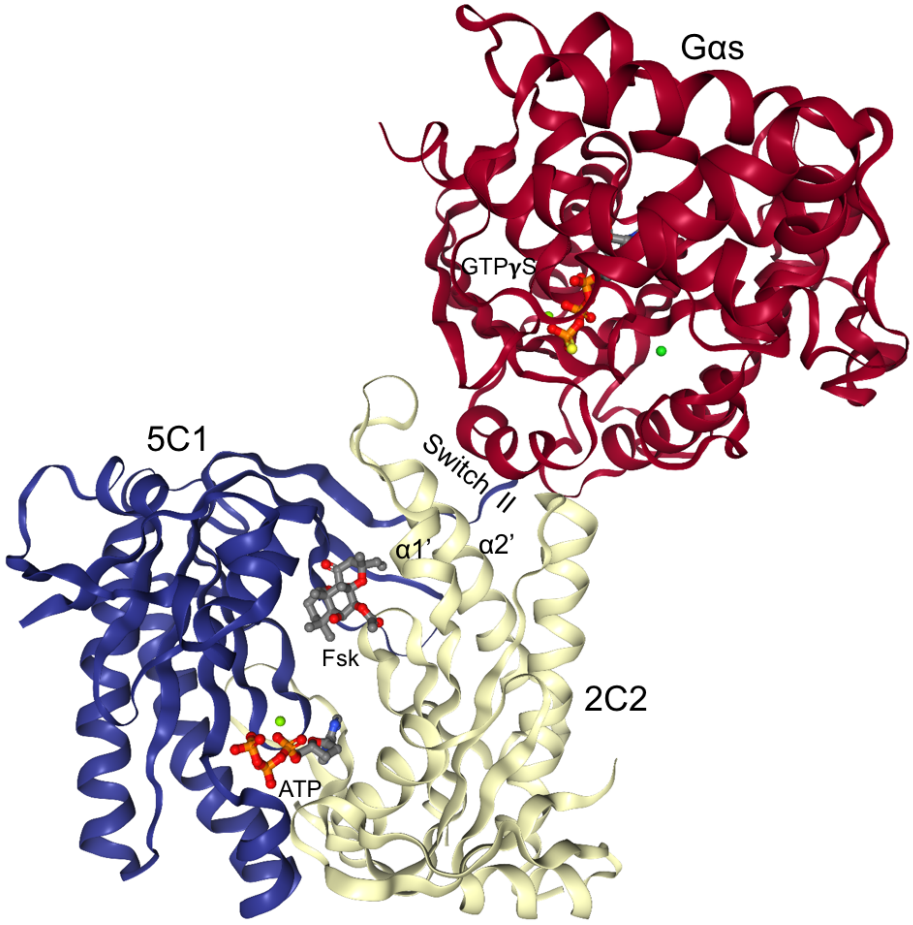

Figure 27. Complex of 5C1:2C2 with forskolin, ATP, and GTPγS-Gαs. AC5 C1 domain, blue; AC2 C2 domain, white; Gαs, red. Model based on the crystal structure PDB 1CJU (Tesmer et al., 1999; Tesmer et al., 1997). NGL viewer: web-based molecular graphics for large complexes. Bioinformatics dio:10.1093/bioinformatics/bty419), and RCSB PDB.

Predicted N-glycosylation sites are conserved among the AC isoforms on the fifth and/or sixth extracellular loops (Wu et al., 2001). The functional relevance of glycosylation varies depending on isoform. Preventing glycosylation of AC6 results in

reduced inhibition by PKC and Gαi (Wu et al., 2001) while prevention of AC9 glycosylation left shifts Gαs-stimulation (Cumbay and Watts, 2004). At first glance, this suggests glycosylation as a mechanism for reduced Gαs sensitivity. This is unlikely as a requirement for increased Gαs has been observed in multiple systems where AC9 would be glycosylated, e.g. in Sf9 or HEK293 cells (Efendiev et al., 2010; Piggott et al., 2008).

Gβγ either conditionally stimulates (AC 2, 4-6, 7) or inhibits (AC 1, 3, 8) all other AC isoforms reviewed in (Dessauer et al., 2017; Sadana and Dessauer, 2009). Gβγ binds the N-termini of several AC isoforms (AC1-3, 5-6, and 9). Mutation of the Gβγ hotspot alters regulation of AC1, 2, 5, and AC6 and disrupts binding to AC1-3, 5-6, 8, and 9 (Brand et al., 2015). Several labs, including this study, have shown that Gβγ does not directly regulate AC9 (Hacker et al., 1998; Premont et al., 1996), although it may indirectly activate AC9 in neutrophils (Liu et al., 2010). Despite not directly regulating AC9, Gβγ binds to the N-terminus of AC9 (Brand et al., 2015), suggesting that the N-termini of AC9 may serve as scaffolding site for heterotrimeric G proteins, as previously shown for AC5 (Sadana et al., 2009).

The lack of direct regulation of AC9 by Gαi/o, although contradictory with some whole cell studies, is not entirely surprising. AC9 has little homology with the Gαi binding site on AC5; only one of six residues required for AC5 inhibition is conserved in AC9 (Dessauer et al., 1998). Moreover, Gi/o-coupled chemokine receptors enhance cAMP production in neutrophils (Mahadeo et al., 2007). In this system, Gi-coupled receptors promote Gβγ activation of mTOR and subsequently PKCβII, ultimately stimulating cAMP production by AC9. Direct inhibition of AC9 by Gαi in this system would be counterproductive to the indirect stimulation of AC9 by Gβγ (Liu et al., 2014; Surve et

al., 2016). Rather, Gαi in neutrophils appears to act on other effectors in a cAMP independent manner, targeting RAP1GAPII (Mochizuki et al., 1999) to regulate neutrophil adhesion (To and Smrcka, 2018).

AC9 was originally cloned as a calcineurin (PP2B) inhibited isoform (Paterson et al., 2000), implying that phosphorylation is an important aspect of AC9 regulation. AC9 contains two predicted PKC sites (T309 and S374; Scansite 4.0, MIT), which are located at the base of TM6 or within an 18 aa insert unique to AC9, prior to the catalytic core. While our *in vitro* results do not support a direct role for PKCβII or CaMKII regulation of AC9, it is possible that a scaffolding protein, absent from our *in vitro* studies, is required to facilitate AC9 phosphorylation (Dessauer, 2009). Alternatively, another PKC isoform could regulate AC9 as other reports of PKC regulation conclude AC9 is inhibited by a novel PKC isoform (Cumbay and Watts, 2004). It is also possible that PKCβII and CaMKII phosphorylate a yet unidentified upstream regulator of AC9.

6.2.3 Regulation of basal cAMP levels.

Examining basal levels of AC activity is difficult; not only are basal levels frequently used to normalize data, but they can be error prone, occurring at the lower limit of detection for some techniques. A few reports have noted differences in AC basal activities, specifically AC1 and AC3 in olfaction (Bakalyar and Reed, 1990) and AC2 and AC6 (Pieroni et al., 1995), suggesting that basal levels of cAMP production are important aspects of their physiological roles. In support of this concept, the most notable effects of AC9 knockout on cardiac function occurred at baseline, where mice had reduced heart rates, diastolic dysfunction, and reduced phosphorylation of the small heat shock protein 20 (Li et al., 2017b). Alterations in basal AC activity with either knockdown or knockout of AC9 in COS-7 cells and splenocytes was revealed under

phosphodiesterase inhibition, a similar effect was recently reported in HEK293 cells (Palvolgyi et al., 2018). Comparison of the Drosophila homolog of AC9 (DAC9) and mouse AC9 also support these findings. Expression of mouse AC9 has enhanced basal activity, which is diminished in cells expressing DAC9. While activation by Gαs is enhanced in DAC9 compared to AC9 (Iourgenko et al., 1997). It should be noted that there is a nuanced difference between these studies. Some of findings show that AC9 contributes to basal cAMP while others show a role in basal AC activity when phosphodiesterase inhibitors are used. Taking into account the reported contributions of AC9 to basal cAMP levels and decreased sensitivity to Gαs, the physiologically significance of AC9 might be dependent on the strength of sympathetic signaling. Where at rest or minimal signal strength AC9 is weakly active and a maximal sympathetic signal would lead to full enzymatic activity.

6.2.4 Whole cell versus in vitro biochemical assessment of AC9 regulation.

Surprisingly, our data supports an indirect mechanism for most previously proposed AC9 regulators. One dilemma is how to access regulatory patterns of AC. For years the gold standard was expression of AC isoforms in Sf9 cells combined with *in vitro* biochemical assays using purified regulators. However, the importance of scaffolding proteins or post translational modifications of AC are lacking in this approach. For example, PKA phosphorylation and inhibition of AC5 and AC6 was originally detected in membranes or with detergent-solubilized preparations of AC using a large excess of kinase; however, regulation of AC5/6 by PKA is readily apparent when in complex with AKAP79-PKA (Bauman et al., 2006; Chen et al., 1997; Iwami et al., 1995). Generally scaffolding proteins simply make these reactions more efficient, thus

we expected to detect any direct PKC regulation of AC9 *in vitro* using an excess of kinase sufficient to activate AC2.

To further evaluate differences between my biochemical results and previous whole cell experiments, a live-cell cAMP assay was utilized in COS-7 cells. HEK293 cells are widely used to study AC regulation but they endogenously express multiple AC isoforms (1, 2, 3, 5, 6, 7 (weakly), 9, and sAC), which limits their utility (Lefkimmiatis et al., 2009). COS-7 cells provided the advantage of using a mammalian cell line, lacking expression of Gαi-inhibitable ACs while endogenously expressing AC7 (Premont, 1994) and AC9 (representing ~40% of Gαs-stimulated activity). Agonist-stimulation of μOR-coupled Gi/o receptors significantly inhibited overexpressed AC6 in COS-7 cells, demonstrating that these cells have all the necessary components for Gαi/o inhibition. The fact that I observed no inhibition of endogenous AC activity or AC9 overexpressed activity in whole-cells by μOR receptors further supports the lack of direct regulation of AC9 by Gαi/o.

6.2.5 AC homo- and heterodimerization

Numerous studies have suggested that AC isoforms form homodimers based on mutational complementation (AC1), cooperative activation (AC5) or co-immunoprecipitation and FRET studies (AC6 and AC8) (Chen-Goodspeed et al., 2005; Gu et al., 2002; Tang et al., 1995). Weak heteromeric formation was reported for AC8 with AC6 (Gu et al., 2002). Evaluation of AC8 homodimers suggests that loss of activity in AC8 mutants can be partially rescue when co-expressed with WT AC8. Structurally, it is thought that oligomers are formed through interactions of the transmembrane domains (Gu et al., 2002). I now show that AC9 not only forms homodimers but can also form heteromers with the Gαi-regulated isoforms AC5 and AC6. The ability of AC9 to

form heteromers may explain why studying AC9 regulation in cell lines that express multiple AC isoforms (i.e. HEK293 cells) has proven difficult.

At this time the physiological importance of AC homo- and heterodimers is unclear. It is tempting to speculate that dimerization of AC9 with AC5/6 could potentially result in Gαi/o inhibition of the complex or even AC9. Heteromer formation may also explain why a reduction of both Gαs- and forskolin-regulated activity is observed upon knockdown or knockout of AC9; given the relative forskolin insensitivity of AC9, we would have expected minimal loss of forskolin-stimulated activity.

More recently, AC5 was shown to interact via its transmembrane helices with adenosine ($A_{2A}R$) and dopamine (D_2R) receptors in striatal neurons; the functional pre-coupling of this complex was suggested to be necessary to promote canonical Gs-Gi regulation of AC5. Minimally this complex should be composed of two AC5 molecules with two heterotetramers of $A_{2A}R$-D_2R. (Navarro et al., 2018). It is easy to imagine tissue dependent variations of this pre-coupled complex. In heart pre-coupled complexes of AC5/6-Gi:GPCR with AC9-Gs:GPCR (Figure 28) could facilitate integration of Gs and Gi regulation. Also, in heart, stimulation of the β-adrenergic receptor enhances phosphorylation of Hsp20 in a cAMP-PKA dependent manner (Fan et al., 2004). While a Gi:GPCR has not been directly implicated in reducing Hsp20 phosphorylation, altering cAMP pools by inhibiting PDEs enhances phosphorylation and inhibiting PKA reduces phosphorylation (Fan et al., 2004; Martin et al., 2014). It is not outside the realm of possibilities that activation of a Gi:GPCR could similarly reduce Hsp20 phosphorylation. Based on the finding that deletion of AC9 only reduced Hsp20 associated AC activity in heart by 30%, we expect that Hsp20 associates with another AC isoform; the most likely candidates being AC5/6. It would be interesting to see whether a pre-coupled AC dimer

complex contributes to the phosphorylation status of Hsp20 or other proteins regulated by Gs and Gi. Oligomerization of ACs may present another mechanism to fine tune regulation of local pools of cAMP and facilitate cross-talk between signaling pathways.

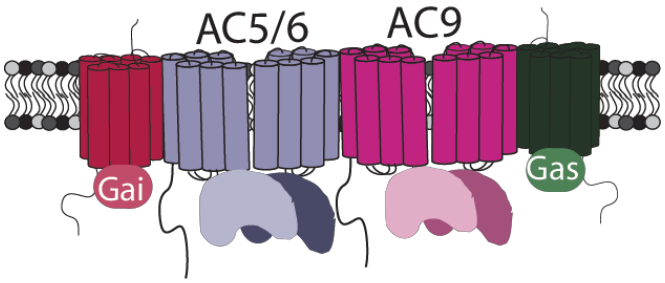

Figure 28. Pre-coupled AC-dimer complex.

6.3 From complex to physiological function

An underlying theme that appears from examination of cardiac phenotypes in AC9$^{-/-}$ mice is that physiological roles of AC9 are vastly dependent on association with macromolecular complexes and tissue distribution (Figure 29). Knockout of either of the

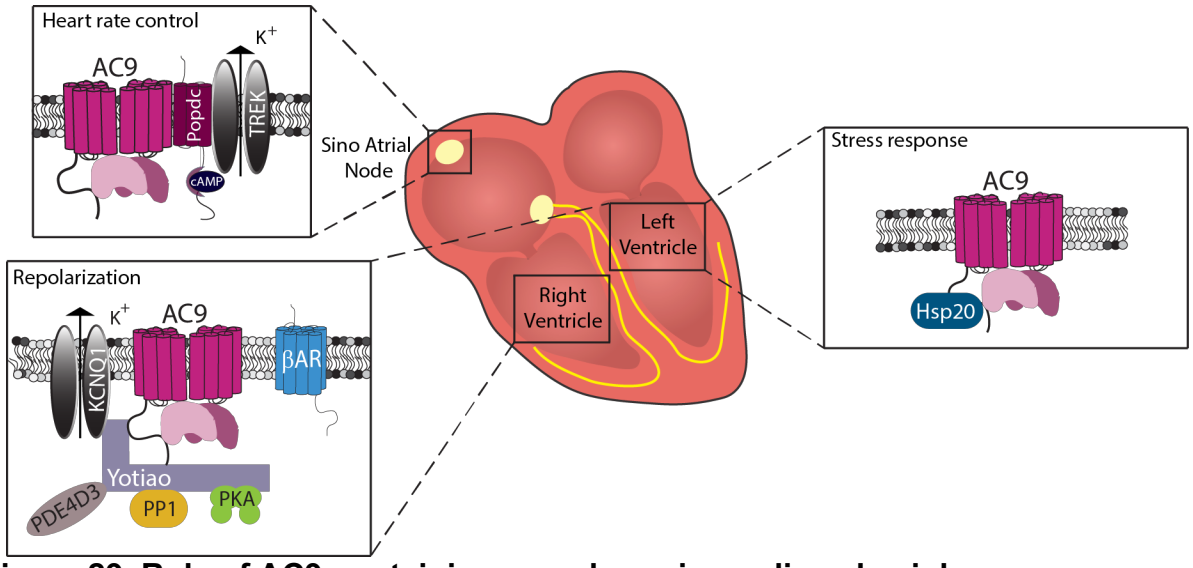

Figure 29. Role of AC9-containing complexes in cardiac physiology.

AC9 expression in the heart is observed in the sinoatrial node (SAN), left ventricle, and right atrium. Contributions of AC9 to cardiac function are dependent on tissue localization and complex formation. Interaction of AC9-Popdc-TREK is hypothesized to

contribute to heart rate control in the SAN. Whereas in the left ventricle AC9-Hsp20 is predicted to play a role in cardiac stress response and the AC9-Yotiao-KNCQ1 complex contributes to repolarization in both ventricles. Parts of this figure are modified from: Baldwin, T. A., and C. W. Dessauer. 2018. Function of Adenylyl Cyclase in Heart: the AKAP Connection. J Cardiovasc Dev Dis 5. distributed under the Creative Commons Attribution License (CC BY 4.0) http://creativecommons.org/licenses/by/4.0/.

major cardiac AC isoforms (AC5 or AC6) significantly reduce total cAMP levels whereas, deletion of AC9 contributes minimally to total cardiac AC activity. Contributions of AC9 could only be revealed in the presence of SQ 22,536, a P-site inhibitor that display > 100 fold selectivity for AC5/6 compared to AC9 (Brand et al., 2013; Li et al., 2017b). Using cardiac membrane from WT or $AC9^{-/-}$ mice, Gs dose response curves were generated with SQ 22,536 revealing that AC9 represents ~3% of Gαs stimulated AC activity. It should be noted that this estimate represents the upper limit for AC9 contribution to total AC activity. Despite this, immunoprecipitated Yotiao associated AC activity, (Bauman et al., 2006; Kapiloff et al., 2009; Piggott et al., 2008), was abolished in $AC9^{-/-}$ heart lysates, confirming that in heart only AC9 can associated with Yotiao (Piggott et al., 2008). AKAP150 associated AC activity was unaltered in $AC9^{-/-}$; suggesting that AC5 and AC6 are the largest contributors of cAMP to the AKAP79/150 local pool (Efendiev et al., 2010; Nichols et al., 2010). Similar to alterations in total cAMP, $AC9^{-/-}$ minimally altered global PKA signaling, although it was important for specific signaling in local complexes. Basal phosphorylation of the small heat shock protein 20 (Hsp20) was reduced in $AC9^{-/-}$ heart lysates. AC9-Hsp20 association was demonstrated by immunoprecipitation and proximity ligation assays and shown the interaction occurs independently of Yotiao.

6.3.1 Cardiac repolarization (AC9-Yotiao-KCNQ1)

As the only cardiac AC isoform associated with the Yotiao-KCNQ1 complex, it was of interest to see whether evidence of AC9 contribution to cardiac repolarization could be observed *in vivo.* Patients with mutations in KCNQ1 (LQT1) have reported bradycardia phenotypes exacerbated by physical activity, swimming in particular (Schwartz et al., 2008; Swan et al., 1999). Although, resting bradycardia phenotypes are typically associated with LQT3,4, or 10 (Amin and Wilde, 2018). A bradycardia phenotype is observed in $AC9^{-/-}$ with no observed prolongation of the QT interval in anesthetized mice. Association of this phenotype with I_{Ks} in mice is complicated. While the I_{Ks} channel is critical for late phase repolarization in humans and AC9 association with Yotiao sensitizes phosphorylation of I_{Ks} *in vitro*, adult mice do not express a functional channel (Honore et al., 1991; Marx et al., 2002; Salama et al., 2009). It is possible the observed bradycardia results from alterations in an unidentified Yotiao-AC9 associated potassium channel. Possible candidates include I_K type channels expressed in mouse, $I_{K,\ slow1/2}$ (Nerbonne and Kass, 2005). Expression of dominant negative $I_{K,\ slow1}$ or $I_{K,\ slow2}$ in mouse both result in prolonged QT intervals (Li et al., 2004; Xu et al., 1999).

Clinically, beta blockers are used to treat LQTS (Schwartz, 2006) with a high degree of success (Hobbs et al., 2006; Itoh et al., 2001), but do not abrogate symptoms for all patients (Priori et al., 2004). Recent efforts to treat arrhythmias have focus on defining macromolecular complexes that modulate ion channel function. AC9 enhances I_{Ks} channel activity when bound to Yotiao by sensitizing PKA phosphorylation of KCNQ1 in response to β adrenergic stimulation *in vitro* (Li et al., 2012). It is conceivable that AC9 could be targeted for treatment of LQTS. While conceivable, effectiveness would be dependent on type of LQTS. Targeting AC9 activity could not overcome disruption of

macromolecular complex formation in mutations that disrupt the binding of Yotiao and KCNQ1.

6.3.2 Cardiac stress (AC9-Hsp20)

Hsp20 has a well-documented cardioprotective role in heart, protecting against various insults including doxorubicin cardiotoxicity, ischemia/reperfusion injury, and prolonged beta-agonist induced hypertrophy (Fan et al., 2006; Fan et al., 2008; Martin et al., 2014). Hsp20 is phosphorylated by protein kinase A (PKA) in response to β-adrenergic stimulation is critical for its cardioprotective role. In response to chronic β-adrenergic stimulation Hsp20 phosphorylation confers cardioprotection by attenuating detrimental cardiac remodeling in mouse models (Fan et al., 2006). Hsp20 is also suggested to protect against human heart failure. Total and phosphorylated Hsp20 are upregulated in human failing hearts by ~2-fold compared controls (Qian et al., 2009). The phosphorylation level of Hsp20 is controlled and facilitated by formation of a macromolecular complex. Regulators of Hsp20 either bind directly (PP1(Qian et al., 2011) or to phosphodiesterase 4D (PDE4D) (Martin et al., 2014)), or complex with Hsp20 through the scaffold, A-kinase anchoring protein-Lbc (AKAP-Lbc) (Edwards et al., 2012a). The binding of PDE4D to Hsp20 decreases phosphorylation through degradation of cAMP; disrupting PDE4D-Hsp20 association enhances phosphorylation and protects against pathological remodeling (Martin et al., 2014). Binding to Hsp20 AKAP-Lbc promotes phosphorylation through coordinating PKA and is cardioprotective in neonatal rat cardiomyocytes (Edwards et al., 2012a). Cardioprotection by phosphorylated Hsp20 is suggested to occur by enhancing cardiac function through regulation of relaxation and contraction (Fan et al., 2005b). At the molecular level, Hsp20

influences calcium handling, promoting the phosphorylation of phospholamban (PLN) by inhibiting the activity of protein phosphatase 1 (PP1) (Qian et al., 2011).

AC9 interaction with Hsp20 adds an additional mode for controlling Hsp20 phosphorylation. Basal phosphorylation of Hsp20 at Ser16 is markedly reduced in AC9$^{-/-}$ mice. Whether AC9 associates with Hsp20 in a novel complex or with previously defined Hsp20 complexes is unclear. Although, Hsp20 associated activity is reduced in AC9$^{-/-}$ mice it is not abolished like Yotiao associated activity. We expected that Hsp20 interacts with other cardiac AC isoforms. Further evidence for AC9 maintaining phosphorylation levels of Hsp20 is observed in neonatal cardiomyocytes expressing catalytically inactive AC9 (AC9d), which attenuates isoproterenol induced phosphorylation of Hsp20. Expression of AC9d appears to work as a dominant negative disrupting Hsp20 association with endogenous WT AC9 and/or other AC isoforms.

Cardiac phenotyping of AC9$^{-/-}$ reveals altered diastolic relaxation with pulsed wave and tissue Doppler measurements. The E/A ratio is significantly reduced due primarily to attenuation of early filling phase velocity (E wave). Although diastolic dysfunction can be observed in LQT1 and LQT2 (Leren et al., 2015), I hesitate to speculate that diastolic dysfunction in AC9$^{-/-}$ mice is simply due to distorted channel regulation. Alternatively, AC9 dependent alterations in Hsp20 phosphorylation could underlie this phenotype. Cardiac remodeling and fibrosis also cause diastolic dysfunction from stiffening of the left ventricle. Hsp20 promotes pathological remodeling and fibrosis by facilitating protein kinase D1 (PKD1) translocation to the nucleus which initiates the fetal gene program (Sin et al., 2015). Disruption of this complex retards pathological phenotypes. The importance of Hsp20 phosphorylation in this process is unknown.

Additional evidence for a cardioprotective role of AC9 comes from observations of upregulated levels of the micro RNA which regulates AC9 (miR-142-3p) in human (non-ischemic dilated cardiomyopathy) and mouse model (hypertrophic cardiomyopathy) cardiac pathologies (Bagnall et al., 2012; Baskerville and Bartel, 2005; Tijsen et al., 2012; Voellenkle et al., 2010).

6.3.3 Heart rate control (AC9-Popdc-TREK)

The AC9-Yotiao-I_K complex represents one possible mechanism underlying the bradycardia phenotype. Another possibility is the AC9-Popdc-TREK complex. TREK functions as a leak potassium channel that maintains the resting membrane potential in addition to modulating action potentials (Honore et al., 1991) and has recently been shown to be important for maintaining sinoatrial node excitability in mice (Unudurthi et al., 2016). Popdc promotes localization of TREK at the plasma membrane increasing channel activity two-fold (Froese et al., 2012). These effects are lost when Popdc binds cAMP. TREK currents are also attenuated by PKA phosphorylation (Terrenoire et al., 2001). It has been suggested that the effect of cAMP bound Popdc represents a second mechanism for reducing TREK current (Froese et al., 2012). It may be hypothesized that AC9 drives one or both of these mechanisms by enhancing cAMP binding to Popdc and PKA phosphorylation of the channel. Additionally, I would add to this and hypothesis that cAMP bound Popdc-AC interactions create a negative feedback loop that could contribute to spatial and temporal components of this signaling pathway. Contrary to what I would have predicted, the TREK knockout mice display a bradycardia phenotype. Although, authors conclude that this phenotype is due to compensatory changes in sympathetic and parasympathetic regulation as the intrinsic heart rate is unaltered (Unudurthi et al., 2016).

6.4 Future directions

As the most divergent membrane bound AC, my further exploration in to the regulation and physiological roles of AC9 have opened the door to novel and exciting research questions in the AC signaling field.

First, an understanding of AC9 regulation *in vivo* is still in its infancy. It was surprising that my findings suggest only Gαs directly regulates AC9. All of the other membrane bound isoforms have multiple regulation mechanisms (Dessauer et al., 2017). Initial looks into AC9 regulation utilized whole cell assay which could have provided components necessary for direct or indirect AC9 regulation such as scaffolds. While I have clearly shown AC9 is not inhibited by Gαi/o, other modes of AC9 regulation were not as closely examined and could simply require a scaffold to localize AC9 with the upstream regulator. It is also possible that additional regulators of AC9 have not been identified. The ability of AC9 to homo- and heterodimerization is particularly intriguing although at this time I can only speculate that this may contribute to overall complex regulation or AC9 regulation and subsequent production of local cAMP pools. Identifying the binding sites of oligomerization is particularly important for further examination of these complexes.

While intriguing, the observed bradycardia phenotype in AC9$^{-/-}$ mice requires further validation. The caveat to the described heart rate measurements is that they were conducted with anesthetized mice; anesthesia has well known effects on heart rate (Ho et al., 2011). Currently, studies are underway to implant telemetry units to determine whether the bradycardia phenotype can be recapitulated in a conscious mouse model. We will not only examine alterations in basal heart rate but utilize various stressors (treadmill, forced swim test, and isoproterenol injection) to see whether AC9 knockout

also displays a stress induced bradycardia similar to Popdc knockout (Froese et al., 2012). It is also unclear whether the observed diastolic dysfunction in $AC9^{-/-}$ is due to alterations in repolarization and subsequent mechanical dysfunction (De Ferrari and Schwartz, 2009; Haugaa et al., 2009), Hsp20 dependent fibrosis (Fan et al., 2006; Martin et al., 2014; Sin et al., 2015), or an alternative mechanism.

A role for AC9 in cardioprotection was postulated based upon alterations of basal Hsp20 phosphorylation. The importance of Hsp20 phosphorylation has primarily been established in response to cardiac stress models (prolong β-agonist stimulation, transverse aortic construction, ischemia/reperfusion, and cardiotoxic drugs), further studies should examine whether AC9 is cardioprotective in similar stress models and determine whether there are other proteins associated with this complex.

The absence of I_{Ks} in adult mice allowed me to evaluate whether AC9 has alterative roles in cardiac function outside of sensitizing I_{Ks} phosphorylation. Although, this complicated the analysis of whether AC9 contributed to cardiac repolarization. The importance of AC9 for sensitizing phosphorylation of I_{Ks} and repolarization *in vivo* still needs to be evaluated. Current work by others in the lab is using a transgenic I_{Ks} mouse model crossed with $AC9^{-/-}$ to examine this.

My findings indicate Popdc is a novel AC scaffold, regulator, and downstream effector synthesized into one protein. While AKAPs are the most studied AC scaffold they function as a scaffold that regulates ACs indirectly via scaffolding of PKA, and anchor downstream effectors. There are a number of important questions to ask in regard to this interaction. How to Popdc-AC interact? My findings would indicate this likely occurs through the Popdc transmembrane domains or near transmembrane domain. Do ACs bind to Popdc homo- or heterodimers (Knight et al., 2003; Schindler,

2013; Vasavada et al., 2004)? The presented findings are evaluated in HEK293 cells, which endogenously express Popdc1. It is possible that the interaction of ACs with Popdc2 in this system could be dependent on Popdc1-Popdc2 heterodimers. Popdc also represents the first direct negative regulator of AC9. Further studies are required to understand the mechanism of Popdc inhibition and how cAMP contributes to this. Additionally, Popdcs facilitates membrane localization of TREK and binds various proteins involved in trafficking. It would also be of interest to see whether Popdc alters membrane localization or trafficking of ACs.

In summary, my findings show definitively that AC9 is not inhibited by Gαi/o and suggest that regulation by Gβγ, PKCβII, or CaMKII occur indirectly. Interestingly, AC9 can form both homodimers and heterodimers with Gαi/o sensitive isoforms (AC5/6); although, the physiological relevance of these interactions is unclear. In heart, deletion of AC9 results in bradycardia and diastolic dysfunction phenotypes likely due to the disruption of AC9 containing complexes. Despite contributing minimally to global cAMP in heart, our evidence suggests that AC9 containing complexes are critical for distinct components of cardiac physiology. AC9 is the only isoform that contributes to cAMP synthesis in Yotiao-dependent complexes, which are essential for cardiac repolarization. The importance of this interaction to facilitate signaling is further emphasized by the decreased sensitivity of AC9 to Gαs observed *in vitro*. Additionally, AC9 contributes to basal AC activity that regulates baseline phosphorylation of Hsp20 and cardiac stress response. My findings also suggest a mechanism for AC9 involvement in heart rate control through an interaction with Popdc, which we propose is a novel regulator and scaffold of AC. Overall, my work supports the idea that the role and regulation of AC9 is fundamentally driven through associations with various macromolecular complexes.

Bibliography

Ackerman MJ and Mohler PJ (2010) Defining a new paradigm for human arrhythmia syndromes: phenotypic manifestations of gene mutations in ion channel- and transporter-associated proteins. *Circ Res* **107**(4): 457-465.

Alcalay Y, Hochhauser E, Kliminski V, Dick J, Zahalka MA, Parnes D, Schlesinger H, Abassi Z, Shainberg A, Schindler RF, Brand T and Kessler-Icekson G (2013) Popeye domain containing 1 (Popdc1/Bves) is a caveolae-associated protein involved in ischemia tolerance. *PLoS One* **8**(9): e71100.

Alig J, Marger L, Mesirca P, Ehmke H, Mangoni ME and Isbrandt D (2009) Control of heart rate by cAMP sensitivity of HCN channels. *Proc Natl Acad Sci U S A* **106**(29): 12189-12194.

Amin AS and Wilde AM (2018) Inheritable Potassium Channel Diseases, in *Cardiac Electrophysiology: From Cell to Bedside* pp 494-503, Elsevier.

Andree B, Fleige A, Hillemann T, Arnold HH, Kessler-Icekson G and Brand T (2002) Molecular and functional analysis of Popeye genes: A novel family of transmembrane proteins preferentially expressed in heart and skeletal muscle. *Exp Clin Cardiol* **7**(2-3): 99-103.

Andree B, Hillemann T, Kessler-Icekson G, Schmitt-John T, Jockusch H, Arnold HH and Brand T (2000) Isolation and characterization of the novel popeye gene family expressed in skeletal muscle and heart. *Dev Biol* **223**(2): 371-382.

Antoni FA (2006) Adenylyl cyclase type 9. *UCSD-Nature Molecule Pages*(doi:10.1038/mp.a000131.01): doi:10.1038/mp.a000131.000101

Antoni FA, Barnard RJO, Shipston MJ, Smith SM, Simpson J and Paterson JM (1995) Calcineurin Feedback Inhibition of Agonist-evoked cAMP Formation. *J Biol Chem* **270**(47): 28055-28061.

Antoni FA, Palkovits M, Simpson J, Smith SM, Leitch AL, Rosie R, Fink G and Paterson JM (1998) Ca2+/calcineurin-inhibited adenylyl cyclase, highly abundant in forebrain regions, is important for learning and memory. *Journal of Neuroscience* **18**(23): 9650-9661.

Antos CL, Frey N, Marx SO, Reiken S, Gaburjakova M, Richardson JA, Marks AR and Olson EN (2001) Dilated cardiomyopathy and sudden death resulting from constitutive activation of protein kinase a. *Circ Res* **89**(11): 997-1004.

Bagnall RD, Tsoutsman T, Shephard RE, Ritchie W and Semsarian C (2012) Global MicroRNA Profiling of the Mouse Ventricles during Development of Severe Hypertrophic Cardiomyopathy and Heart Failure. *PLoS One* **7**(9): e44744.

Bakalyar HA and Reed RR (1990) Identification of a specialized adenylyl cyclase that may mediate odorant detection. *Science* **250**(4986): 1403-1406.

Baskerville S and Bartel DP (2005) Microarray profiling of microRNAs reveals frequent coexpression with neighboring miRNAs and host genes. *RNA* **11**(3): 241-247.

Bauman AL, Soughayer J, Nguyen BT, Willoughby D, Carnegie GK, Wong W, Hoshi N, Langeberg LK, Cooper DM, Dessauer CW and Scott JD (2006) Dynamic regulation of cAMP synthesis through anchored PKA-adenylyl cyclase V/VI complexes. *Molecular Cell* **23**(6): 925-931.

Bavencoffe A, Li Y, Wu Z, Yang Q, Herrera J, Kennedy EJ, Walters ET and Dessauer CW (2016) Persistent Electrical Activity in Primary Nociceptors after Spinal Cord Injury Is Maintained by Scaffolded Adenylyl Cyclase and Protein Kinase A and Is

Associated with Altered Adenylyl Cyclase Regulation. *J Neurosci* **36**(5): 1660-1668.

Beall A, Bagwell D, Woodrum D, Stoming TA, Kato K, Suzuki A, Rasmussen H and Brophy CM (1999) The small heat shock-related protein, HSP20, is phosphorylated on serine 16 during cyclic nucleotide-dependent relaxation. *J Biol Chem* **274**(16): 11344-11351.

Benesh EC, Miller PM, Pfaltzgraff ER, Grega-Larson NE, Hager HA, Sung BH, Qu X, Baldwin HS, Weaver AM and Bader DM (2013) Bves and NDRG4 regulate directional epicardial cell migration through autocrine extracellular matrix deposition. *Mol Biol Cell* **24**(22): 3496-3510.

Berndt SI, Gustafsson S, Magi R, Ganna A, Wheeler E, Feitosa MF, Justice AE, Monda KL, Croteau-Chonka DC, Day FR, Esko T, Fall T, Ferreira T, Gentilini D, Jackson AU, Luan Ja, Randall JC, Vedantam S, Willer CJ, Winkler TW, Wood AR, Workalemahu T, Hu Y-J, Lee SH, Liang L, Lin D-Y, Min JL, Neale BM, Thorleifsson G, Yang J, Albrecht E, Amin N, Bragg-Gresham JL, Cadby G, den Heijer M, Eklund N, Fischer K, Goel A, Hottenga J-J, Huffman JE, Jarick I, Johansson A, Johnson T, Kanoni S, Kleber ME, Konig IR, Kristiansson K, Kutalik Z, Lamina C, Lecoeur C, Li G, Mangino M, McArdle WL, Medina-Gomez C, Muller-Nurasyid M, Ngwa JS, Nolte IM, Paternoster L, Pechlivanis S, Perola M, Peters MJ, Preuss M, Rose LM, Shi J, Shungin D, Smith AV, Strawbridge RJ, Surakka I, Teumer A, Trip MD, Tyrer J, Van Vliet-Ostaptchouk JV, Vandenput L, Waite LL, Zhao JH, Absher D, Asselbergs FW, Atalay M, Attwood AP, Balmforth AJ, Basart H, Beilby J, Bonnycastle LL, Brambilla P, Bruinenberg M, Campbell H, Chasman DI, Chines PS, Collins FS, Connell JM, Cookson WO, de Faire U,

de Vegt F, Dei M, Dimitriou M, Edkins S, Estrada K, Evans DM, Farrall M, Ferrario MM, Ferrieres J, Franke L, Frau F, Gejman PV, Grallert H, Gronberg H, Gudnason V, Hall AS, Hall P, Hartikainen A-L, Hayward C, Heard-Costa NL, Heath AC, Hebebrand J, Homuth G, Hu FB, Hunt SE, Hypponen E, Iribarren C, Jacobs KB, Jansson J-O, Jula A, Kahonen M, Kathiresan S, Kee F, Khaw K-T, Kivimaki M, Koenig W, Kraja AT, Kumari M, Kuulasmaa K, Kuusisto J, Laitinen JH, Lakka TA, Langenberg C, Launer LJ, Lind L, Lindstrom J, Liu J, Liuzzi A, Lokki M-L, Lorentzon M, Madden PA, Magnusson PK, Manunta P, Marek D, Marz W, Leach IM, McKnight B, Medland SE, Mihailov E, Milani L, Montgomery GW, Mooser V, Muhleisen TW, Munroe PB, Musk AW, Narisu N, Navis G, Nicholson G, Nohr EA, Ong KK, Oostra BA, Palmer CNA, Palotie A, Peden JF, Pedersen N, Peters A, Polasek O, Pouta A, Pramstaller PP, Prokopenko I, Putter C, Radhakrishnan A, Raitakari O, Rendon A, Rivadeneira F, Rudan I, Saaristo TE, Sambrook JG, Sanders AR, Sanna S, Saramies J, Schipf S, Schreiber S, Schunkert H, Shin S-Y, Signorini S, Sinisalo J, Skrobek B, Soranzo N, Stancakova A, Stark K, Stephens JC, Stirrups K, Stolk RP, Stumvoll M, Swift AJ, Theodoraki EV, Thorand B, Tregouet D-A, Tremoli E, Van der Klauw MM, van Meurs JBJ, Vermeulen SH, Viikari J, Virtamo J, Vitart V, Waeber G, Wang Z, Widen E, Wild SH, Willemsen G, Winkelmann BR, Witteman JCM, Wolffenbuttel BHR, Wong A, Wright AF, Zillikens MC, Amouyel P, Boehm BO, Boerwinkle E, Boomsma DI, Caulfield MJ, Chanock SJ, Cupples LA, Cusi D, Dedoussis GV, Erdmann J, Eriksson JG, Franks PW, Froguel P, Gieger C, Gyllensten U, Hamsten A, Harris TB, Hengstenberg C, Hicks AA, Hingorani A, Hinney A, Hofman A, Hovingh KG, Hveem K, Illig T, Jarvelin M-R, Jockel K-H, Keinanen-

Kiukaanniemi SM, Kiemeney LA, Kuh D, Laakso M, Lehtimaki T, Levinson DF, Martin NG, Metspalu A, Morris AD, Nieminen MS, Njolstad I, Ohlsson C, Oldehinkel AJ, Ouwehand WH, Palmer LJ, Penninx B, Power C, Province MA, Psaty BM, Qi L, Rauramaa R, Ridker PM, Ripatti S, Salomaa V, Samani NJ, Snieder H, Sorensen TIA, Spector TD, Stefansson K, Tonjes A, Tuomilehto J, Uitterlinden AG, Uusitupa M, van der Harst P, Vollenweider P, Wallaschofski H, Wareham NJ, Watkins H, Wichmann HE, Wilson JF, Abecasis GR, Assimes TL, Barroso I, Boehnke M, Borecki IB, Deloukas P, Fox CS, Frayling T, Groop LC, Haritunian T, Heid IM, Hunter D, Kaplan RC, Karpe F, Moffatt MF, Mohlke KL, O'Connell JR, Pawitan Y, Schadt EE, Schlessinger D, Steinthorsdottir V, Strachan DP, Thorsteinsdottir U, van Duijn CM, Visscher PM, Di Blasio AM, Hirschhorn JN, Lindgren CM, Morris AP, Meyre D, Scherag A, McCarthy MI, Speliotes EK, North KE, Loos RJF and Ingelsson E (2013) Genome-wide meta-analysis identifies 11 new loci for anthropometric traits and provides insights into genetic architecture. *Nature genetics* **45**(5): 501-512.

Braeunig JH, Schweda F, Han PL and Seifert R (2013) Similarly potent inhibition of adenylyl cyclase by P-site inhibitors in hearts from wild type and AC5 knockout mice. *PLoS One* **8**(7): e68009.

Brand CS, Hocker HJ, Gorfe AA, Cavasotto CN and Dessauer CW (2013) Isoform selectivity of adenylyl cyclase inhibitors: characterization of known and novel compounds. *J Pharmacol Exp Ther* **347**(2): 265-275.

Brand CS, Sadana R, Malik S, Smrcka AV and Dessauer CW (2015) Adenylyl Cyclase 5 Regulation by Gbetagamma Involves Isoform-Specific Use of Multiple Interaction Sites. *Mol Pharmacol* **88**(4): 758-767.

Brand T (2018) The Popeye Domain Containing Genes and Their Function as cAMP Effector Proteins in Striated Muscle. *J Cardiovasc Dev Dis* **5**(1).

Brand T, Simrick SL, Poon KL and Schindler RF (2014) The cAMP-binding Popdc proteins have a redundant function in the heart. *Biochem Soc Trans* **42**(2): 295-301.

Bravo CA, Vatner DE, Pachon R, Zhang J and Vatner SF (2016) A Food and Drug Administration-Approved Antiviral Agent that Inhibits Adenylyl Cyclase Type 5 Protects the Ischemic Heart Even When Administered after Reperfusion. *J Pharmacol Exp Ther* **357**(2): 331-336.

Bronte V and Pittet MJ (2013) The spleen in local and systemic regulation of immunity. *Immunity* **39**(5): 806-818.

Chen L, Marquardt ML, Tester DJ, Sampson KJ, Ackerman MJ and Kass RS (2007) Mutation of an A-kinase-anchoring protein causes long-QT syndrome. *Proc Natl Acad Sci U S A* **104**(52): 20990-20995.

Chen Y, Harry A, Li J, Smit MJ, Bai X, Magnusson R, Pieroni JP, Weng G and Iyengar R (1997) Adenylyl cyclase 6 is selectively regulated by protein kinase A phosphorylation in a region involved in Galphas stimulation. *Proc Natl Acad Sci U S A* **94**(25): 14100.

Chen YZ, Friedman JR, Chen DH, Chan GC, Bloss CS, Hisama FM, Topol SE, Carson AR, Pham PH, Bonkowski ES, Scott ER, Lee JK, Zhang G, Oliveira G, Xu J, Scott-Van Zeeland AA, Chen Q, Levy S, Topol EJ, Storm D, Swanson PD, Bird TD, Schork NJ, Raskind WH and Torkamani A (2014) Gain-of-function ADCY5 mutations in familial dyskinesia with facial myokymia. *Ann Neurol* **75**(4): 542-549.

Chen YZ, Matsushita MM, Robertson P, Rieder M, Girirajan S, Antonacci F, Lipe H, Eichler EE, Nickerson DA, Bird TD and Raskind WH (2012) Autosomal dominant familial dyskinesia and facial myokymia: single exome sequencing identifies a mutation in adenylyl cyclase 5. *Arch Neurol* **69**(5): 630-635.

Chen-Goodspeed M, Lukan AN and Dessauer CW (2005) Modeling of G alpha(s) and G alpha(i) regulation of human type V and VI adenylyl cyclase. *J Biol Chem* **280**(3): 1808-1816.

Cumbay MG and Watts VJ (2004) Novel Regulatory Properties of Human Type 9 Adenylate Cyclase. *J Pharmacol Exp Ther* **310**(1): 108-115.

Cumbay MG and Watts VJ (2005) Galphaq potentiation of adenylate cyclase type 9 activity through a Ca2+/calmodulin-dependent pathway. *Biochem Pharmacol* **69**(8): 1247-1256.

de Rooji J, Zwartkruis FJT, Verheijen MHG, Cool RH, Nijman SMB, Wittinghofer A and Bos JL (1998) Epac is a Rap1 guanine-nucleotide-exchange factor directly activated by cyclic AMP. *Nature* **396**: 474-477.

De Ferrari GM and Schwartz PJ (2009) Long QT syndrome, a purely electrical disease? Not anymore. *Eur Heart J* **30**(3): 253-255.

Delcarpio JB, Claycomb WC and Moses RL (1989) Ultrastructural morphometric analysis of cultured neonatal and adult rat ventricular cardiac muscle cells. *Am J Anat* **186**(4): 335-345.

Dessauer CW (2002) Kinetic analysis of the action of P-site analogs. *Methods in Enzymology* **345**: 112-126.

Dessauer CW (2009) Adenylyl cyclase--A-kinase anchoring protein complexes: the next dimension in cAMP signaling. *Mol Pharmacol* **76**(5): 935-941.

Dessauer CW, Scully TT and Gilman AG (1997) Interactions of forskolin and ATP with the cytosolic domains of mammalian adenylyl cyclase. *J Biol Chem* **272**(35): 22272-22277.

Dessauer CW, Tesmer JJ, Sprang SR and Gilman AG (1998) Identification of a Gialpha binding site on type V adenylyl cyclase. *J Biol Chem* **273**(40): 25831-25839.

Dessauer CW, Watts VJ, Ostrom RS, Conti M, Dove S and Seifert R (2017) International Union of Basic and Clinical Pharmacology. CI. Structures and Small Molecule Modulators of Mammalian Adenylyl Cyclases. *Pharmacol Rev* **69**(2): 93-139.

Diel S, Klass K, Wittig B and Kleuss C (2006) Gbetagamma activation site in adenylyl cyclase type II. Adenylyl cyclase type III is inhibited by Gbetagamma. *J Biol Chem* **281**(1): 288-294.

Dodge KL, Khouangsathiene S, Kapiloff MS, Mouton R, Hill EV, Houslay MD, Langeberg LK and Scott JD (2001) mAKAP assembles a protein kinase A/PDE4 phosphodiesterase cAMP signaling module. *EMBO Journal* **20**(8): 1921-1930.

Dodge-Kafka KL, Bauman A, Mayer N, Henson E, Heredia L, Ahn J, McAvoy T, Nairn AC and Kapiloff MS (2010) cAMP-stimulated protein phosphatase 2A activity associated with muscle A kinase-anchoring protein (mAKAP) signaling complexes inhibits the phosphorylation and activity of the cAMP-specific phosphodiesterase PDE4D3. *J Biol Chem* **285**(15): 11078-11086.

Dodge-Kafka KL, Soughayer J, Pare GC, Carlisle Michel JJ, Langeberg LK, Kapiloff MS and Scott JD (2005) The protein kinase A anchoring protein mAKAP coordinates two integrated cAMP effector pathways. *Nature* **437**(7058): 574-578.

Duggal P, Vesely MR, Wattanasirichaigoon D, Villafane J, Kaushik V and Beggs AH (1998) Mutation of the gene for IsK associated with both Jervell and Lange-

Nielsen and Romano-Ward forms of Long-QT syndrome. *Circulation* **97**(2): 142-146.

Edwards HV, Scott JD and Baillie GS (2012a) The A-kinase-anchoring protein AKAP-Lbc facilitates cardioprotective PKA phosphorylation of Hsp20 on Ser(16). *Biochem J* **446**(3): 437-443.

Edwards HV, Scott JD and Baillie GS (2012b) PKA phosphorylation of the small heat-shock protein Hsp20 enhances its cardioprotective effects. *Biochem Soc Trans* **40**(1): 210-214.

Efendiev R, Bavencoffe A, Hu H, Zhu MX and Dessauer CW (2013) Scaffolding by A-kinase anchoring protein enhances functional coupling between adenylyl cyclase and TRPV1 channel. *J Biol Chem* **288**(6): 3929-3937.

Efendiev R and Dessauer CW (2011) A kinase-anchoring proteins and adenylyl cyclase in cardiovascular physiology and pathology. *J Cardiovasc Pharmacol* **58**(4): 339-344.

Efendiev R, Samelson BK, Nguyen BT, Phatarpekar PV, Baameur F, Scott JD and Dessauer CW (2010) AKAP79 interacts with multiple adenylyl cyclase (AC) isoforms and scaffolds AC5 and -6 to alpha-amino-3-hydroxyl-5-methyl-4-isoxazole-propionate (AMPA) receptors. *J Biol Chem* **285**(19): 14450-14458.

Ejendal KF, Conley JM, Hu CD and Watts VJ (2013) Bimolecular fluorescence complementation analysis of G protein-coupled receptor dimerization in living cells. *Methods Enzymol* **521**: 259-279.

Escobar M, Cardenas C, Colavita K, Petrenko NB and Franzini-Armstrong C (2011) Structural evidence for perinuclear calcium microdomains in cardiac myocytes. *J Mol Cell Cardiol* **50**(3): 451-459.

Fan GC, Chu G and Kranias EG (2005a) Hsp20 and its cardioprotection. *Trends Cardiovasc Med* **15**(4): 138-141.

Fan GC, Chu G, Mitton B, Song Q, Yuan Q and Kranias EG (2004) Small heat-shock protein Hsp20 phosphorylation inhibits beta-agonist-induced cardiac apoptosis. *Circulation Research* **94**(11): 1474.

Fan GC, Ren X, Qian J, Yuan Q, Nicolaou P, Wang Y, Jones WK, Chu G and Kranias EG (2005b) Novel cardioprotective role of a small heat-shock protein, Hsp20, against ischemia/reperfusion injury. *Circulation* **111**(14): 1792-1799.

Fan GC, Yuan Q, Song G, Wang Y, Chen G, Qian J, Zhou X, Lee YJ, Ashraf M and Kranias EG (2006) Small heat-shock protein Hsp20 attenuates beta-agonist-mediated cardiac remodeling through apoptosis signal-regulating kinase 1. *Circ Res* **99**(11): 1233-1242.

Fan GC, Zhou X, Wang X, Song G, Qian J, Nicolaou P, Chen G, Ren X and Kranias EG (2008) Heat shock protein 20 interacting with phosphorylated Akt reduces doxorubicin-triggered oxidative stress and cardiotoxicity. *Circ Res* **103**(11): 1270-1279.

Fink MA, Zakhary DR, Mackey JA, Desnoyer RW, Apperson-Hansen C, Damron DS and Bond M (2001) AKAP-Mediated Targeting of Protein Kinase A Regulates Contractility in Cardiac Myocytes. *Circulation Research* **88**(3): 291-297.

Froese A and Brand T (2008) Expression pattern of Popdc2 during mouse embryogenesis and in the adult. *Dev Dyn* **237**(3): 780-787.

Froese A, Breher SS, Waldeyer C, Schindler RF, Nikolaev VO, Rinne S, Wischmeyer E, Schlueter J, Becher J, Simrick S, Vauti F, Kuhtz J, Meister P, Kreissl S, Torlopp A, Liebig SK, Laakmann S, Muller TD, Neumann J, Stieber J, Ludwig A, Maier

SK, Decher N, Arnold HH, Kirchhof P, Fabritz L and Brand T (2012) Popeye domain containing proteins are essential for stress-mediated modulation of cardiac pacemaking in mice. *J Clin Invest* **122**(3): 1119-1130.

Gao B and Gilman AG (1991) Cloning and expression of a widely distributed (type IV) adenylyl cyclase. *Proceedings of the National Academy of Sciences in the United States of America* **88**: 10178.

Gao M, Ping P, Post S, Insel PA, Tang R and Hammond HK (1998) Increased expression of adenylylcyclase type VI proportionately increases beta-adrenergic receptor-stimulated production of cAMP in neonatal rat cardiac myocytes. *Proc Natl Acad Sci U S A* **95**(3): 1038-1043.

Gao MH, Lai NC, Giamouridis D, Kim YC, Guo T and Hammond HK (2017) Cardiac-directed expression of a catalytically inactive adenylyl cyclase 6 protects the heart from sustained beta-adrenergic stimulation. *PLoS One* **12**(8): e0181282.

Gao T, Puri TS, Gerhardstein BL, Chien AJ, Green RD and Hosey MM (1997) Identification and subcellular localization of the subunits of L-type calcium channels and adenylyl cyclase in cardiac myocytes. *Journal of Biological Chemistry* **272**(31): 19401-19407.

Gao X, Sadana R, Dessauer CW and Patel TB (2007) Conditional stimulation of type V and VI adenylyl cyclases by G protein beta gamma subunits. *J Biol Chem* **282**(1): 294-302.

Gu C, Cali JJ and Cooper DM (2002) Dimerization of mammalian adenylate cyclases. *European Journal of Biochemistry* **269**(2): 413.

Guellich A, Gao S, Hong C, Yan L, Wagner TE, Dhar SK, Ghaleh B, Hittinger L, Iwatsubo K, Ishikawa Y, Vatner SF and Vatner DE (2010) Effects of cardiac overexpression

of type 6 adenylyl cyclase affects on the response to chronic pressure overload. *Am J Physiol Heart Circ Physiol* **299**(3): H707-712.

Hacker BM, Tomlinson JE, Wayman GA, Sultana R, Chan G, Villacres E, Disteche C and Storm DR (1998) Cloning, Chromosomal Mapping, and Regulatory Properties of the Human Type 9 Adenylyl Cyclase (ADCY9). *Genomics* **50**(1): 97-104.

Hager HA, Roberts RJ, Cross EE, Proux-Gillardeaux V and Bader DM (2010) Identification of a novel Bves function: regulation of vesicular transport. *EMBO J* **29**(3): 532-545.

Hammond HK, Penny WF, Traverse JH, Henry TD, Watkins MW, Yancy CW, Sweis RN, Adler ED, Patel AN, Murray DR, Ross RS, Bhargava V, Maisel A, Barnard DD, Lai NC, Dalton ND, Lee ML, Narayan SM, Blanchard DG and Gao MH (2016) Intracoronary Gene Transfer of Adenylyl Cyclase 6 in Patients With Heart Failure: A Randomized Clinical Trial. *JAMA Cardiol* **1**(2): 163-171.

Haugaa KH, Edvardsen T, Leren TP, Gran JM, Smiseth OA and Amlie JP (2009) Left ventricular mechanical dispersion by tissue Doppler imaging: a novel approach for identifying high-risk individuals with long QT syndrome. *Eur Heart J* **30**(3): 330-337.

Heijman J, Spatjens RL, Seyen SR, Lentink V, Kuijpers HJ, Boulet IR, de Windt LJ, David M and Volders PG (2012) Dominant-negative control of cAMP-dependent IKs upregulation in human long-QT syndrome type 1. *Circ Res* **110**(2): 211-219.

Ho D, Zhao X, Gao S, Hong C, Vatner DE and Vatner SF (2011) Heart Rate and Electrocardiography Monitoring in Mice. *Curr Protoc Mouse Biol* **1**: 123-139.

Hobbs JB, Peterson DR, Moss AJ, McNitt S, Zareba W, Goldenberg I, Qi M, Robinson JL, Sauer AJ, Ackerman MJ, Benhorin J, Kaufman ES, Locati EH, Napolitano C, Priori SG, Towbin JA, Vincent GM and Zhang L (2006) Risk of aborted cardiac arrest or sudden cardiac death during adolescence in the long-QT syndrome. *JAMA* **296**(10): 1249-1254.

Honore E, Attali B, Romey G, Heurteaux C, Ricard P, Lesage F, Lazdunski M and Barhanin J (1991) Cloning, expression, pharmacology and regulation of a delayed rectifier K+ channel in mouse heart. *EMBO J* **10**(10): 2805-2811.

Hu CL, Chandra R, Ge H, Pain J, Yan L, Babu G, Depre C, Iwatsubo K, Ishikawa Y, Sadoshima J, Vatner SF and Vatner DE (2009) Adenylyl cyclase type 5 protein expression during cardiac development and stress. *Am J Physiol Heart Circ Physiol* **297**(5): H1776-1782.

Huttlin EL, Ting L, Bruckner RJ, Gebreab F, Gygi MP, Szpyt J, Tam S, Zarraga G, Colby G, Baltier K, Dong R, Guarani V, Vaites LP, Ordureau A, Rad R, Erickson BK, Wuhr M, Chick J, Zhai B, Kolippakkam D, Mintseris J, Obar RA, Harris T, Artavanis-Tsakonas S, Sowa ME, De Camilli P, Paulo JA, Harper JW and Gygi SP (2015) The BioPlex Network: A Systematic Exploration of the Human Interactome. *Cell* **162**(2): 425-440.

Ikoma E, Tsunematsu T, Nakazawa I, Shiwa T, Hibi K, Ebina T, Mochida Y, Toya Y, Hori H, Uchino K, Minamisawa S, Kimura K, Umemura S and Ishikawa Y (2003) Polymorphism of the type 6 adenylyl cyclase gene and cardiac hypertrophy. *J Cardiovasc Pharmacol* **42 Suppl 1**: S27-32.

International Mouse Knockout C, Collins FS, Rossant J and Wurst W (2007) A mouse for all reasons. *Cell* **128**(1): 9-13.

Iourgenko V, Kliot B, Cann MJ and Levin LR (1997) Cloning and characterization of a Drosophila adenylyl cyclase homologous to mammalian type IX. *FEBS Lett* **413**(1): 104-108.

Itoh T, Kikuchi K, Odagawa Y, Takata S, Yano K, Okada S, Haneda N, Ogawa S, Nakano O, Kawahara Y, Kasai H, Nakayama T, Fukutomi T, Sakurada H, Shimizu A, Yazaki Y, Nagai R, Nakamura Y and Tanaka T (2001) Correlation of genetic etiology with response to beta-adrenergic blockade among symptomatic patients with familial long-QT syndrome. *J Hum Genet* **46**(1): 38-40.

Iwami G, Kawabe J-i, Ebina T, Cannon PJ, Homcy CJ and Ishikawa Y (1995) Regulation of Adenylyl Cyclase by Protein Kinase A. *J Biol Chem* **270**(21): 12481-12484.

Iwatsubo K, Minamisawa S, Tsunematsu T, Nakagome M, Toya Y, Tomlinson JE, Umemura S, Scarborough RM, Levy DE and Ishikawa Y (2004) Direct inhibition of type 5 adenylyl cyclase prevents myocardial apoptosis without functional deterioration. *J Biol Chem* **279**(39): 40938-40945.

Kapiloff MS, Piggott LA, Sadana R, Li J, Heredia LA, Henson E, Efendiev R and Dessauer CW (2009) An adenylyl cyclase-mAKAPbeta signaling complex regulates cAMP levels in cardiac myocytes. *J Biol Chem* **284**(35): 23540-23546.

Kapiloff MS, Schillace RV, Westphal AM and Scott JD (1999) mAKAP: an A-kinase anchoring protein targeted to the nuclear membrane of differentiated myocytes. *J Cell Sci* **112**(16): 2725-2736.

Kawaguchi M, Hager HA, Wada A, Koyama T, Chang MS and Bader DM (2008) Identification of a novel intracellular interaction domain essential for Bves function. *PLoS One* **3**(5): e2261.

Kawasaki H, Springett GM, Mochizuki N, Toki S, Nakaya M, Matsuda M, Housman DE and Graybiel AM (1998) A Family of cAMP-Binding Proteins That Directly Activate Rap1. *Science* **282**.

Kirchmaier BC, Poon KL, Schwerte T, Huisken J, Winkler C, Jungblut B, Stainier DY and Brand T (2012) The Popeye domain containing 2 (popdc2) gene in zebrafish is required for heart and skeletal muscle development. *Dev Biol* **363**(2): 438-450.

Knight RF, Bader DM and Backstrom JR (2003) Membrane topology of Bves/Pop1A, a cell adhesion molecule that displays dynamic changes in cellular distribution during development. *J Biol Chem* **278**(35): 32872-32879.

Korfali N, Wilkie GS, Swanson SK, Srsen V, de Las Heras J, Batrakou DG, Malik P, Zuleger N, Kerr AR, Florens L and Schirmer EC (2012) The nuclear envelope proteome differs notably between tissues. *Nucleus* **3**(6): 552-564.

Kozasa T and Gilman AG (1995) Purification of recombinant G proteins from Sf9 cells by hexa-histidine tagging of associated subunits. Characterization of a 12 and inhibition of adenylyl cyclase by a z *Journal of Biological Chemistry* **270**: 1734-1741.

Kritzer MD, Li J, Passariello CL, Gayanilo M, Thakur H, Dayan J, Dodge-Kafka K and Kapiloff MS (2014) The scaffold protein muscle A-kinase anchoring protein beta orchestrates cardiac myocyte hypertrophic signaling required for the development of heart failure. *Circ Heart Fail* **7**(4): 663-672.

Kurokawa J, Motoike HK, Rao J and Kass RS (2004) Regulatory actions of the A-kinase anchoring protein Yotiao on a heart potassium channel downstream of PKA phosphorylation (vol 101, pg 16374, 2004). *Proceedings of the National Academy of Sciences, USA* **101**(51): 17884-17884.

Lai NC, Tang T, Gao MH, Saito M, Takahashi T, Roth DM and Hammond HK (2008) Activation of cardiac adenylyl cyclase expression increases function of the failing ischemic heart in mice. *J Am Coll Cardiol* **51**(15): 1490-1497.

Landa LR, Jr., Harbeck M, Kaihara K, Chepurny O, Kitiphongspattana K, Graf O, Nikolaev VO, Lohse MJ, Holz GG and Roe MW (2005) Interplay of Ca2+ and cAMP signaling in the insulin-secreting MIN6 beta-cell line. *J Biol Chem* **280**(35): 31294-31302.

Lash LH and Jones DP (1993) *Methods in Toxicology: Mitochondrial Dysfunction*. Academic Press, San Diego, CA.

Lefkimmiatis K, Srikanthan M, Maiellaro I, Moyer MP, Curci S and Hofer AM (2009) Store-operated cyclic AMP signalling mediated by STIM1. *Nat Cell Biol* **11**(4): 433-442.

Leren IS, Hasselberg NE, Saberniak J, Håland TF, Kongsgård E, Smiseth OA, Edvardsen T and Haugaa KH (2015) Cardiac Mechanical Alterations and Genotype Specific Differences in Subjects With Long QT Syndrome. *JACC: Cardiovascular Imaging* **8**(5): 501-510.

Li H, Guo W, Yamada KA and Nerbonne JM (2004) Selective elimination of I(K,slow1) in mouse ventricular myocytes expressing a dominant negative Kv1.5alpha subunit. *Am J Physiol Heart Circ Physiol* **286**(1): H319-328.

Li J, Kritzer MD, Michel JJ, Le A, Thakur H, Gayanilo M, Passariello CL, Negro A, Danial JB, Oskouei B, Sanders M, Hare JM, Hanauer A, Dodge-Kafka K and Kapiloff MS (2013a) Anchored p90 ribosomal S6 kinase 3 is required for cardiac myocyte hypertrophy. *Circ Res* **112**(1): 128-139.

Li J, Negro A, Lopez J, Bauman AL, Henson E, Dodge-Kafka K and Kapiloff MS (2010) The mAKAPbeta scaffold regulates cardiac myocyte hypertrophy via recruitment of activated calcineurin. *J Mol Cell Cardiol* **48**(2): 387-394.

Li L, Li J, Drum BM, Chen Y, Yin H, Guo X, Luckey SW, Gilbert ML, McKnight GS, Scott JD, Santana LF and Liu Q (2017a) Loss of AKAP150 promotes pathological remodelling and heart failure propensity by disrupting calcium cycling and contractile reserve. *Cardiovasc Res* **113**(2): 147-159.

Li X, Nooh MM and Bahouth SW (2013b) Role of AKAP79/150 protein in beta1-adrenergic receptor trafficking and signaling in mammalian cells. *J Biol Chem* **288**(47): 33797-33812.

Li Y, Baldwin TA, Wang Y, Subramaniam J, Carbajal AG, Brand CS, Cunha SR and Dessauer CW (2017b) Loss of type 9 adenylyl cyclase triggers reduced phosphorylation of Hsp20 and diastolic dysfunction. *Scientific Reports* **7**(1): 5522.

Li Y, Chen L, Kass RS and Dessauer CW (2012) The A-kinase anchoring protein Yotiao facilitates complex formation between type 9 adenylyl cyclase and the IKs potassium channel in heart. *J Biol Chem* **287**(35): 29815-29824.

Li Y and Dessauer CW (2015) Identifying Complexes of Adenylyl Cyclase with A-kinase Anchoring Proteins, in *Cyclic Nucleotide Signaling* (Cheng X ed) pp 147-164, CRC Press, Boca Raton, FL.

Lin JW, Wyszynski M, Madhavan R, Sealock R, Kim JU and Sheng M (1998) Yotiao, a novel protein of neuromuscular junction and brain that interacts with specific splice variants of NMDA receptor subunit NR1. *Journal of Neuroscience* **18**(6): 2017-2027.

Linder ME, Middleton P, Hepler JR, Taussig R, Gilman AG and Mumby SM (1993) Lipid modifications of G proteins: à subunits are palmitoylated. *Proceedings of the National Academy of Sciences in the United States of America* **90**: 3675.

Linder ME, Pang IH, Duronio RJ, Gordon JI, Sternweis PC and Gilman AG (1991) Lipid modifications of G protein subunits. Myristoylation of G o à increases its affinity for áç. *Journal of Biological Chemistry* **266**: 4654.

Liu L, Das S, Losert W and Parent CA (2010) mTORC2 regulates neutrophil chemotaxis in a cAMP- and RhoA-dependent fashion. *Dev Cell* **19**(6): 845-857.

Liu L, Gritz D and Parent CA (2014) PKCbII acts downstream of chemoattractant receptors and mTORC2 to regulate cAMP production and myosin II activity in neutrophils. *Molecular Biology of the Cell*.

Mahadeo DC, Janka-Junttila M, Smoot RL, Roselova P and Parent CA (2007) A chemoattractant-mediated Gi-coupled pathway activates adenylyl cyclase in human neutrophils. *Mol Biol Cell* **18**(2): 512-522.

Martin TP, Hortigon-Vinagre MP, Findlay JE, Elliott C, Currie S and Baillie GS (2014) Targeted disruption of the heat shock protein 20-phosphodiesterase 4D (PDE4D) interaction protects against pathological cardiac remodelling in a mouse model of hypertrophy. *FEBS Open Bio* **4**: 923-927.

Marx SO, Kurokawa J, Reiken S, Motoike H, D'Armiento J, Marks AR and Kass RS (2002) Requirement of a macromolecular signaling complex for beta adrenergic receptor modulation of the KCNQ1-KCNE1 potassium channel. *Science* **295**(5554): 496-499.

Matheus AS, Tannus LR, Cobas RA, Palma CC, Negrato CA and Gomes MB (2013) Impact of diabetes on cardiovascular disease: an update. *Int J Hypertens* **2013**: 653789.

Mattick P, Parrington J, Odia E, Simpson A, Collins T and Terrar D (2007) Ca2+-stimulated adenylyl cyclase isoform AC1 is preferentially expressed in guinea-pig sino-atrial node cells and modulates the I(f) pacemaker current. *Journal of Physiology (London)* **582**(Pt 3): 1195-1203.

Metrich M, Laurent AC, Breckler M, Duquesnes N, Hmitou I, Courillau D, Blondeau JP, Crozatier B, Lezoualc'h F and Morel E (2010) Epac activation induces histone deacetylase nuclear export via a Ras-dependent signalling pathway. *Cell Signal* **22**(10): 1459-1468.

Mochizuki N, Ohba Y, Kiyokawa E, Kurata T, Murakami T, Ozaki T, Kitabatake A, Nagashima K and Matsuda M (1999) Activation of the ERK/MAPK pathway by an isoform of rap1GAP associated with G alpha(i). *Nature* **400**(6747): 891-894.

Nakano SJ, Sucharov J, van Dusen R, Cecil M, Nunley K, Wickers S, Karimpur-Fard A, Stauffer BL, Miyamoto SD and Sucharov CC (2017) Cardiac Adenylyl Cyclase and Phosphodiesterase Expression Profiles Vary by Age, Disease, and Chronic Phosphodiesterase Inhibitor Treatment. *J Card Fail* **23**(1): 72-80.

Navarro G, Cordomi A, Casado-Anguera V, Moreno E, Cai NS, Cortes A, Canela EI, Dessauer CW, Casado V, Pardo L, Lluis C and Ferre S (2018) Evidence for functional pre-coupled complexes of receptor heteromers and adenylyl cyclase. *Nat Commun* **9**(1): 1242.

Navedo MF, Nieves-Cintron M, Amberg GC, Yuan C, Votaw VS, Lederer WJ, McKnight GS and Santana LF (2008) AKAP150 Is Required for Stuttering Persistent Ca2+ Sparklets and Angiotensin II-Induced Hypertension. *Circ Res* **102**(2): e1-11.

Nerbonne JM and Kass RS (2005) Molecular physiology of cardiac repolarization. *Physiol Rev* **85**(4): 1205-1253.

Nichols CB, Rossow CF, Navedo MF, Westenbroek RE, Catterall WA, Santana LF and McKnight GS (2010) Sympathetic stimulation of adult cardiomyocytes requires association of AKAP5 with a subpopulation of L-type calcium channels. *Circ Res* **107**(6): 747-756.

Nicolaou P, Knoll R, Haghighi K, Fan GC, Dorn GW, 2nd, Hasenfub G and Kranias EG (2008) Human mutation in the anti-apoptotic heat shock protein 20 abrogates its cardioprotective effects. *J Biol Chem* **283**(48): 33465-33471.

Nicolas CS, Park KH, El Harchi A, Camonis J, Kass RS, Escande D, Merot J, Loussouarn G, Le Bouffant F and Baro I (2008) IKs response to protein kinase A-dependent KCNQ1 phosphorylation requires direct interaction with microtubules. *Cardiovasc Res* **79**(3): 427-435.

Nieves-Cintron M, Hirenallur-Shanthappa D, Nygren PJ, Hinke SA, Dell'Acqua ML, Langeberg LK, Navedo M, Santana LF and Scott JD (2016) AKAP150 participates in calcineurin/NFAT activation during the down-regulation of voltage-gated K(+) currents in ventricular myocytes following myocardial infarction. *Cell Signal* **28**(7): 733-740.

Nikolaev VO, Moshkov A, Lyon AR, Miragoli M, Novak P, Paur H, Lohse MJ, Korchev YE, Harding SE and Gorelik J (2010) Beta2-adrenergic receptor redistribution in heart failure changes cAMP compartmentation. *Science* **327**(5973): 1653-1657.

Okumura S, Kawabe J, Yatani A, Takagi G, Lee MC, Hong C, Liu J, Takagi I, Sadoshima J, Vatner DE, Vatner SF and Ishikawa Y (2003a) Type 5 adenylyl cyclase disruption alters not only sympathetic but also parasympathetic and calcium-mediated cardiac regulation. *Circulation Research* **93**(4): 364-371.

Okumura S, Takagi G, Kawabe J, Yang G, Lee MC, Hong C, Liu J, Vatner DE, Sadoshima J, Vatner SF and Ishikawa Y (2003b) Disruption of type 5 adenylyl cyclase gene preserves cardiac function against pressure overload. *Proc Natl Acad Sci U S A* **100**(17): 9986-9990.

Okumura S, Vatner DE, Kurotani R, Bai Y, Gao S, Yuan Z, Iwatsubo K, Ulucan C, Kawabe J, Ghosh K, Vatner SF and Ishikawa Y (2007) Disruption of type 5 adenylyl cyclase enhances desensitization of cyclic adenosine monophosphate signal and increases Akt signal with chronic catecholamine stress. *Circulation* **116**(16): 1776-1783.

Osler ME, Smith TK and Bader DM (2006) Bves, a member of the Popeye domain-containing gene family. *Dev Dyn* **235**(3): 586-593.

Ostrom RS, Naugle JE, Hase M, Gregorian C, Swaney JS, Insel PA, Brunton LL and Meszaros JG (2003) Angiotensin II enhances adenylyl cyclase signaling via Ca2+/calmodulin. Gq-Gs cross-talk regulates collagen production in cardiac fibroblasts. *Journal of Biological Chemistry* **278**(27): 24461-24468.

Palvolgyi A, Simpson J, Bodnar I, Biro J, Palkovits M, Radovits T, Skehel P and Antoni FA (2018) Auto-inhibition of adenylyl cyclase 9 (AC9) by an isoform-specific motif in the carboxyl-terminal region. *Cell Signal* **51**: 266-275.

Pare GC, Bauman AL, McHenry M, Michel JJ, Dodge-Kafka KL and Kapiloff MS (2005a) The mAKAP complex participates in the induction of cardiac myocyte hypertrophy by adrenergic receptor signaling. *J Cell Sci* **118**(Pt 23): 5637-5646.

Pare GC, Easlick JL, Mislow JM, McNally EM and Kapiloff MS (2005b) Nesprin-1alpha contributes to the targeting of mAKAP to the cardiac myocyte nuclear envelope. *Experimental Cell Research* **303**(2): 388-399.

Paterson JM, Smith SM, Harmar AJ and Antoni FA (1995) Control of a novel adenylyl cyclase by calcineurin. *BiochemBiophysResCommun* **214**(3): 1000.

Paterson JM, Smith SM, Simpson J, Grace OC, Sosunov AA, Bell JE and Antoni FA (2000) Characterisation of human adenylyl cyclase IX reveals inhibition by Ca(2+)/Calcineurin and differential mRNA plyadenylation. *JNeurochem* **75**(4): 1358.

Pieroni JP, Harry A, Chen J, Jacobowitz O, Magnusson RP and Iyengar R (1995) Distinct characteristics of the basal activities of adenylyl cyclases 2 and 6. *Journal of Biological Chemistry* **270**(36): 21368.

Piggott LA, Bauman AL, Scott JD and Dessauer CW (2008) The A-kinase anchoring protein Yotiao binds and regulates adenylyl cyclase in brain. *Proc Natl Acad Sci U S A* **105**(37): 13835-13840.

Ping P, Anzai T, Gao M and Hammond HK (1997) Adenylyl cyclase and G protein receptor kinase expression during development of heart failure. *American Journal of Physiology: Heart and Circulatory Physiology* **273**(2): H707-717.

Premont RT (1994) Identification of adenylyl cyclases by amplification using degenerate primers. *Methods in Enzymology* **238**: 116.

Premont RT, Matsuoka I, Mattei M-G, Pouille Y, Defer N and Hanoune J (1996) Identification and Characterization of a Widely Expressed Form of Adenylyl Cyclase. *J Biol Chem* **271**(23): 13900-13907.

Priori SG, Napolitano C, Schwartz PJ, Grillo M, Bloise R, Ronchetti E, Moncalvo C, Tulipani C, Veia A, Bottelli G and Nastoli J (2004) Association of long QT syndrome loci and cardiac events among patients treated with beta-blockers. *JAMA* **292**(11): 1341-1344.

Qian J, Ren X, Wang X, Zhang P, Jones WK, Molkentin JD, Fan GC and Kranias EG (2009) Blockade of Hsp20 phosphorylation exacerbates cardiac ischemia/reperfusion injury by suppressed autophagy and increased cell death. *Circ Res* **105**(12): 1223-1231.

Qian J, Vafiadaki E, Florea SM, Singh VP, Song W, Lam CK, Wang Y, Yuan Q, Pritchard TJ, Cai W, Haghighi K, Rodriguez P, Wang HS, Sanoudou D, Fan GC and Kranias EG (2011) Small heat shock protein 20 interacts with protein phosphatase-1 and enhances sarcoplasmic reticulum calcium cycling. *Circ Res* **108**(12): 1429-1438.

Rall TW and Sutherland EW (1958) Formation of a cyclic adenine ribonucleotide by tissue particles. *Journal of Biological Chemistry* **232**: 1065.

Randhawa PK and Jaggi AS (2017) TRPV1 channels in cardiovascular system: A double edged sword? *Int J Cardiol* **228**: 103-113.

Reddy AK, Jones AD, Martono C, Caro WA, Madala S and Hartley CJ (2005) Pulsed Doppler signal processing for use in mice: design and evaluation. *IEEE Trans Biomed Eng* **52**(10): 1764-1770.

Reese DE, Zavaljevski M, Streiff NL and Bader D (1999) bves: A Novel Gene Expressed during Coronary Blood Vessel Development *Developmental Biology* **209**: 159-171.

Roth DM, Bayat H, Drumm JD, Gao MH, Swaney JS, Ander A and Hammond HK (2002) Adenylyl cyclase increases survival in cardiomyopathy. *Circulation* **105**(16): 1989-1994.

Roth DM, Gao MH, Lai NC, Drumm J, Dalton N, Zhou JY, Zhu J, Entrikin D and Hammond HK (1999) Cardiac-directed adenylyl cyclase expression improves heart function in murine cardiomyopathy. *Circulation* **99**(24): 3099-3102.

Ruehr ML, Russell MA and Bond M (2004) A-kinase anchoring protein targeting of protein kinase A in the heart. *JMolCell Cardiol* **37**(3): 653.

Ruehr ML, Russell MA, Ferguson DG, Bhat M, Ma JJ, Damron DS, Scott JD and Bond M (2003) Targeting of protein kinase A by muscle a kinase-anchoring protein (mAKAP) regulates phosphorylation and function of the skeletal muscle ryanodine receptor. *J Biol Chem* **278**(27): 24831-24836.

Russ PK, Pino CJ, Williams CS, Bader DM, Haselton FR and Chang MS (2011) Bves modulates tight junction associated signaling. *PLoS One* **6**(1): e14563.

Sadana R, Dascal N and Dessauer CW (2009) N terminus of type 5 adenylyl cyclase scaffolds Gs heterotrimer. *Mol Pharmacol* **76**(6): 1256-1264.

Sadana R and Dessauer CW (2009) Physiological Roles for G Protein-Regulated Adenylyl Cyclase Isoforms: Insights from Knockout and Overexpression Studies. *NeuroSignals* **17**: 5-22.

Salama G, Baker L, Wolk R, Barhanin J and London B (2009) Arrhythmia phenotype in mouse models of human long QT. *J Interv Card Electrophysiol* **24**(2): 77-87.

Sandoz G, Thummler S, Duprat F, Feliciangeli S, Vinh J, Escoubas P, Guy N, Lazdunski M and Lesage F (2006) AKAP150, a switch to convert mechano-, pH- and arachidonic acid-sensitive TREK K(+) channels into open leak channels. *EMBO J* **25**(24): 5864-5872.

Scarpace PJ, Matheny M and Tumer N (1996) Myocardial adenylyl cyclase type V and VI mRNA: differential regulation with age. *J Cardiovasc Pharmacol* **27**(1): 86-90.

Schindler RF (2013) Protein biochemistry of Popdc1 and -2 in heart and skeletal muscle, in *Harefield Heart Science Center*, Imperial College London, London, England.

Schindler RF and Brand T (2016) The Popeye domain containing protein family--A novel class of cAMP effectors with important functions in multiple tissues. *Prog Biophys Mol Biol* **120**(1-3): 28-36.

Schindler RF, Scotton C, French V, Ferlini A and Brand T (2016a) The Popeye Domain Containing Genes and their Function in Striated Muscle. *J Cardiovasc Dev Dis* **3**(2): 22.

Schindler RF, Scotton C, Zhang J, Passarelli C, Ortiz-Bonnin B, Simrick S, Schwerte T, Poon KL, Fang M, Rinne S, Froese A, Nikolaev VO, Grunert C, Muller T, Tasca G, Sarathchandra P, Drago F, Dallapiccola B, Rapezzi C, Arbustini E, Di Raimo FR, Neri M, Selvatici R, Gualandi F, Fattori F, Pietrangelo A, Li W, Jiang H, Xu X, Bertini E, Decher N, Wang J, Brand T and Ferlini A (2016b) POPDC1(S201F) causes muscular dystrophy and arrhythmia by affecting protein trafficking. *J Clin Invest* **126**(1): 239-253.

Schwartz PJ (2006) The congenital long QT syndromes from genotype to phenotype: clinical implications. *J Intern Med* **259**(1): 39-47.

Schwartz PJ, Vanoli E, Crotti L, Spazzolini C, Ferrandi C, Goosen A, Hedley P, Heradien M, Bacchini S, Turco A, La Rovere MT, Bartoli A, George AL, Jr. and Brink PA (2008) Neural control of heart rate is an arrhythmia risk modifier in long QT syndrome. *J Am Coll Cardiol* **51**(9): 920-929.

Scott JD, Dessauer CW and Tasken K (2013) Creating order from chaos: cellular regulation by kinase anchoring. *Annu Rev Pharmacol Toxicol* **53**: 187-210.

Sin YY, Martin TP, Wills L, Currie S and Baillie GS (2015) Small heat shock protein 20 (Hsp20) facilitates nuclear import of protein kinase D 1 (PKD1) during cardiac hypertrophy. *Cell Commun Signal* **13**: 16.

Small KM, Brown KM, Theiss CT, Seman CA, Weiss ST and Liggett SB (2003) An Ile to Met polymorphism in the catalytic domain of adenylyl cyclase type 9 confers reduced beta2-adrenergic receptor stimulation. *Pharmacogenetics* **13**(9): 535-541.

Smith TK and Bader DM (2006) Characterization of Bves expression during mouse development using newly generated immunoreagents. *Dev Dyn* **235**(6): 1701-1708.

Sosunov EA, Anyukhovsky EP, Gainullin RZ, Plotnikov A, Danilo P, Jr. and Rosen MR (2001a) Long-term electrophysiological effects of regional cardiac sympathetic denervation of the neonatal dog. *Cardiovasc Res* **51**(4): 659-669.

Sosunov SA, Kemaikin SP, Kurnikova IA, Antoni FA and Sosunov AA (2001b) Expression of adenylyl cyclase type IX and calcineurin in synapses of the central nervous system. *Bull Exp Biol Med* **131**(2): 172-175.

Steiner D, Saya D, Schallmach E, Simonds WF and Vogel Z (2006) Adenylyl cyclase type-VIII activity is regulated by G[beta][gamma] subunits. *Cellular Signalling* **18**(1): 62-68.

Sunahara RK, Dessauer CW, Whisnant RE, Kleuss C and Gilman AG (1997) Interaction of G(s alpha) with the cytosolic domains of mammalian adenylyl cyclase. *J Biol Chem* **272**(35): 22265-22271.

Surve CR, To JY, Malik S, Kim M and Smrcka AV (2016) Dynamic regulation of neutrophil polarity and migration by the heterotrimeric G protein subunits Galphai-GTP and Gbetagamma. *Sci Signal* **9**(416): ra22.

Swan H, Viitasalo M, Piippo K, Laitinen P, Kontula K and Toivonen L (1999) Sinus node function and ventricular repolarization during exercise stress test in long QT syndrome patients with KvLQT1 and HERG potassium channel defects. *J Am Coll Cardiol* **34**(3): 823-829.

Tajada S, Moreno CM, O'Dwyer S, Woods S, Sato D, Navedo MF and Santana LF (2017) Distance constraints on activation of TRPV4 channels by AKAP150-bound PKCalpha in arterial myocytes. *J Gen Physiol* **149**(6): 639-659.

Tall GG, Krumins AM and Gilman AG (2003) Mammalian Ric-8A (synembryn) is a heterotrimeric Galpha protein guanine nucleotide exchange factor. *J Biol Chem* **278**(10): 8356-8362.

Tang M, Zhang X, Li Y, Guan Y, Ai X, Szeto C, Nakayama H, Zhang H, Ge S, Molkentin JD, Houser SR and Chen X (2010) Enhanced basal contractility but reduced excitation-contraction coupling efficiency and beta-adrenergic reserve of hearts with increased Cav1.2 activity. *Am J Physiol Heart Circ Physiol* **299**(2): H519-528.

Tang T, Gao MH, Lai NC, Firth AL, Takahashi T, Guo T, Yuan JX, Roth DM and Hammond HK (2008) Adenylyl cyclase type 6 deletion decreases left ventricular function via impaired calcium handling. *Circulation* **117**(1): 61-69.

Tang T, Lai NC, Roth DM, Drumm J, Guo T, Lee KW, Han PL, Dalton N and Gao MH (2006) Adenylyl cyclase type V deletion increases basal left ventricular function and reduces left ventricular contractile responsiveness to beta-adrenergic stimulation. *Basic Res Cardiol* **101**(2): 117-126.

Tang T, Lai NC, Wright AT, Gao MH, Lee P, Guo T, Tang R, McCulloch AD and Hammond HK (2013) Adenylyl cyclase 6 deletion increases mortality during sustained beta-adrenergic receptor stimulation. *J Mol Cell Cardiol* **60**: 60-67.

Tang WJ and Gilman AG (1991) Type-specific regulation of adenylyl cyclase by G protein beta gamma subunits. *Science* **254**(5037): 1500-1503.

Tang WJ, Krupinski J and Gilman AG (1991) Expression and characterization of calmodulin-activated (Type-I) adenylyl cyclase. *Journal of Biological Chemistry* **266**: 8595.

Tang WJ, Stanzel M and Gilman AG (1995) Truncation and alanine-scanning mutants of type I adenylyl cyclase. *Biochemistry* **34**: 14563.

Taussig R, Tang WJ, Hepler JR and Gilman AG (1994) Distinct patterns of bidirectional regulation of mammalian adenylyl cyclases. *J Biol Chem* **269**(8): 6093-6100.

Tepe NM, Lorenz JN, Yatani A, Dash R, Kranias EG, Dorn GW, 2nd and Liggett SB (1999) Altering the receptor-effector ratio by transgenic overexpression of type V adenylyl cyclase: enhanced basal catalytic activity and function without increased cardiomyocyte beta-adrenergic signalling. *Biochemistry* **38**(50): 16706-16713.

Terrenoire C, Houslay MD, Baillie GS and Kass RS (2009) The cardiac IKs potassium channel macromolecular complex includes the phosphodiesterase PDE4D3. *J Biol Chem* **284**(14): 9140-9146.

Terrenoire C, Lauritzen I, Lesage F, Romey G and Lazdunski M (2001) A TREK-1-like potassium channel in atrial cells inhibited by beta-adrenergic stimulation and activated by volatile anesthetics. *Circ Res* **89**(4): 336-342.

Tesmer JJ, nbsp, G, Sunahara RK, Johnson RA, Gosselin G, Gilman AG and Sprang SR (1999) Two-Metal-Ion Catalysis in Adenylyl Cyclase. *Science* **285**(5428): 756-760.

Tesmer JJ, Sunahara RK, Gilman AG and Sprang SR (1997) Crystal structure of the catalytic domains of adenylyl cyclase in a complex with Gsalpha.GTPgammaS. *Science* **278**(5345): 1907-1916.

Tewson PH, Martinka S, Shaner NC, Hughes TE and Quinn AM (2016) New DAG and cAMP Sensors Optimized for Live-Cell Assays in Automated Laboratories. *J Biomol Screen* **21**(3): 298-305.

Tijsen AJ, Pinto YM and Creemers EE (2012) Circulating microRNAs as diagnostic biomarkers for cardiovascular diseases. *Am J Physiol Heart Circ Physiol* **303(9)**: H1085-1095.

Timofeyev V, Myers RE, Kim HJ, Woltz RL, Sirish P, Heiserman JP, Li N, Singapuri A, Tang T, Yarov-Yarovoy V, Yamoah EN, Hammond HK and Chiamvimonvat N (2013) Adenylyl cyclase subtype-specific compartmentalization: differential regulation of L-type Ca2+ current in ventricular myocytes. *Circ Res* **112**(12): 1567-1576.

Timofeyev V, Porter CA, Tuteja D, Qiu H, Li N, Tang T, Singapuri A, Han PL, Lopez JE, Hammond HK and Chiamvimonvat N (2010) Disruption of adenylyl cyclase type V does not rescue the phenotype of cardiac-specific overexpression of Galphaq protein-induced cardiomyopathy. *Am J Physiol Heart Circ Physiol* **299**(5): H1459-1467.

To JY and Smrcka AV (2018) Activated heterotrimeric G protein alphai subunits inhibit Rap-dependent cell adhesion and promote cell migration. *J Biol Chem* **293**(5): 1570-1578.

Toyota T, Hattori E, Meerabux J, Yamada K, Saito K, Shibuya H, Nankai M and Yoshikawa T (2002) Molecular analysis, mutation screening, and association study of adenylate cyclase type 9 gene (ADCY9) in mood disorders. *Am J Med Genet* **114**(1): 84-92.

Unudurthi SD, Wu X, Qian L, Amari F, Onal B, Li N, Makara MA, Smith SA, Snyder J, Fedorov VV, Coppola V, Anderson ME, Mohler PJ and Hund TJ (2016) Two-Pore K+ Channel TREK-1 Regulates Sinoatrial Node Membrane Excitability. *J Am Heart Assoc* **5**(4): e002865.

Vargas MA, Tirnauer JS, Glidden N, Kapiloff MS and Dodge-Kafka KL (2012) Myocyte enhancer factor 2 (MEF2) tethering to muscle selective A-kinase anchoring protein (mAKAP) is necessary for myogenic differentiation. *Cell Signal* **24**(8): 1496-1503.

Vasavada TK, DiAngelo JR and Duncan MK (2004) Developmental Expression of Pop1/Bves. *Journal of Histochemistry & Cytochemistry* **52(3)**: 371-377.

Vedantham V, Galang G, Evangelista M, Deo RC and Srivastava D (2015) RNA sequencing of mouse sinoatrial node reveals an upstream regulatory role for Islet-1 in cardiac pacemaker cells. *Circ Res* **116**(5): 797-803.

Vercellino I, Rezabkova L, Olieric V, Polyhach Y, Weinert T, Kammerer RA, Jeschke G and Korkhov VM (2017) Role of the nucleotidyl cyclase helical domain in catalytically active dimer formation. *Proc Natl Acad Sci U S A* **114**(46): E9821-E9828.

Voellenkle C, van Rooij J, Cappuzzello C, Greco S, Arcelli D, Di Vito L, Melillo G, Rigolini R, Costa E, Crea F, Capogrossi MC, Napolitano M and Martelli F (2010) MicroRNA signatures in peripheral blood mononuclear cells of chronic heart failure patients. *Physiol Genomics* **42**(3): 420-426.

Westphal RS, Tavalin SJ, Lin JW, Alto NM, Fraser ID, Langeberg LK, Sheng M and Scott JD (1999) Regulation of NMDA receptors by an associated phosphatase-kinase signaling complex. *Science* **285**(5424): 93-96.

Willoughby D and Cooper DM (2007) Organization and Ca2+ regulation of adenylyl cyclases in cAMP microdomains. *Physiol Rev* **87**(3): 965-1010.

Wong W, Goehring AS, Kapiloff MS, Langeberg LK and Scott JD (2008) mAKAP compartmentalizes oxygen-dependent control of HIF-1alpha. *Sci Signal* **1**(51): ra18.

Wu GC, Lai HL, Lin YW, Chu YT and Chern Y (2001) N-glycosylation and residues Asn805 and Asn890 are involved in the functional properties of type VI adenylyl cyclase. *Journal of Biological Chemistry* **276**(38): 35450.

Wu HC, Yamankurt G, Luo J, Subramaniam J, Hashmi SS, Hu H and Cunha SR (2015) Identification and characterization of two ankyrin-B isoforms in mammalian heart. *Cardiovascular Research* **107**(4): 466-477.

Wu YS, Chen CC, Chien CL, Lai HL, Jiang ST, Chen YC, Lai LP, Hsiao WF, Chen WP and Chern Y (2017) The type VI adenylyl cyclase protects cardiomyocytes from beta-adrenergic stress by a PKA/STAT3-dependent pathway. *J Biomed Sci* **24**(1): 68.

Xu H, Barry DM, Li H, Brunet S, Guo W and Nerbonne JM (1999) Attenuation of the slow component of delayed rectification, action potential prolongation, and triggered activity in mice expressing a dominant-negative Kv2 alpha subunit. *Circ Res* **85**(7): 623-633.

Yan L, Vatner DE, O'Connor JP, Ivessa A, Ge H, Chen W, Hirotani S, Ishikawa Y, Sadoshima J and Vatner SF (2007) Type 5 adenylyl cyclase disruption increases longevity and protects against stress. *Cell* **130**(2): 247-258.

Yan S-Z, Huang Z-H, Andrews RK and Tang W-J (1998) Conversion of Forskolin-Insensitive to Forskolin-Sensitive (Mouse-Type IX) Adenylyl Cyclase. *Mol Pharmacol* **53**(2): 182-187.

Yoshimura M, Ikeda H and Tabakoff B (1996) mu-Opioid receptors inhibit dopamine-stimulated activity of type V adenylyl cyclase but enhance dopamine-stimulated activity of type VII adenylyl cyclase. *Mol Pharmacol* **50**(1): 43-51.

Younes A, Lyashkov AE, Graham D, Sheydina A, Volkova MV, Mitsak M, Vinogradova TM, Lukyanenko YO, Li Y, Ruknudin AM, Boheler KR, van Eyk J and Lakatta EG (2008) Ca(2+) -stimulated basal adenylyl cyclase activity localization in

membrane lipid microdomains of cardiac sinoatrial nodal pacemaker cells. *J Biol Chem* **283**(21): 14461-14468.

Zeng C, Wang J, Li N, Shen M, Wang D, Yu Q and Wang H (2014) AKAP150 mobilizes cPKC-dependent cardiac glucotoxicity. *Am J Physiol Endocrinol Metab* **307**(4): E384-397.

Zhang L, Malik S, Kelley GG, Kapiloff MS and Smrcka AV (2011) Phospholipase C epsilon scaffolds to muscle-specific A kinase anchoring protein (mAKAPbeta) and integrates multiple hypertrophic stimuli in cardiac myocytes. *J Biol Chem* **286**(26): 23012-23021.

Zhang L, Malik S, Pang J, Wang H, Park KM, Yule DI, Blaxall BC and Smrcka AV (2013) Phospholipase Cepsilon hydrolyzes perinuclear phosphatidylinositol 4-phosphate to regulate cardiac hypertrophy. *Cell* **153**(1): 216-227.

Zhang R, Zhao J, Mandveno A and Potter JD (1995) Cardiac troponin I phosphorylation increases the rate of cardiac muscle relaxation. *Circ Res* **76**(6): 1028-1035.

Zimmermann G and Taussig R (1996) Protein kinase C alters the responsiveness of adenylyl cyclases to G protein alpha and betagamma subunits. *J Biol Chem* **271**(43): 27161-27166.

Vita

Tanya Ann Baldwin was born in South Dakota, the daughter of Kirk and Janis Baldwin. After completing her work at Milbank High School, Milbank, South Dakota in 2009, she entered South Dakota State University in Brookings, South Dakota. She received the degree of Bachelor of Science with a major in biochemistry and minors in biology and mathematics from SD State in May 2013. In August 2013 she entered The University of Texas MD Anderson Cancer Center UTHealth Graduate School of Biomedical Sciences.

Permanent address:

902 S. 2nd St

Milbank, SD 57252